ISTANBUL TECHNICAL UNIVERSITY ★ GRADUATE SCHOOL

MOLECULAR CHARACTERIZATION OF SILVER-RESISTANT *Saccharomyces cerevisiae*

Ph.D. THESIS

Ergi TERZİOĞLU

Department of Molecular Biology – Genetics and Biotechnology

Molecular Biology – Genetics and Biotechnology Programme

AUGUST 2021

ISTANBUL TECHNICAL UNIVERSITY ★ GRADUATE SCHOOL

MOLECULAR CHARACTERIZATION OF SILVER-RESISTANT *Saccharomyces cerevisiae*

Ph.D. THESIS

Ergi TERZİOĞLU
(521092065)

Department of Molecular Biology – Genetics and Biotechnology

Molecular Biology – Genetics and Biotechnology Programme

Thesis Advisor: Prof. Dr. Zeynep Petek ÇAKAR
Thesis Co-Advisor: Prof. Dr. Cenk SELÇUKİ

AUGUST 2021

ISTANBUL TEKNİK ÜNİVERSİTESİ ★ LİSANSÜSTÜ EĞİTİM ENSTİTÜSÜ

GÜMÜŞ STRESİNE DİRENÇLİ *Saccharomyces cerevisiae*'nin MOLEKÜLER KARAKTERİZASYONU

DOKTORA TEZİ

Ergi TERZİOĞLU
(521092065)

Moleküler Biyoloji – Genetik ve Biyoteknoloji Anabilim Dalı

Moleküler Biyoloji – Genetik ve Biyoteknoloji Programı

Tez Danışmanı: Prof. Dr. Zeynep Petek ÇAKAR
Eş Danışman: Prof. Dr. Cenk SELÇUKİ

AĞUSTOS 2021

Ergi TERZIOGLU, a Ph.D. student of ITU Graduate School student ID 521092065, successfully defended the thesis entitled "MOLECULAR CHARACTERIZATION OF SILVER-RESISTANT *Saccharomyces cerevisiae*", which he prepared after fulfilling the requirements specified in the associated legislations, before the jury whose signatures are below.

Thesis Advisor :	**Prof. Dr. Zeynep Petek ÇAKAR** İstanbul Technical University	.....
Co-advisor :	**Prof.Dr. Cenk SELÇUKİ** Ege University	.....
Jury Members :	**Prof. Dr. Ayten KARATAŞ** Istanbul Technical University	.....
	Prof. Dr. Süleyman AKMAN Istanbul Technical University	.....
	Prof. Dr. Gamze TORUN KÖSE Yeditepe University	.....
	Prof. Dr. Fatma Neşe KÖK Istanbul Technical University	.....
	Assoc. Prof. Dr. Nagehan ERSOY TUNALI Istanbul Medeniyet University	.....

Date of Submission : 24 June 2021
Date of Defense : 02 August 2021

To my family,

FOREWORD

First of all, I owe my thesis supervisor Prof. Dr. Zeynep Petek ÇAKAR a debt of gratitude for giving me a chance to study with her and for her encouragement when I was lost. Thanks for your patience and serving as a model of being in such a personality including hard working, respectfulness, and tolerance.

I am also grateful to my co-advisor, Prof. Cenk SELÇUKİ for his contribution to my thesis work and my graduate education. My thesis advisory board members, Prof. Dr. Ayten KARATAŞ, Prof. Dr. Süleyman AKMAN and Prof. Dr. Gamze TORUN KÖSE are also gratefully acknowledged for the time they devoted to follow the progress of my work and for their valuable comments.

Secondly, I want to thank to my friends who were also studying in ITU Yeast Lab and helped me without hesitation when I needed. Thank you Ceren for your guidance with your deep experience on experiments, Mevlut for your huge support on my article, Öykü for your accompany as a specialist on difficult tasks, Gülçin for your editing role on my manuscript, Burcu for your friendship during my doctorate programme, and Alican for your technical help.

Additionally, I will never forget the time I spent with Murat Kemal, Ayşe Burcu, and Erdem during studying exams and for celebrations; I hope you will be happy what you will be doing in the future. And also I have to thank all my colleagues and my team leader Mrs. Sönmez in Turkish Airlines, I would not be able to start and finish such a doctorate programme without your permission and support.

The financial support for this research from the Scientific and Technological Research Council of Turkey (TÜBİTAK) (project no: 109T638, PI: Z.P. Çakar) as a COST Action (CM0902) project is gratefully acknowledged.

And finally, I dedicate this study to my family whom I owe a debt of gratitude for their support and encourage. This graduation is just one more step through the happiness in my family.

June 2021

Ergi TERZİOĞLU
(Industrial Engineer)

TABLE OF CONTENTS

Page

ABBREVIATIONS

AgNPs : Silver Nanoparticles
AORS : Antioxidative Redox System
cDNA : Complementary Deoxyribonucleic Acid
CDW : Cell Dry Weight
CFU : Colony-forming units
Chr : Chromosome
cRNA : Complementary Ribonucleic Acid
DEGs : Differentially expressed genes
DNA : Deoxyribonucleic Acid
EMS : Ethyl Methanesulfonate
et al. : And others
F-AAS : Flame Atomic Absorption Spectrometry
HPLC : High Performance Liquid Chromatography
MPN : Most Probable Number
ORF : Open Reading Frame
PDB : Protein Data Bank
RIN : RNA integrity number
RNA : Ribonucleic Acid
ROS : Reactive Oxygen Species
TCA : Tricarboxylic Acid
YMM : Yeast Minimal Medium
YPD : Yeast extract-peptone-dextrose medium

SYMBOLS

µM	**:** Micromolar
$AgNO_3$	**:** Silver Nitrate
H_2O_2	**:** Hydrogen Peroxide
Mg^{+2}	**:** Magnesium ion
Ca^{+2}	**:** Calcium ion
K^+	**:** Potassium ion
Na^+	**:** Sodium ion
u	**:** Dalton (Da) or unified atomic mass unit
ppm	**:** Parts per million
µg/litre	**:** Microgram per liter
µm	**:** Micrometer
μm^3	**:** Cubic micrometer
w/v (%)	**:** Weight/volume percentage concentration
^oC	**:** Degrees Celsius
Ag^+	**:** Silver ion
mL	**:** Milliliter
xg	**:** Times gravity
min	**:** Minute
%	**:** Percentage
v/v	**:** Volume per volume
rpm	**:** Rotation per minute
nm	**:** Nanometer
ng	**:** Nanogram

LIST OF TABLES

Page

LIST OF FIGURES

Page

MOLECULAR CHARACTERIZATION OF SILVER-RESISTANT *Saccharomyces cerevisiae*

SUMMARY

In molecular biology and metabolic engineering, one of the most widely used organisms is the yeast *Saccharomyces cerevisiae* that has been involved in biological applications for thousands of years among different cultures in different parts of the world. As a eukaryotic organism, *S. cerevisiae* reproduces by budding or sporulation, as a consequence of being able to have genetically haploid and diploid forms. It has a high level of similarity with human cells in regard of proteins and their functions, which leads to the popularity of this budding yeast in a wide range of researches related to humans.

Yeast can resist many types of stress factors in the environment at various levels. Metal stress is one of these stresses that yeast may show resistance against, but the mechanism of metal stress tolerance in yeast has not been fully enlightened yet. When these metal resistance pathways are revealed, it will be also possible to increase resistance, which leads to an improved productivity in metal recovery in industrial applications for biotechnological processes and in bioremediation of metal-polluted environments.

Silver stress resistance in yeast was studied in this thesis and after obtaining a silver-resistant *S. cerevisiae* mutant by using evolutionary engineering methods, the mutant was subjected to genetic and physiological characterization by comparison with the reference strain.

Ethyl methanesulfonate (EMS) treated *S. cerevisiae* was the initial culture in this study, and this chemical mutagenesis caused a wide range of random mutations in the genome of the yeast cells in the population. To select a target mutant with the character of silver-resistance in the population, evolutionary engineering method was applied. To determine the initial level of silver stress for the evolutionary selection, this culture and the reference strain were both cultivated at different silver concentrations. The survival rates calculated at different silver concentrations demonstrated the most appropriate initial silver concentration with the minimum effect of silver stress on the cells. Next populations were subjected to higher concentrations of silver than the previous ones, until a significant decrease in the survival rate. While 5 µM $AgNO_3$ was the initial stress level for the first population of the selection, the 29^{th} population was exposed to 250 µM $AgNO_3$. Ten individual mutants were randomly chosen from the final population, based on their high resistance to silver stress. Among these mutants, the most resistant one, called as 2E, was tested for genetic stability that revealed a genetically stable trait.

The silver-resistant mutant 2E and the reference strain were subjected to cross-resistance tests against other stresses, using spot assay. Spot assay results showed that 2E was also highly resistant to copper stress and had a significant resistance against cobalt and oxidative (H_2O_2) stresses. On the other hand, it was observed that 2E was sensitive against chromium, manganese, aluminum, and ethanol stress. Reference strain and the silver-resistant mutant 2E showed similar stress responses against nickel, zinc, and lithium stresses.

Transcriptomic analysis for the whole genome of the silver-resistant mutant 2E and the reference strain was applied to investigate the mechanism of silver resistance in the cell. DNA microarray analysis revealed that while 780 genes were upregulated, 877 genes were downregulated. Totally 1657 open reading frames (ORFs) had differential expression between 2E and the reference strain. By using Gene Ontology analysis, it was indicated that in the silver-resistant mutant, the highly upregulated genes were related to carbohydrate metabolic process, precursor metabolite generation, energy generation, oxidation-reduction, oxidative stress, and extracellular stimulus response. On the other hand, mutant 2E seemed to have generally repressed its protein synthesis by downregulation of the genes involved in ribosome biogenesis, ribosomal subunit and RNA metabolic processes.

When compared to the reference strain, there were 64 mutations in the silver resistant mutant 2E, based on the results of whole genome re-sequencing. These mutations were composed of 61 nonsynonymous and 3 stop-loss ones. The most relevant mutation in 2E that may have caused an improvement in silver resistance was the one on *CCC1* gene, a transporter of Fe^{2+}/Mn^{2+} in vacuole, since silver has similar atomic properties with copper. This study also implied that the resistance of 2E against silver might be by upregulating copper resistance genes, *CTR3*, *CUP2*, *CUP1-1*, and *CUP1-2*, that bind copper and are responsible for copper-homeostasis in the yeast cell.

Silver causes oxidative stress in cell and the mutant 2E had oxidative stress resistance. This study showed that a number of oxidative stress responsive genes were oppositely expressed in the mutant 2E and the reference strain that showed no resistance against neither silver nor oxidative stress. Oxidative stress resistance of 2E was also supported by the missense mutation detected on the DNA helicase gene *PIF1*. In addition to this, 2E had a highly differentiated mitochondrial gene expression profile that led to a more active aerobic metabolism and electron transfer system, which may explain the better growth of the mutant 2E under silver stress condition.

The membrane-bound transport and cell wall proteins are damaged when subjected to silver ions and nanoparticles during growth phase, that leads to disruption in cell wall and membrane integrity. However, while 2E upregulated some of the mannoprotein genes (such as *YPK2*, *USV1*, *YPS6*, *SRL1*) to keep its cell wall integrity, it downregulated the ones related to anaerobic growth (*TIP1* and *TIR1-4* genes). Additionally, some ergosterol synthesis genes and many of the sugar transporter genes along with some TCA cycle genes for NADH regeneration were significantly upregulated. All these findings indicated a strong aerobic metabolism in the evolved strain 2E, but a more robust cell wall was most likely provided by the upregulation of other cell wall-associated genes and the observed mutations in some cell wall-associated genes, particularly *RLM1*, a gene that encodes a transcription factor responsible for the activation of the *MPK1* mitogen-activated protein kinase pathway, and the maintenance of cell wall integrity.

Some of the missense mutations of 2E were found in vesicle protein sorting and vacuole biogenesis (*VPS45*, *PEP5*), and endocytosis (*ENT1*, *YAP1802*, *MYO5*, *AKR2*) genes. Also *AAC1* that encodes a vesicular transport protein was upregulated in 2E. As a result, the silver-resistant evolved strain 2E kept higher levels of silver in/on itself, compared to the reference strain, according to Flame Atomic Absorption Spectrometry (F-AAS) analysis results, that possibly made a significant contribution to its silver resistance.

This study was about selecting and characterizing a silver-resistant mutant of *S.cerevisiae* at a molecular level. The possible reasons for the silver resistance in yeast cell were discussed, regarding molecular and functional factors. Some potentially important genes and pathways for the silver resistance mechanism have been identified in this study, which have been discussed, based on the previous studies found in the literature about silver response. Despite these major findings, further investigations are still needed to fully enlighten the complex molecular mechanisms of silver resistance, regarding copper resistance, oxidative stress, cell wall integrity, aerobic metabolism and vesicular transport.

GÜMÜŞ STRESİNE DİRENÇLİ *Saccharomyces cerevisiae*'nin MOLEKÜLER KARAKTERİZASYONU

ÖZET

Dünyanın farklı bölgelerindeki farklı kültürlerde binlerce yıldır biyolojik uygulamalarda kullanılan *Saccharomyces cerevisiae* mayası, günümüzde de moleküler biyoloji ve metabolik mühendislik alanlarında en çok kullanılan organizmalardan birisidir. Ökaryotik bir organizma olan *S. cerevisiae*, genetik olarak haploid ve diploid formlarda bulunabilmesinin bir sonucu olarak tomurcuklanarak (eşeysiz) veya spor oluşturarak (mayoz bölünme) üreyebilir. Protein yapıları ve fonksiyonları açısından insan hücreleri ile önemli ölçüde benzerlikler gösterdiği için, insan ile ilgili farklı araştırmalarda da bu maya türü, bir model organizma olarak yaygın bir şekilde kullanılmaktadır.

Maya hücreleri, ortamlarında bulunan birçok stres faktörüne karşı, farklı seviyelerde direnç gösterebilir. Maya hücrelerinin direnç gösterebildiği bu stres faktörlerinden biri de metal stresidir; fakat mayaların metal stresine karşı gösterebildikleri direncin moleküler mekanizmaları henüz tam olarak aydınlatılamamıştır. Bu metal direnç yolizleri ortaya çıkarılabildiğinde, sahip olunan direncin arttırılması sağlanabilecek, böylece endüstriyel uygulamalarda metallerin biyolojik proseslerle geri kazanımında ve metal kirliliğinin görüldüğü çevrelerde, biyoıslah çalışmalarında üretkenlik yükseltilebilecektir.

Bu çalışmada, maya hücrelerindeki gümüş direnci incelenmiştir ve evrimsel mühendislik metodu ile gümüşe dirençli *S.cerevisiae* mutantı elde edildikten sonra, referans maya suşu ile karşılaştırmalı olarak bu mutantın genetik ve fizyolojik karakterizasyonu gerçekleştirilmiştir.

Çalışmada kullanılan başlangıç kültürü, etil metansülfonat uygulanmış, dolayısıyla rastgele mutasyonlar ile genetik çeşitliliği artırılmış bir *S. cerevisiae* maya popülasyonudur. Bu popülasyon içinde gümüş stresine direnç özelliği gösteren hedef mutant, evrimsel mühendislik metodu uygulanarak seçilmiştir. Seleksiyonda uygulanacak başlangıç gümüş stres direnç düzeyinin tespiti için bu kültür ve referans *S.cerevisiae* suşu, farklı gümüş konsantrasyonları varlığında üretilerek hayatta kalma oranları belirlenmiştir. Buna göre, gümüş stresinin hücreler üzerinde minimum etki ettiği en uygun gümüş konsantrasyonu, başlangıç gümüş stress değeri olarak belirlenmiştir. Birbirini takip eden iki popülasyon arasında, hayatta kalma oranları ciddi düzeyde düşene kadar, besiyerindeki gümüş konsantrasyonu kademeli olarak artırılmıştır. İlk popülasyon için gümüş stresi seviyesi 5 µM $AgNO_3$ iken, en son 29. popülasyon için 250 µM $AgNO_3$ kullanılmıştır. Bu son popülasyon içerisinden, gümüş stresi varlığında daha hızlı gelişme gösteren 10 farklı mutant birey seri seyreltme ve katı besiyerine ekilerek rastgele olarak seçilmiş ve bunlar arasından gümüş stresine en

dirençli olan mutant birey 2E olarak adlandırılmıştır. 2E bireyine uygulanan genetik kararlılık testi de olumlu sonuç vermiştir.

Gümüşe dirençli suş 2E ile referans suşu için, fizyolojik özelliklerinin belirlenebilmesi amacıyla çapraz stres direnç testleri yapılmıştır. Bu testler, 2E'nin, referans suşa kıyasla, gümüş ile birlikte bakır stresine karşı da yüksek bir dirence, kobalt ve oksidatif (H_2O_2) strese karşı da anlamlı düzeyde dirence sahip olduğunu göstermiştir. Fakat aynı testler sonucunda 2E'nin, kroma, manganeze, alüminyuma ve etanole karşı hassasiyeti olduğu ortaya çıkmıştır. Bununla birlikte, referans suş ve gümüş stresine dirençli suş 2E; nikel, çinko ve lityum stres direnci açısından anlamlı bir farklılık göstermemiştir.

Mutant maya bireyindeki gümüş stresine direncin moleküler mekanizmasının incelenmesi için, gümüşe dirençli suş 2E'nin ve referans suşun tüm genomunu kapsayan transkriptomik analizler gerçekleştirilmiştir. Bu doğrultuda yapılan DNA mikrodizin analizleri, 2E ile referans suş arasında toplam 1657 genin ekspresyonunda farklılık olduğunu göstermiştir. Bunlardan 780 genin ekspresyon düzeyi artarken, 877 geninki ise azalmıştır. Gümüşe dirençli suş 2E; özellikle karbonhidrat metabolizması, metabolit üretimi, enerji üretimi, oksidasyon-redüksiyon ve oksidatif stres süreçlerinde yer alan genleri çok yüksek oranda eksprese ederken, ribozom biyogenezi, ribozoma ait altbirimler ve RNA metabolik süreçlerinde yer alan genlerin ekspresyonunu ise düşürerek protein sentezini baskılamıştır.

Referans suş ile karşılaştırıldığında, tüm genomun yeniden dizilenmesi sonuçlarına göre, gümüşe dirençli suş 2E'nin, 64 mutasyona sahip olduğu görülmüştür. Bu mutasyonların 61 tanesi nokta mutasyon iken, 3 tanesi durdurucu mutasyondur. Bu mutasyonlar arasında, 2E'nin gümüş direnci geliştirmesiyle muhtemelen en ilişkili olanı, vakuol içinde Fe^{2+}/Mn^{2+} taşınımı ile ilgili gen olan *CCC1* üzerindekidir, çünkü bu gen bakır direnciyle doğrudan ilişkilidir ve gümüş, bakır ile benzer atom özelliklerine sahiptir. Bu çalışma ayrıca 2E'nin, maya hücrelerinde bakır bağlayan ve bakır homeostaz sürecinden sorumlu *CTR3*, *CUP2*, *CUP1-1* ve *CUP1-2* bakır direnç genlerini çok daha fazla eksprese ederek gümüşe karşı direnç kazanmış olabileceğini göstermektedir.

Gümüş, hücre içerisinde oksidatif strese sebep olur ve bu çalışmada, mutant 2E'nin oksidatif strese karşı da direnci olduğu görülmüştür. Referans maya suşu, gümüş stresine ve oksidatif strese karşı bir direnç gösteremezken, mutant 2E, referans suşun, oksidatif strese cevap genekspresyonuna neredeyse zıt olacak şekilde ekspresyon göstermiştir. 2E'nin oksidatif stres direnci, aynı zamanda DNA helikaz geni *PIF1*'deki nokta mutasyonu ile de desteklenmiştir. Ayrıca, 2E'nin referans suşa kıyasla oldukça farklı bir mitokondrial gen ekspresyon profiline sahip olması, onun muhtemelen daha aktif bir aerobik metabolizmaya ve elektron transfer sistemine sahip olmasını sağlamıştır. Böylece mutant 2E, gümüş stresi şartlarında daha iyi gelişebilmiştir.

Maya hücrelerinin gelişme fazında gümüş iyonlarına ve nanopartiküllerine maruz kalması durumunda, membran taşınım ve hücre duvarı proteinleri zarar görür. Bu durum hücre duvarında ve membran bütünlüğünde bozulmalara sebep olur. Ama 2E, hücre duvarının bütünlüğünü koruyabilmek için bazı mannoproteinlerin gen ekspresyonunu arttırırken (*YPK2*, *USV1*, *YPS6*, *SRL1* gibi), anaerobik büyümeyle ilgili genlerin ise ekspresyonunu azaltmıştır (*TIP1* and *TIR1-4* gibi). Ayrıca, bazı ergosterol sentez genlerinin, NADH rejenerasyonu için gereken bazı Krebs döngüsü genlerinin ve birçok şeker taşınım genlerinin ekspresyonunun da arttığı tespit edilmiştir. Tüm bu bulgular, 2E suşunda güçlü bir aerobik metabolizmanın var olduğuna işaret etmektedir. 2E'nin, muhtemelen daha sağlam bir hücre duvarını sağlayabilmek için

hücre duvarıyla ilişkili diğer genlerin ekspresyonunu arttırdığı da gözlenmiştir. Ayrıca, bazı hücre duvarı bağlantılı genlerdeki ve özellikle, *MPK1* protein kinaz yolizinin aktivasyonundan ve hücre duvarı bütünlüğünün korunmasından sorumlu bir transkripsiyon faktörü olan *RLM1* genindeki mutasyonların, bu sağlamlığa katkı sağladığı tahmin edilmektedir.

2E'deki bazı nokta mutasyonlar vesikül protein etiketleme ve vakuol biyogenez (*VPS45*, *PEP5*) ve endositoz (*ENT1*, *YAP1802*, *MYO5*, *AKR2*) genlerinde yer almaktadır. Buna ilave olarak 2E, bir vesikül taşınım proteinini kodlayan *AAC1*'in ekspresyonunu arttırmıştır. Böylece, Alevli Atomik Absorpsiyon Spektrometri analizlerine göre, referans suş ile karşılaştırıldığında 2E suşu, hücre içinde ve hücre duvarı üzerinde yüksek miktarda gümüş iyonunu tutabilmektedir.

Bu tez çalışmasının amacı gümüş stresine dirençli bir *S. cerevisiae* maya mutantı elde ederek bu suşun moleküler karakterizasyonunu yapabilmektir. Tez çalışması kapsamında evrimsel mühendislik yaklaşımıyla elde edilen dirençli şuşun sahip olduğu gümüş direncinin, olası moleküler ve fizyolojik nedenleri tartışılmıştır. Gümüş direncinin olası moleküler mekanizmaları hakkında kritik bilgiler edinilmekle birlikte, bu mekanizmaların tam olarak aydınlatılabilmesi için daha kapsamlı araştırmalar gerekmektedir. Fakat, daha önceki bazı çalışmalarda gümüş direnci ile ilişkisi tespit edilmiş olan bazı genlerin, 2E'nin gümüş stresine direnç kazanmasında da muhtemelen görev aldığı görülmüştür. Ayrıca bu çalışmada, yakın zamanda, gümüş direnci ile ilişkisi olabileceği liteartürde belirtilmiş olan bazı genlerle ilgili teorileri destekleyici bazı sonuçlar da elde edilmiştir. Sonuç olarak, bu tez çalışması kapsamında elde edilmiş olan, mayada gümüş stresine direnç ile ilgili tüm önemli bulgulara rağmen, gümüş direncinin karmaşık moleküler mekanizmasının aydınlatılabilmesi için bakır direnci, oksidatif stress, hücre duvarı bütünlüğü, aerobik metabolizma ve vesiküler taşınım mekanizmaları odaklı daha ileri araştırmalar gerekmektedir.

1. INTRODUCTION

1.1 Transition Metals

Microorganisms need metals for their biological functions because metals participate in different and critical cell processes related to physiology, structure, and catalytic functions. For example, having key roles in muscle and nerve cells, magnesium (Mg^{+2}), calcium (Ca^{+2}), potassium (K^{+}), and sodium (Na^{+}) are the metals that are found prevailingly in the cells. According to Protein Data Bank (PDB), 25% of the proteins involve metal ions (Argüello *et al.*, 2012; Shi *et al.*, 2005). Among metal ions, probably due to their coordination and redox chemistry, transition metal ions (Figure 1.1) are much more covered than alkali metal ions by cell for their protein structure (Bleackley *et al.*, 2011).

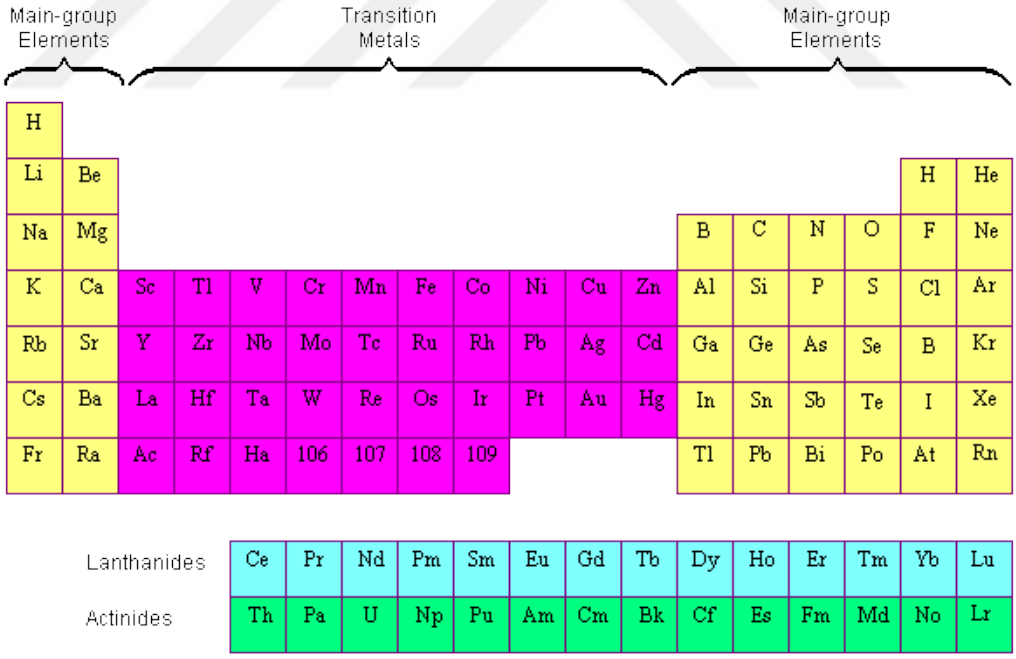

Figure 1.1 : Transition metals in the Periodic Table (URL-1).

Transition matels are generally required in the cell for protein activities. While some eukaryotes and prokaryotes need transition metals like nickel, manganese, and copper; iron and zinc are required nearly by all types of organisms (Galaris and Pantopoulos, 2008).

1.2 Silver in Nature

Silver is a metal symbolized with Ag. Its atomic number and molecular weight are 47 and 107,87 u respectively. As a transition metal, silver is in the same group (11) with copper and gold. Most stable and main oxidation state of silver is +1 but highly oxidising state of +2 is also common, in addition to rare oxidation states 0 and +3. The ratio of silver within the Earth's crust is 0.08 ppm. The three forms of silver found in nature are free elemant, as alloy with metals and gold, and in minerals. Generally, production of silver is the formation as a byproduct during the refinement process of lead, zinc, gold, and copper (Greenwood and Earnshaw, 1997).

1.3 Metals in the Cell

From a biological point of view, some metals (such as iron and copper) are trace elements and very low amounts of them are needed by living organisms. Living organisms have certain mechanisms including uptake, storage, and excretion to maintain the amount of those specific metals at low levels (Figure 1.2). On the other hand, high concentrations of essential and non-essential metals (silver, mercury…) cause toxicity by damaging DNA and its repair mechanism, interfering with protein functionality participating in important cell processes, and leading to oxidative stress by forming reactive oxygen species (Wysocki and Tamas, 2010).

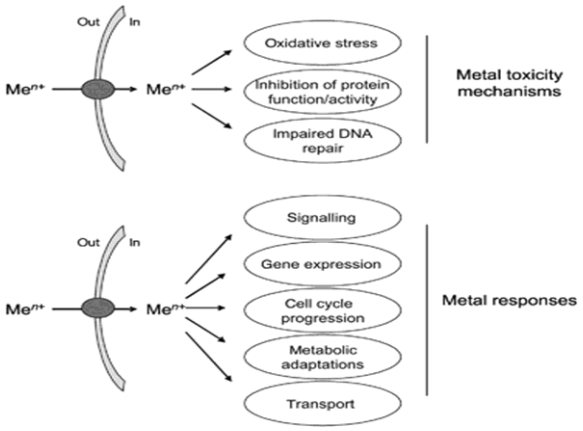

Figure 1.2 : Toxicity of metals and responses in cell (Wysocki and Tamas, 2010).

Microorganisms resist toxicity of metals by postponing the progression of the cell cycle and changing gene expression and metabolism in order to change membrane permeability against metals and remove metals from cytosol including membrane metal exporters, cysteine-rich proteins-peptides with low molecular weight, and

vacuolar sequestration. There are common metal response mechanisms as well as specialized ones depending on the chemical properties of the metal (Tamas et al., 2005).

1.4 Silver in the Industry and Its Effects on Human Health

Silver (Ag) is one of the non-essential heavy metals. Jewellery, electronics, brazing alloys and chemical aquipment are some applications that silver is used in. It is also used in biotechnological applications such as wound management and dental devices (for antibiotic coating) due to its antimicrobial effects (Chopra, 2007; Limberger, Westphalen, Menezes, Medina-Silva, 2011). The use of antimicrobial property of silver regarding resistance and toxicity has been reviewed in many researches such as the one by Mijnendonckx, Leys, Mahillon, Silver, and Van Houdt in 2013. Additionally, in the last decade, silver is used increasingly in medical and especially dental coating applications by nanotechnology. Therefore, toxicity of silver nanoparticles has also been investigated (Limberger et al., 2011; Niazi, Sang, Kim, Gu, 2011; Saulou et al., 2010).

Treatment and diagnosis of disease are popular fields for nanomedicine. While optimizing nanotechnological benefits with nanoparticle production costs, biological and toxicological effects should be evaluated in detail by negative effects on the cell (Figure 1.3). The toxic effects of nanoparticles are based on their size, structure, and surface chemistry (Warheit et al., 2008). Generally, smaller size is the most important factor for toxicity because the physical and chemical properties of the particle change. Additionally, structure and surface lead to transfer of the nanoparticles in the organism and interaction with the components of the cell (Fadeel and Garcia-Bennett, 2010). Silver nanoparticles provide silver ions uninterruptedly because of their very low rate of dissolution which is the reason for their use in medical coating. On the other hand, this causes occurrence of reactive oxygen species (ROS) interacting cell wall, nucleic acids, and some other molecules in the cell (Greulich et al., 2012).

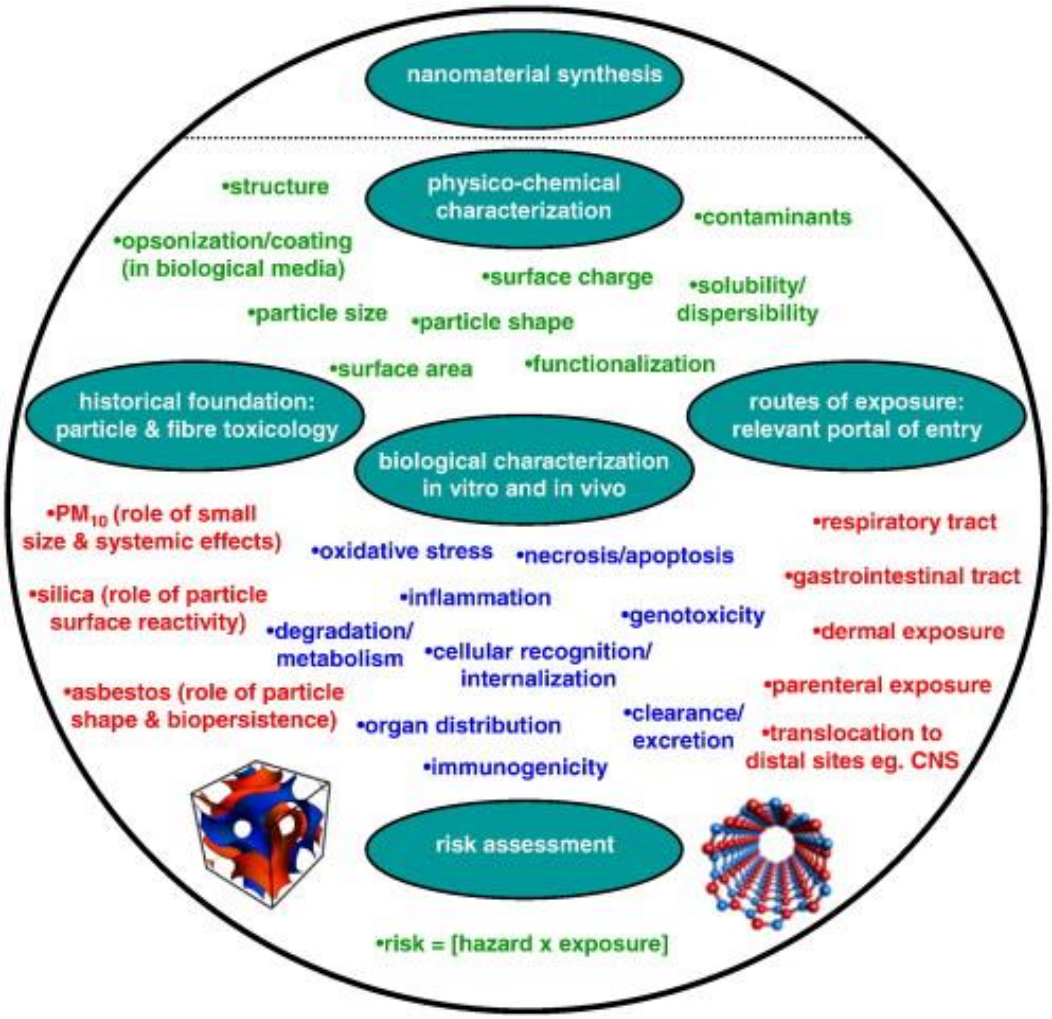

Figure 1.3 : Nanotoxicology: nanomaterial synthesis, physical-chemical-biological characterization, and risk assessment (Fadeel and Garcia-Bennett, 2010).

Although silver has benefits for health applications, due to being a metal it is dangerous for humans and the environment (Jin et al., 2008). Mines are the main source of silver leached into the sea and rivers in addition to industrial waste that causes pollution in water with high acid and metal levels (Holland et al., 2011). Clean techniques indicated that while unpolluted areas of lakes and rivers had nearly 0.01 µg/litre silver level, it was between 0.01 µg/litre and 0.1 µg/litre in industrialized ones. Just in the USA, the estimated amount of silver discharged into the environment (main part into the aquatic and terrestrial ecosystem) in 1978 was 2.5 milliom kilogram, 47% of which was from industry regarding photography. Silver accumulates in human body in brain, kidney, and liver through drinking-water and diet (Howe and Dobson, 2002). Organ damage, nervous system disorders, defects on birth, and cancer are some of the diseases that high silver concentrations cause against human health (Jin et al., 2008).

1.5 *Saccharomyces cerevisiae* as a Model Organism

Saccharomyces cerevisiae is a eukaryotic organism that has been studied genetically since 1935. It has been the microorganism used in production of beer, wine, and baking for thousands of years. It has also been commonly used in molecular biological and genetic studies as a model organism since the last century (Botstein, Chervitz, Cherry, 1997). Whole genome of one of the *S.cerevisiae* strains was sequenced and it was the first time for a eukaryotic organism. As the biochemistry and the genetic properties of *S. cerevisiae* are known well, its cultivation and genetic manipulation are also easy (Botstein et al., 1997; Galagan, Henn, Ma, Cuomo, Birren, 2005; Goffeau et al., 1996; Sherman, 2002).

S.cerevisiae genome consists of 16 chromosomes and 12 million base pair. 70% of the *S.cerevisiae* genome covers approximately 6000 open reading frames (ORFs), that is much more denser than eukaryotic microorganisms and human (5% of its genome consists of ORF). Dense ORF means most of the DNA sequences in *S.cerevisiae* contain coding genes. As a result, it is easy to identify a gene, determine its function, and investigate the similar protein regarding its DNA sequence and function (Dujon, 1996).

Two forms of *S.cerevisiae*, haploid and diploid states, have different cell properties as shown in Table 1.1. These properties also differ according to growth phase and strain. In general, spheroidal haploid cells have a diameter of 4 μm and ellipsoidal diploid cells have the dimensions of 5x6 μm. Diploid cultures reach less number of cells in a cluster compared to haploid cultures at the exponential phase of the growth. While the buds of diploid cells occur at the opposite pole, the buds of the haploid one are seen bordering (Sherman, 2002).

Table 1.1 : Yeast cells' composition and size (Sherman, 2002).

Characteristic	Volume (μm^3)	Composition (10^{-12}g)				
		Wet weight	Dry weight	DNA	RNA	Protein
Haploid cell	70	60	15	0.017	1.2	6
Diploid cell	120	80	20	0.034	1.9	8

The yeast *S.cerevisiae* uses carbon sources for fermentation and grows through 4 differential phases, as shown in Figure 1.4. Lag phase is the initial period of time when cells experience growth as soon as they are cultured into a fresh medium. Prediauxic

phase is a period in which cells produce ethanol during fermentation by using dextrose as a carbon source and logarithmic growth is seen after lag phase. As dextrose is consumed in the media, cells start respiration (postdiauxic phase) and produce carbon dioxide by using ethanol that has been produced during fermentation. The stationary phase is the final phase where the growth turns into a plateau because yeast cells stop dividing (Matmati and Hannun, 2008).

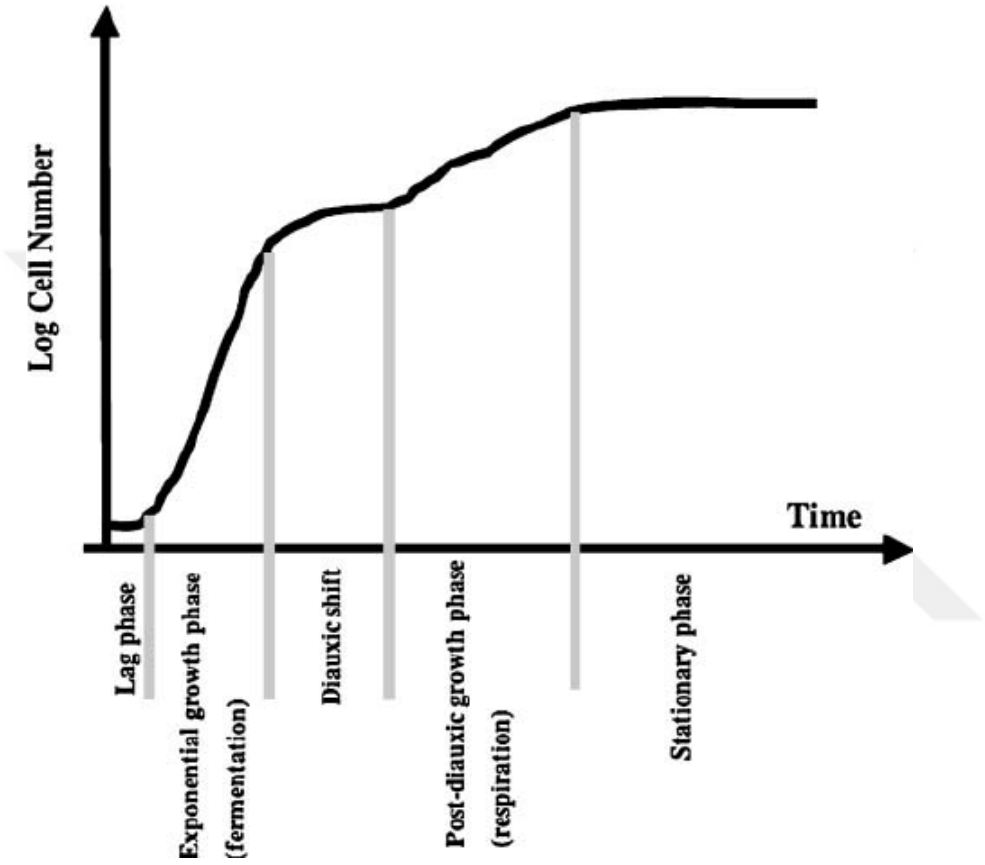

Figure 1.4 : Four growth phases of the yeast *S.cerevisiae* (Matmati and Hannun, 2008).

Regarding medium types, both YPD and synthetic yeast minimal medium (YMM) are used for *S.cerevisiae* strain. While YPD consists of 1% yeast extract, 2% peptone, and 2% glucose (all in w/v), YMM consists of 0.67% yeast nitrogen base and 2% dextrose (all in w/v). Doubling time during exponential growth phase differs according to medium (90 minutes for YPD and 140 minutes for YMM). 30^{o}C is required for an optimum yeast growth.

Many *S.cerevisiae* strains were obtained in many important laboratories in the world. CEN.PK is a widespread *S.cerevisiae* strain that is used in many studies in laboratories

(Schacherer et al., 2007). When compared with other *S.cerevisiae* strains, it was demonstrated that CEN.PK strain family was more preferable regarding characteristics of growth in shake-flask, growth rates during respiratory phase, and efficiency in genetic transformation. Additionally, its physiological character is similar in both haploid and diploid forms, many gene-replacement mutants are produced, productivity of heterologous protein production was high, and DNA microarrays are easily accessible (van Dijken et al., 2000).

1.6 Silver Stress in *S.cerevisiae*

All metal ions are able to bind to cell wall of yeast by anionic groups on it without any specific cell affinity effort (Fuhrman and Rothstein, 1968). On the other hand, some metals like iron and copper are essenital so yeast cell has to take in, sequester into cell compartment and detoxify through complicated mechanisms in order to keep the optimal levels of it in cytosol (Nies, 1999). Silver is a nonessential metal and does not participate in any protein for its structure or catalytic function. Since there is no biological significance of silver ions, there is no known transport, maintainence, or export system specialized and targeted on silver inside the cell. However, because of its structural resemblance to copper, silver is also transported by copper transport system especially under copper deficiency and many copper ATPases are activated to carry silver ions (Solioz and Odermatt, 1995).

If copper increases in cytosol, Ace1p, transcription factor of copper, is activated that leads to the expression of *CUP1-1* and *CUP1-2* metallothionein genes (Winge, 1998). In addition to these metallothioneins, *CCC2* gene is induced during high-level copper conditions to export copper to the extracytosolic compartment from cytosol. *CCC2* gene is also responsible for iron uptake (Yuan et al., 1995). When yeast cell is subjected to silver ions, *CUP1-1*, *CUP1-2*, and *CCC2* genes are also induced (Niazi et al, 2011). In Figure 1-5, it is shown how silver and some other metals are detoxified in general. Copper transport system is stimulated in the cell to prevent toxicity of silver during this detoxification, which includes chelation of silver ions by metallothionein and glutathione, reduction of reactive oxygen species by antioxidative redox system (AORS), sequestration into the vacuole where silver is stored and proteins are degraded. Most of the metals (such as zinc, nickel, and cobalt) accumulate in vacuole

and this accumulation of metals preserves the cell from toxicity of metals (Ramsay et al., 1997).

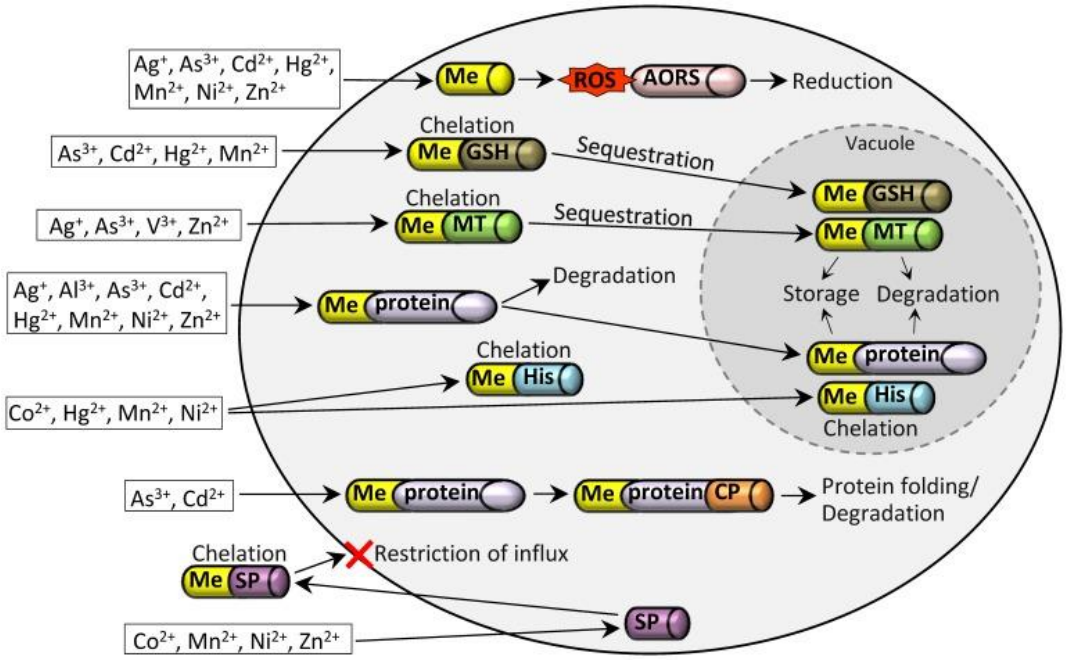

Figure 1.5 : Detoxification patterns against silver stress in *S.cerevisiae*. The abbreviations for patterns regarding Ag^{+} (silver ion) are Me: Metal ion, GSH: Glutathione, MT: Metallothionein (Hosiner et al., 2014).

When the yeast cell is overexposed to silver, the resistance mechanisms are not able to handle the inhibitory influences of it. Silver stress leads to growth rate defect, instability of cell wall and oxidative stress inside the cell. Additionally, cell membrane integrity is damaged and oxidative stress causes impairment in RNA processing, ribosome biogenesis, protein folding and cellular respiration. Both silver ions and silver nanoparticles (AgNPs) have toxic effects on the yeast cell but free silver ions have worse effect than silver nanoparticles (Horstmann et al., 2019). Cellular processes and cell compartments impaired by silver stress are shown in Figure 1.6.

Silver nanoparticles and silver ions response of the yeast consists of complicated and unrevealed molecular mechanisms. In order to investigate these mechanisms, the omic technologies provide detailed information. There are many researches covering deletome and transcriptome analysis focusing on silver ion exposure of yeast and silver (such as Jin et al., 2008) as well as covering transcriptome profile focusing on silver nanoparticle treatment (such as Horstmann et al., 2019).

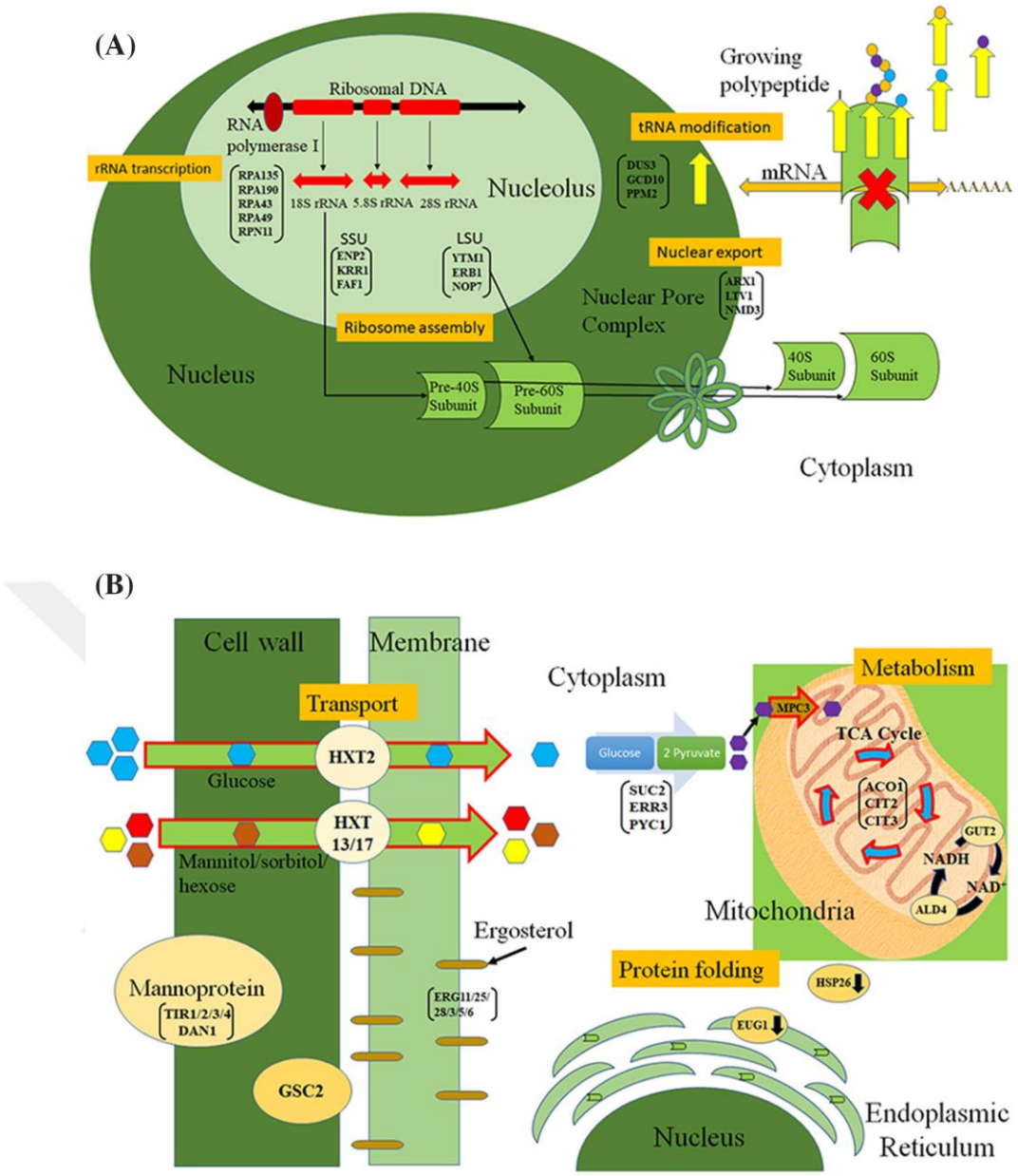

Figure 1.6 : Cellular processes and cell compartments impaired by silver stress. (A) Impairment of ribosome integrity and its consequence of upregulation of rRNA processing and ribosome subunit biogenesis genes. (B) Downregulation of genes participated in respiration, protein folding, cytosolic metabolism, sugar import, integrity of cell wall (Horstmann et al., 2019).

1.7 Metabolic Engineering

In 1970s, there were many advances in recombinant DNA technology which led to outstanding discoveries and novelties in biology. Thus, scientists started to work on genomes of both eukaryotic and prokaryotic cells, thoroughly. In the 2000s, these improvements have reached a high level such that producing pharmaceutical proteins in large amounts and forming a productive mutant strain under extreme conditions

became possible now (Porro et al., 2005). Metabolic engineering is described as changing or installing biochemical reactions in the cell by using recombinant DNA technology, in order to improve cellular properties and biological products (Stephanopoulos, 1999). Gene deletions and new metabolic pathway introduction are achieved by execution of genetic engineering techniques and using the data gathered from biochemical analysis (Ostergaard et al., 2000). *S. cerevisiae* is also a preferable microorganism for metabolic engineering, because unnecessary mutations can be ruled out and heterologous genes can be expressed (Nevoigt, 2008).

There are complex relationships between many metabolic pathways and sometimes it is nearly impossible to understand the regulations of all cellular activities being investigated, asit requires the recognition of the whole metabolic network. Thus, inverse metabolic engineering can be an alternative approach for metabolic studies, overcoming those difficulties associated with the rational metabolic engineering (Cakar, 2009).

1.8 Evolutionary Engineering as an Inverse Metabolic Engineering Strategy

In order to enhance the product formation or the production rate of microorganisms, metabolic engineering is an ideal tool. However, inverse metabolic engineering is applied for complex metabolic systems about which there is a limited amount of information.that Inverse metabolic engineering consists of three major steps: identification or description of a desired phenotype, , determination of the genetic basis of that phenotype, and introduction of the relevant genes of that phenotype to a suitable host for industrial production (Bailey et al., 1996).

As an inverse metabolic engineering strategy, adaptive laboratory evolution or evolutionary engineering enables improvement of genetically complex microbial phenotypes (Cakar, et al., 2012). Iron-resistant (Balaban et al., 2020), caffeine-resistant (Surmeli et al., 2019), coniferyl aldehyde-resistant (Hacısalihoğlu et al., 2019), ethanol-resistant (Turanli-Yildiz et al., 2017), nickel-resistant (Kucukgoze et al. 2013), cobalt-resistant (Cakar et al., 2009; Alkim et al., 2013), and multi-stress resistant (Cakar et al., 2005) strains of *S. cerevisiae* have been previously obtained by applying evolutionary engineering. In addition to these stress-resistant mutants, an evolved *S.cerevisiae* strain that has an increased chronological life span has also been obtained by using evolutionary engineering strategy (Arslan et al., 2018). In order to

identify the complicated molecular mechanisms these stress-resistant evolved strains, transcriptomic, physiological, and/or genomic analyses have also been performed in those studies.

1.9 The Aim of the Study

Despite the common use of silver in various applications and the limited information about copper-related genes and tolerance pathways in *S. cerevisiae* that may also be involved in silver tolerance, the molecular basis of silver resistance in yeast has not been clarified yet. There are no reports on transcriptomic and genomic analyses of silver-resistant *S. cerevisiae*. Additionally, there are no previous studies which employed evolutionary engineering strategy to obtain highly silver stress-resistant *S. cerevisiae*.

In this study, the aim was to obtain a *S. cerevisiae* strain which is resistant against silver stress by using evolutionary engineering and to investigate the molecular mechanisms of the silver resistance of the evolved strain by using genomic, transcriptomic, and physiological analyses.

2. MATERIALS AND METHODS

2.1 Materials

The materials used in this study consist of the yeast strain, media, chemicals, buffers, solutions, enzymes, kits, equipments, and websites. All materials, except for the strain, are listed in tables.

2.1.1 Strain

The prototrophic *Saccharomyces cerevisiae* strain CEN.PK 113-7D (*MATa*, *MAL2-8*^{c}, *SUC2*) (van Dijken et al., 2000) was used as the reference strain (also called as 905) in this study. The reference strain is provided by Prof. Dr. Jean Marie François and Dr. Laurent Benbadis (University of Toulouse, France).

One mL of exponentially growing cells were rotated at 10,000 xg for 5 min in a 1.5 mL microfuge tube in order to prepare stock cultures. 30% (v/v) glycerol was used for resuspension of the pellet. The stock cultures were stored at -80^{o}C.

2.1.2 Media

Yeast minimal medium (YMM) containing 2% (w/v) glucose and 6.7 g/L yeast nitrogen base without amino acids (Difco) was used for cultivations (Burke et al., 2000). For solid media, 2% (w/v) agar was added to YMM (Table 2.1).

Table 2.1 : Contents of YMM.

Content	YMM Percentage (w/v)
Yeast nitrogen based without amino acids	0.67
Glucose	2.00
Agar for solid media	2.00
Distilled water	1 L

Yeast extract-peptone-dextrose medium (YPD) containing 1% (w/v) yeast extract, 2% (w/v) peptone and 2% (w/v) glucose was used for growth of the yeast cells (Sherman et al., 1979). For solid media, 2% (w/v) agar was added to YPD (Table 2.2).

Table 2.2 : Contents of YPD.

Content	YPD Percentage (w/v)
Yeast extract	1.00
Peptone	2.00
Glucose	2.00
Agar for solid media	2.00
Distilled water	1 L

2.1.3 Chemicals

The chemicals used in this study are listed in Table 2.3.

Table 2.3 : Chemicals used in the study.

Chemical	Company	Country
5-fluoro-orotic acid	Euromedex	France
Acetic acid glacial	MERCK	Germany
Aluminum chloride hexahydrate $AlCl_3 6H_2O$	MERCK	Germany
Ammonium iron(II) sulfate hexahydrate $(NH_4)_2Fe(SO_4)_2 6H_2O$	MERCK	Germany
Ethylenediaminetetraacetic acid disodium salt dehydrate EDTA	MERCK	Germany
Glucose	VWR BDH PROLABO	UK
Cobalt chloride $CoCl_2$	Fluka	USA
Cyanine 3	Amersham Bioscience	Sweden
DNA markers	Fermentas	Lithuania
IPTG dioxane-free	Fermentas	Lithuania
X-gal	Fermentas	Lithuania
Ethanol	J.T.Baker	Netherlands
Glucose standard solution	Sigma	USA
Manganese(II) sulphate monohydrate $MnSO_4H_2O$	Sigma	USA
o-Dianisidine dihydrochloride	Sigma	USA
PEG-400	Sigma	USA
Hydrogen peroxide	MERCK	Germany
Magnesium chloride hexahydrate $MgCl_2 6H_2O$	MERCK	Germany
Nickel(II) chloride hexahydrate $NiCl_2 6H_2O$	MERCK	Germany
Potassium acetate	MERCK	Germany
Silver nitrate $AgNO_3$	MERCK	Germany
Sorbitol	MERCK	Germany
Tris HCl	MERCK	Germany
Tryptone	MERCK	Germany
Yeast Extract	MERCK	Germany
Ampicillin	Roche	Switzerland
Agarose	Applichem	Germany
Ammonium sulphate	VWR BDH PROLABO	UK

Table 2.3 (continued) : Chemicals used in the study.

Chemical	Company	Country
Trehalase	Sigma	USA
NaCl	Carlo Erba	Italy
Glucose oxidase/peroxidase reagent	Sigma ALDRICH	USA
Lithium acetate	Sigma ALDRICH	USA
NaOH	Carlo Erba	Italy
Nouseothricine (ClonNAT)	Werner Bioagents	Germany
Mercaptoethanol	MERCK	Germany
Amyloglycosidase (3500 U)	Roche	Switzerland
G-418 (Geneticine) solution	Roche	Switzerland
RNase A	Roche	Switzerland
β-Glucuronidase/Arylsulfatase	Roche	Switzerland
Bacto peptone	BD DifcoTM	USA
Yeast nitrogen base without amino acid and ammonium sulphate salt	BD DifcoTM	USA
Calcium chloride hexahydrate $CaCl_26H_2O$	Sigma ALDRICH	USA
Lithium chloride anhydrous LiCl2	Sigma ALDRICH	USA
Potassium acetate	Sigma ALDRICH	USA
SDS	Sigma ALDRICH	USA
Zinc sulphate heptahydrate ZnSO47H2O	Sigma ALDRICH	USA
Copper(II) sulphate pentahydrate $CuSO_45H_2O$	Sigma ALDRICH	USA
DAPI 4',6-diamidino-2-phenylindole	Sigma ALDRICH	USA
Glycerol	Sigma ALDRICH	USA

2.1.4 Buffers and solutions

The buffer and solution names and their content are listed in Table 2.4.

Table 2.4 : Buffers and solutions used in the study.

Solution/Buffer	Content
Potassium phosphate buffer	50 mM and pH 7
Sodium thiosulphate	10% (w/v)
Glycerol	30% (v/v)
Solution I	50 mM Tris HCl pH 8, 10 mM EDTA, 100 mg/L RNase A
Solution II	200 mM NaOH and 1% SDS
Solution III	Potassium acetate and acetic acid glacial

2.1.5 Kits and enzymes

The kits and enzymes used in this study are listed in Table 2.5.

Table 2.5 : Kits and enzymes used in the study.

Kit/Enzyme	Company	Country
DNase	Qiagen	Germany

Table 2.5 (continued) : Kits and enzymes used in the study.

Kit/Enzyme	Company	Country
RNeasy Mini Kit	Qiagen	Germany
RNA Spike-In Kit One-color	Agilent	USA
Absolutely RNA Nanoprep Kit	Agilent	USA
Gene expression Hybridization Kit	Agilent	USA
Gene Expression Wash Buffers	Agilent	USA
Hybridization Chamber gasket slides (8 microarrays/slide)	Agilent	USA
Low Input Quick Amp Labeling Kit	Agilent	USA
RNA 6000 Nano LabChip Kit	Agilent	USA
Agilent RNA 6000 Nano Kit	Agilent	USA
Lyticase	Sigma	USA

2.1.6 Equipment

The equipment used in this study are listed in Table 2.6.

Table 2.6 : Equipment used in the study.

Equipment	Company	Country
Hybridization Chamber	Agilent	USA
Hybridization oven rotator for Agilent Microarray Hybridization Chambers	Agilent	USA
Hybridization oven	Agilent	USA
Bioanalyzer 2100	Agilent	USA
Microarray Scanner	Agilent	USA
Glass slides for microarray analysis	Agilent	USA
Refrigerator (+4ºC, -20ºC) 3011 NY	Arçelik	Turkey
Benchtop Centrifuge Allegra 25R	Beckman Coulter	USA
Ultracentrifuge Avanti J-30I	Beckman Coulter	Germany
Microwave oven	Beko	Turkey
Gel illustration system	Biolab	Turkey
Laminar Flow Hood Faster BH-EN 2003	Biolab	Italy
Electrophoresis system	BioRad	USA
Aminex©HPX-87H column	BioRad	USA
Microplate Reader 3550 UV	BioRad	USA
Orbital Shaker Incubator Certomat S II	Sartorius AG	Germany
Thermomixers	Eppendorf	Germany
Micropipettes	Eppendorf	Germany
Centrifuge 5424	Eppendorf	Germany
pH-meter MP220	Mettler Toledo	Germany
REAX top Vortex mixer	Heidolph	Germany
Water Bath SW22	Julabo	Germany
Magnetic Stirrer	Labworld	Germany
Incubator EN400 - EN500	Nüve	Turkey
Light Microscope CH30	Olympus	USA

Table 2.6 (continued) : Equipment used in the study.

Equipment	Company	Country
Balance BJ 610 C - 620 SCS	Precisa	Switzerland
Vortex mixer for chip MS2-S8/MS2-S9	IKA	China
Spectrophotometer UV-1700	Shimadzu	Japan
Thermal Cycler TC-412	Techne	USA
NanoDrop 2000Spectrophotometer	Thermo Fisher Scientific	USA
High Pressure Liquid Chromatography	Shimadzu	Japan
UHQ Ultrapure Water System	USF-Elga	USA
Deep Freezer (-80ºC) Ultra Low MDT- U40865	Sanyo	Japan
Rotor JA-30.50i	Beckman Coulter	USA
280FS AA	Varian	USA
Autoclave GR110DF	Zealway	USA
Autoclave 2540mL - 2870ELVC	Tuttnauer Systec	Switzerland
Autoclave SX 700E	Tomy	China

2.1.7 Websites and software

The websites and software used in this study are listed in Table 2.7.

Table 2.7 : Website and software used in the study.

Website/Software Name	Website/Company
2100 Expert software	Agilent Tech.
GeneSpring	GeneSpring 12.6 version, Agilent Tech.
Primer-3-Plus	http://www.bioinformatics.nl/cgi-bin/primer3plus/primer3plus.cgi
Saccharomyces genome database (SGD)	http://www.yeastgenome.org/
SGD, GO Slim Mapper	http://www.yeastgenome.org/cgi-bin/GO/goSlimMapper.pl
YEASTRACT	http://www.yeastract.com

2.1.8 Cultivation of yeast

Yeast strains were cultivated at 150 rpm and 30°C in YMM or YPD (medium rich in nutrient). Yeast strains' stock cultures were kept in a -80°C deep freezer in 1.5 mL microcentrifuge tubes containing 30% (v/v) glycerol. After inoculation of the frozen stock cultures in 50 mL culture tubes in 10 mL of YPD medium, they were incubated overnight on a rotary shaker of 150 rpm at 30ºC. The overnight cultures grown in YPD medium were used to prepare precultures of yeast strains, unless otherwise stated. The cultures grown overnight in YPD were washed with 2% YMM twice and then incubated approximately for 16 hours at 150 rpm and 30ºC.

2.2 Methods

2.2.1 Growth analysis tests

Growth analysis consists of spectrophotometric measurements, determination of specific growth rate, colony-forming units (CFU) numbers, and cell dry weight of the cultures.

2.2.1.1 Spectrophotometry

Shimadzu UV-1700 spectrophotometer was used to measure the optical density at 600 nm (OD_{600}) in order to monitor growth of the cultures. The yeast cultures grown under different stress conditions were compared with the non-stressed (control) ones by dividing their OD_{600} values to those of the control cultures that indicated growth fitness or survival rate.

2.2.1.2 Colony-forming units (cfu) determination

To monitor the growth of the cultures, the colonies on the agar plates were counted manually by using a pen, as described previously (Goldman and Green, 2008).

2.2.1.3 Specific growth rate determination

A growth physiological experiment was applied in order to determine the growth behavior of the cultures. It involves the determination of OD_{600} values of the overnight cultures in YPD, twice-wash of the cells with sterile distilled water, and inoculation to an initial OD_{600} of 0.2 into 20 mL fresh 2% YMM (in 100 mL flasks). The cultures were incubated approximately for 16 hours at 150 rpm and 30ºC. Pre-cultivation of the cells was performed in 0.5% YMM for growth in silver-containing medium. Precultures were inoculated to an initial OD_{600} of 0.2 in 1l flasks inoculated into fresh 200 mL 2% YMM. Cultures were incubated at 150 rpm and 30ºC. During incubation, withdrawal of samples from the culture was performed at specific time intervals. The OD_{600} values of the cultures were measured. For statistical purposes, the experiment was performed in triplicate, where arithmetic averages and standard deviations were also calculated.

Logarithmic values of the OD_{600} ($LnOD_{600}$) were also calculated, to plot growth curves and calculate the generation time and the specific growth rate (μ), using the natural logarithmic values, as shown in the Equations 2.1 and 2.2, respectively.

$$\text{Generation time (h)} = \frac{Ln2}{\mu} \quad (2.1)$$

$$\text{Specific growth rate } (h^{-1}) = \frac{\Delta \ln OD600}{\Delta t} \quad (2.2)$$

2.2.1.4 Cell dry weight determination

In order to measure the biomass production of the evolved strain and the reference strain, cell dry weight (CDW) analysis was performed. Microcentrifuge tubes of 2 mL were dried in an oven for 48 h at 80ºC. The tubes were kept in a desiccator for 3 h. To specify initial weight, they were weighted. Two mL samples were withdrawn from cultures at specific time intervals during the growth, and put into the preweighed microcentrifuge tubes. Centrifugation was applied for 5 min at 14,000 xg. After the removal of the supernatant, cell pellets in the tubes were placed in the oven at 80ºC for 48 h. Right after the desiccation for 3 h in the desiccator, the tubes were weighed for final weight. The difference between the final weight and the inital weight indicated the biomass. CDW analysis was conducted in triplicate.

2.2.2 Stress resistance determination

Most Probable Number (MPN) assay, spot assay and replica plating were performed for the determination of stress resistance of yeast cells. Stress resistance was determined by comparison of the survival of the yeast strains in the media containing different stress factors and stress levels.

2.2.2.1 Most Probable Number (MPN) assay

Most probable number assay was used to estimate resistance of a cell to different stress types (Russek and Colwell, 1983). Serial dilutions in 96-well plates covering 180 µL YMM allowed the determination of viable cell numbers. Five parallel samples in the range between 10^{-1} and 10^{-8} were diluted in order to estimate the most probable number of survivors according to the ability of growth of the yeast cells at higher dilutions.

Cells were grown in 200 µM $AgNO_3$ containing YMM for 72 h. MPN table was used to determine the viable cell numbers. Survival rate, the resistance to stress conditions, was calculated as the ratio of stress-treated viable cell number and non-treated viable cell number (Cakar et al., 2009).

2.2.2.2 Spot assay

In order to determine yeast strains' sensitivity and resistance against various stress factors, spot assay was applied as described previously (Memarian et al., 2007). Cells were cultivated in 10 mL liquid YMM in 50 mL culture tubes. After they reached logarithmic growth phase at 150 rpm and 30°C, yeast cells were divided into equal numbers and centrifuged for 5 min at 10,000 xg. The pellets were resuspended in 100 µL water, as soon as the supernatant was withdrawn. They were diluted in 96-well plates serially at 10^{-1}, 10^{-2}, 10^{-3}, and 10^{-4} dilution rates. The diluted suspensions of 2 µL were spread onto solid plates with and without stress factor in the media. All of them were incubated at 30°C.

2.2.2.3 Replica plating

Replica plating method was applied to reveal and compare various phenotypes of yeast cells, as described previously (Lederberg and Lederberg, 1952). Firstly, yeast cultures to be compared were grown in solid YPD medium in petri dishes, called as master plate. The master plate was then used to inoculate the control plate and the plates containing different stress factors in either YPD or the minimal medium YMM. The plates were incubated for 1-2 days at 30°C to produce colonies.

2.2.3 Obtaining silver-resistant *Saccharomyces cerevisiae* by evolutionary engineering

Evolutionary engineering strategy was performed in this study as an inverse metabolic engineering approach in order to obtain silver-resistant *Saccharomyces cerevisiae* mutant. After mutagenization of *S.cerevisiae* with ethyl methane sulfonate (EMS), initial silver stress level was determined. A culture surviving under conditions with high silver concentrations was obtained by gradually increasing silver stress level in the media. Finally, silver-resistant individual mutants were selected from the final population.

2.2.3.1 EMS mutagenesis of *Saccharomyces cerevisiae*

The reference strain (905) was subjected to chemical mutagenesis (EMS), as described previously (Lawrence, 2002). Approximately 10% of the initial culture survived after the EMS mutagenesis, thus a starting population containing genetically diverse individuals was obtained. Evolutionary engineering batch selection experiments were

applied to a chemically mutagenized culture (called 906) containing genetically diverse individuals, as described previously (Turanli-Yildiz et al., 2017; Çakar et al., 2009; Küçükgöze et al., 2013). In this thesis study, silver-resistant *S. cerevisiae* mutant was selected by increasing silver concentration gradually in the environment as the stress factor.

2.2.3.2 Initial silver stress level determination for selection experiments

The growth of *S.cerevisiae* in 2% YMM was compared with the growth in media containing 0.125 mM, 0.25 mM, 0.5 mM, 1 mM, 2 mM, 5 mM, and 10 mM $AgNO_3$ in order to determine the initial stress level for the evolutionary selection experiments. The growth was detected by spectrophotometric analyses at 600 nm wavelength and also colony-forming units (CFU). The cultures of both 905 and 906 were grown in 2% YMM overnight and then inoculated in 50 mL-test tubes into 10 mL fresh 2% YMM for control and 10 mL of seven media at different $AgNO_3$ concentrations indicated above to an initial OD_{600} of 0.35. They were incubated at 150 rpm and 30ºC. The growth of 905 and 906 in all media types were determined at the 24^{th} h of incubation using a spectrophotometer. For the determeination of colony-forming units, it was determined between 24^{th} and 72^{nd} h of incubation. The growth ratio was calculated by dividing OD_{600} of the silver-stress culture to that of the control culture as shown in Equation 2.3 and by dividing cell number of the silver-stress culture to that of the control culture as shown in Equation 2.4.

$$Growth\ ratio = \frac{OD_{600}\ value\ of\ the\ silver\ stress\ group}{OD_{600}\ value\ of\ the\ control\ group} \tag{2.3}$$

$$Growth\ ratio = \frac{Cell\ number\ of\ the\ silver\ stress\ group}{Cell\ number\ of\ the\ control\ group} \tag{2.4}$$

2.2.3.3 Obtaining silver-resistant mutant generations

In order to select a silver-resistant mutant generation, the EMS-mutagenized culture (906) was cultivated in successive batch cultures where the silver stress level was increased gradually. The initial silver concentration of the medium was 5 µM $AgNO_3$ and it was increased gradually until it reached 250 µM $AgNO_3$ at the final passage.

EMS-mutagenized culture (906) grown in 2% YMM overnight was inoculated in two different 100 mL flasks to an initial OD_{600} of 0.35: one of the flasks contained 20 mL

2% YMM without silver (control) and the other contained 20 mL 2% YMM with a silver concentration of 5 µM $AgNO_3$. They were incubated for 24 h at 150 rpm and 30ºC. The growth ratio of the cultures were calculated by using both the Equations (2.3) and (2.4) where OD_{600} values of the cultures were detected by a spectrophotometer. The initial culture grown for 24 h in the presence of 5 µM $AgNO_3$ was named as the first population of the study. After the first population was centrifuged for 3 min at 10,000xg, it was washed twice with sterile distilled water. It was inoculated into fresh YMM and YMM with 10 µM $AgNO_3$ (in two separate culture tubes) and grown for 24 h (called as the second population). CFU and OD_{600} values of the second population were measured. The aliquot of 1 mL population was washed twice with sterile distilled water and stored at -80°C in 30% (v/v) glycerol for every passage. Cultivations were repeated until the 29th population by gradually increasing the silver concentration at each successive population up to 250 µM $AgNO_3$ at the final (29th) population.

2.2.3.4 Individual mutants selection from the last population

In order to obtain colonies from the final (29th) population of the mutant culture, it was spread onto solid YMM plates containing 200 µM $AgNO_3$ and incubated for 72 h and 30ºC where 10 colonies were randomly selected after 72 hours according to their approximate colony volume. Ten individual mutants (Table 2.8), final population and the reference strain were subjected to silver resistance test on YMM plates containing 200 µM $AgNO_3$.

Table 2.8 : Individual mutants chosen from the 29th population.

Mutant Name	
1E	6E
2E	7E
3E	8E
4E	9E
5E	10E

2.2.4 Determination of cross-resistance against other stress types

Spot assay method was used to estimate stress cross-resistance. The strain precultures were inoculated for 18-20 h at 150 rpm and 30ºC after they were cultivated in 50-mL test tubes containing 10 mL liquid YMM. The overnight precultures were incubated at 150 rpm and 30 ºC and they were transferred into 50 mL culture tubes containing 10

mL fresh YMM to an initial OD_{600} of 0.2 (approximately 2.8 x 10^6 cells/mL). Spectrophotometrical (Shimadzu UV-1700, Japan) values at 600 nm were measured for growth. When reached mid-exponential phase where the OD_{600} values were about 2 (approximately 2.8 x 10^7 cells/mL), supernatants that occured at the end of the centrifugation for 5 min at 10,000 xg were discarded, and 2 mL cells were collected. In order to obtain 4 OD_{600} units/cells in 1 mL, the cells were resuspended in 1 mL sterile distilled water after they were washed with sterile distilled water. They were diluted for ten-fold (from 10^{-1} to 10^{-4}) by using sterile distilled water. Finally, 5 µL 10-fold diluted cells were spotted onto plates that were containing YMM with standard contents, 0 - 500 µM $AgNO_3$, and also various stress factors (25 and 50 mM $(NH_4)_2Fe(SO_4)_2$, 10 mM $ZnCl_2$, 10 mM $LiCl_2$, 0.25 mM $NiCl_2$, 8% (v/v) ethanol, 7.5 mM $AlCl_3$, 2 mM $CrCl_3$, 20 mM $MnCl_2$, 3 mM $CoCl_2$, 1 mM H_2O_2, and 0.3 mM $CuSO_4$,) shown in Table 2.9. All plates were incubated for 72 h at 30 ºC.

Table 2.9 : Stress factors and their concentrations for stress cross-resistance tests.

Stress Factor	mM or %
$CuSO_4$	0.3
H_2O_2	1
$CoCl_2$	3
$CrCl_3$	2
$AlCl_3$	7.5
Ethanol	8% (v/v)
$MnCl_2$	20
$NiCl_2$	0.25
$LiCl_2$	10
$ZnCl_2$	10
$(NH_4)_2Fe(SO_4)_2$	25
$(NH_4)_2Fe(SO_4)_2$	50

2.2.5 Genetic stability analysis of individual mutants

In order to test the genetic stability of the mutants, firstly, the mutant strains stored as frozen stocks at -80ºC were inoculated to solid YPD medium before incubation at 30ºC for 2 days. The culture on the YPD agar plate was innoculated in 50 ml culture tube containing 10 mL YMM and then transferred to 50 ml culture tube to an initial OD_{600} of 0.35 with 10 ml fresh YMM. The first passage was produced by incubation of the culture for 24 h at 150 rpm and 30ºC. Five successive passages were obtained by repeating the same steps with the culture obtained at the end of every process. All of the five stock cultures in addition to the reference strain were grown in liquid YMM

and inoculated on agar plates with silver and without silver (control). Thus, all 5 passages were tested for their silver resistance levels by using MPN method.

2.2.6 Growth analysis of the mutant and the reference strain

Precultures of the reference strain and the mutant strain were grown until they reached early stationary phase on a rotary shaker at 30°C. They were cultured in 20 mL YMM at 150 rpm and 30ºC in 100-mL Erlenmeyer flasks. They were then inoculated into two separate 500 mL flasks containing fresh YMM of 100 mL, with and without 220 µM $AgNO_3$, and incubated at 150 rpm and 30ºC. Cell growth was measured as CFU and also by spectrophotometry.

2.2.7 Physiological characterization of the mutant and the reference strain

Reference strain and the mutant precultures were prepared in 250-mL flasks at 30°C and 150 rpm. They were inoculated upon 12 h of incubation into 400-mL YMM and YMM containing 200 µM $AgNO_3$ in 2-L flasks by setting the initial OD_{600} as 0.35. OD_{600} values were monitored throughout 12 h by 1.5 h time intervals and the final OD_{600} was measured at 24 h of incubation.

2.2.8 Further analysis for growth

Further analyses were required for detailed investigation of growth parameters of the reference strain and the silver-resistant mutant. Glucose consumption, ethanol, acetate, and glycerol production, trehalose and glycogen contents were measured.

2.2.8.1 Glucose consumption and ethanol, acetate, glycerol production

The silver-resistant strain's and the reference strain's overnight precultures were incubated in 250-ml flasks at 30 °C and 150 rpm for 12 h in 50 ml YMM. Precultures were inoculated in 2-liter flasks at 30 °C and 150 rpm to an initial OD_{600} of 0.35 (approximately 4.9 x 10^6 cells/ml) into fresh 400 ml YMM and 400 ml YMM containing 200 µM $AgNO_3$. The growth of the cultures were measured as OD_{600} values. Concentrations of the residual glucose, glycerol, acetate, and ethanol of the cultures were measured by using HPLC, as described previously (Küçükgöze et al., 2013).

Solution I and Solution II, given in Table 2.10, were used to prepare standard solutions for HPLC, as shown in Table 2.11. Tha standard solutions enabled to measure the

standard concentrations of metabolites in HPLC, as indicated in Table 1.12. The unknown concentrations of the unknown metobolites in the culture were calculated by using these standard concentrations of metabolites in HPLC. The experiment was performed in triplicate, and the standard deviations and average values were calculated.

Table 2.10 : Contents of Solution I and Solution II.

Solution I	
Glucose	120 g
Final volume by adding dH_2O	1000 mL
Solution II	
Ethanol	30 g
Glycerol	2 g
Acetate	4 g
Final volume by adding dH_2O	1000 mL

Table 2.11 : Standard solutions of HPLC standards.

Standard solution (Std)	Mixing Volumes	Eluent Volume	Final Volume
Standard 1	1 ml Solution I 3 ml Solution II	2 mL Eluent	6 mL
Standard 2	0.75 mL Std1	0.25 mL Eluent	1 mL
Standard 3	0.50 mL Std1	0.50 mL Eluent	1 mL
Standard 4	0.25 mL Std1	0.75 mL Eluent	1 mL
Standard 5	0.125 mL Std1	0.875 mL Eluent	1 mL
Standard 6	0.063 mL Std1	0.937 mL Eluent	1 mL
Standard 7	0.010 mL Std1	0.990 mL Eluent	1 mL

Table 2.12 : Retention time (given in ± 0.2 min range) and concentrations of metabolites in HPLC standards.

Metabolite(g/L)	Glucose	Ethanol	Glycerol	Acetate
Standard 1	20	15	1	2
Standard 2	15	11.25	0.75	1.5
Standard 3	10	7.5	0.5	1
Standard 4	5	3.75	0.25	0.5
Standard 5	2.5	1.875	0.125	0.25
Standard 6	1.125	0.937	0.0625	0.125
Standard 7	0.2	0.15	0.01	0.02
Retention Time (min)	8.43	19.95	12.5	13.81

2.2.8.2 Trehalose content

The measurement of the trehalose content in cells was performed as described previously (Parrou and François, 1997). First, cell pellet was collected from the culture of an OD_{600} value of 25. After the pellet was suspended in screw-top microfuge tubes (Corning, USA) containing 250 µL of 0.25 M Na_2CO_3, it was kept for 4 h at 95^{o}C.

Before 600 µL of 0.2 M $C_2H_3NaO_2$ buffer at pH 5.2 was mixed inside, 150 µL of 1 M CH_3COOH added into the suspension. Final solution was incubated with trehalase (Sigma) at 37ºC overnight. The glucose oxidase/peroxidase method was used for glucose determination, as described previously (Cramp, 1967).

2.2.9 Microarray analysis

Whole genome transcriptomic analysis was performed in order to obtain detailed information about silver resistance of the mutant. Agilent DNA Microarray System was used to analyze and compare the whole genome transcriptome of the mutant and the reference strain. Extraction of total RNA, extracted total RNA samples quality analysis, synthesis of cDNA, cRNA labeling, hybridization on microarray chips, and analysis of data were the steps of DNA microarray analysis.

2.2.9.1 Extraction of total RNA

RNeasy Mini Kit (Qiagen) was used for total RNA extraction. In brief, after being grown in 50 ml culture tubes containing 10 ml 2% YMM for about 16 h at 150 rpm and 30ºC, reference strain and the silver-resistant mutant cultures were inoculated to an initial OD_{600} of 0.1 in 20 ml fresh YMM and incubated at 150 rpm and 30°C. Total RNA isolation was performed in accordance with manufacturer's procedure (RNeasy Mini Kit, Qiagen) after the growth of the cultures were at the mid-exponential phase where OD_{600} values reached 1 (≈ $2x10^7$cells/ml). Table 2.13 shows the buffers of the RNA extraction kit and their contents.

Table 2.13 : Buffers of Qiagen RNA Extraction Kit and their contents.

Buffer	Content
Y1 Buffer	0.1 M EDTA and 1 M sorbitol were prepared and adjusted to pH 7.4. Just before use, lyticase and 0.1% β-mercaptoethanol were added.
RW1	Not indicated.
RPE Buffer	Before use, four volumes of ethanol were added to RPE buffer.
RLT Buffer	10 µl β-mercaptoethanol per 1 mL RLT.

After the harvest of the culture of ≈ $2x10^7$cells per mL by centrifugation at room temperature for 3 min at 10,000 xg, supernatants were discarded and pellets were washed twice with sterile distilled water. Cell wall of yeast cells was disrupted by enzymatic lysis procedure. First, 0.1% β-mercaptoethanol and lyticase (50 U final concentration) were added into 1.5 mL Y1 solution and cells were transferred into this freshly prepared solution. Gentle shaking was performed during incubation of cells for

30 min at 30°C. After the centrifugation of spheroplasts for 5 min at 300 xg, supernatants were discarded. After adding 350 µL Buffer RLT with 1% β-mercaptoethanol, spheroplasts were lysed by vortexing vigorously. The lysate was mixed by using pipette after 350 µL 70% (v/v) ethanol was added. The mixture, transferred to RNeasy spin columns in 2 mL collection tube, was centrifuged for 15 sec at 8,000 xg. After the addition of 700 µL Buffer RW1 to spin columns, the mixture was centrifuged for 15 sec at 8,000 xg. Before centrifugation for 15 sec at 8,000 xg, 500 µL Buffer RPE was added to spin columns. Before centrifugation for 2 min at 8,000 xg to the re-wash spin column, 500 µL Buffer RPE was added to the spin columns. The spin columns were installed in new collection tubes of 2 mL and centrifuged for 1 min at 16,000 xg. Final step was placing spin columns in a new 1.5 mL RNase-free microfuge tube. RNase-free water of 40 µL was added onto spin columns and centrifuged for 1 min at 8,000 xg in order to elute RNAs from spin columns. Total RNAs purified at the end of this procedure were kept at -80°C.

2.2.9.2 Purified total RNA quality analysis

A UV-Vis spectrophotometer (NanoDrop 2000, Thermo Scientific) was used to determine purified total RNA concentrations. For quality analysis, RNA concentrations of >150 ng/µL were required. The RNA 6000 Nano Assay Kit (Cat: 5067-1511, Agilent, USA) and Agilent 2100 Bioanalyzer instruments were used to determine RNA integrity numbers (RIN) of RNA samples. Analysis of RNA samples' electropherograms and determination of RIN values were performed by the manufacturer's instructions. For DNA microarray analysis, samples with RIN values of > 9 were selected.

2.2.9.3 Synthesis of cDNA and labeling of cRNA

RNase-free water was used for dilution of RNA samples with sufficient quality to 133 ng/µL. An amount of 1.5 µL of this diluted RNA (total 200 ng) was used for microarray analysis of DNA. Spike RNA (Agilent One-color RNA Spike-in Kit) was used as the control unit. For 200 ng total RNA, dilution rates of Spike RNA were 1:10, 1:20, and 1:25 (totally 1:5000). Two µL from the last dilution was added to samples of RNA. Afterwards, 1.8 µL of T7 primer mix, as shown in Table 2.14, was added to each tube with 3.5 µL of total RNA and diluted RNA spike-in controls.

Table 2.14 : Composition of T7 primer mix.

Content	Volume (µL) per reaction
Nuclease-free Water	1
T7 Primer	0.8

In order to denature RNA, the tubes were incubated for 10 min at 65ºC before they were cooled down for 5 min to 4ºC. Each tube was added 4.7 µL cDNA master mix, content of which is shown in Table 2.15. The tubes were incubated firstly for 2 h at 40ºC and secondly for 15 min at 70ºC. Finally they were cooled down and kept at 4ºC for denaturation.

Table 2.15 : Composition of cDNA mster mix.

Content	Volume (µL) per reaction
Affinity Script RNase Block Mix	1.2
10 mM dNTP Mix	0.5
5× First Strand Buffer	2
0.1 M Dithiothreitol (DTT)	1

cDNA was synthesized before cRNA was labelled with Transcription Master Mix. The composition of Transcription Master Mix is shown in Table 2.16. Addition of the T7 RNA Polymerase Blend enzyme was just before the use of the mix. Six µL of the Transcription Master Mix was put into each sample tube. Labeling (Cy3) and synthesis of cRNA were performed by incubation of the tubes for 2 h at 40ºC.

Table 2.16 : Transcription Master Mix composition.

Content	Volume (µL) per reaction
5× Transcription Buffer	3.2
NTP Mix	1
Nuclease-free water	0.75
0.1 M DTT	0.6
Cyanine 3-CTP	0.24
T7 RNA Polymerase Blend	0.21
Total volume	6

Absolutely RNA Nanoprep Kit was used to purify Cy3-labeled cRNA in accordance with manufacturer's instructions. Spectrophotometric measurements were used to determine the concentrations of Cyanine dye and Purifed Cy3-labeled cRNA. Finally, samples' specific activities were detected.

2.2.9.4 Microarray hibridization

In order to hybridize Cy3-labeled cRNA to the microarrays, after dilution of purified Cy3-labeled cRNA to 100 ng per µL with RNase-DNase-free water, the Cy3-labeled cRNA was fragmented by fragmentation mix. The components of the fragmentation mix is shown in Table 2.17. The fragmentation mix was incubated for exactly 30 min at 60°C and then cooled immediately for 1 min on ice in order to fragment the Cy3-labeled cRNA.

Table 2.17 : Mix of fragmentation.

Content	Volume (µL) per sample
Nuclease-free water	13
Cy3-labeled cRNA (diluted 100 ng/ µl)	6
10x Gene expression blocking reagent	5
25x Fragmentation buffer	1

In order to stop the reaction of fragmentation, 25 µl of 2×Hi-RPM Hybridization Buffer was added into each tube after the process of fragmentation. As a result, hybridization mix of 50 µL was gained, as its content is shown in Table 2.18.

Table 2.18 : Hybridization mix.

Content	Volume (µL) per sample
2×Hi-RPM Hybridization Buffer	25
25x Fragmentation mix	25

Before the slides were chambered, hybridization mix of 40 µL was loaded on the microarray slides (Yeast Gene Expression Array V2). Installing the slide chambers into the hybridization oven was followed by hybridization for 17 h at 10 rpm and 65°C.

2.2.9.5 Transcript data analysis

Agilent C Scanners were used to scan the slides after the microarray slides were washed in accordance with the manufacturer's instructions. Agilent GeneSpring GX (Version 12.6) software was used to analyze the primary data. At least one of two conditions with acceptible value of 100% condition was used to filter probes after the application of Quantile Normalization on the signals. Cut-off value was 50% for CV (coefficient of variation) error filter that was used for filtering probes obtained. Moderated t-test with Bonferroni FEWR (Family Wise Error Rate) correction was used to determine statistical significance. The probes that had corrected-p value <0.05 were approved as they were expressed differentially. Filtration of the probe sets

according to fold-change values lower than 2-fold resulted in determination of 2-fold and higher up- or downregulated genes.

SGD Slim Mapper based on Gene Ontology (GO) annotations for yeast genes (URL-2) was used to analyze the biological processes of upregulated and downregulated genes obtained from microarray data. The transcription factors regulating the induced genes in the mutant were determined by using Yeastract database (Abdulrehman et al., 2011). Additionally, GO enrichment analysis (*enrichGO*) of the differentially expressed genes (DEGs) was performed by an R package, 'ClusterProfiler' (Yu, Wang, Han, He, 2012). GSE143335 is the accession number at GEO repository for accessing the complete microarray data (Terzioğlu, Arslan, Kısakesen, Çakar, 2020).

2.2.10 Atomic absorption spectrophotometry to determine silver content

Yeast precultures were inoculated in 1 L flasks containing 150 mL YMM to an initial OD_{600} value of 0.35 and incubated overnight at 150 rpm and 30°C. They were transferred into 50 ml-culture tubes containing 10 mL YMM without silver (as a control) and with 50µM $AgNO_3$, 100µM $AgNO_3$ and 250µM $AgNO_3$, respectively, when the OD_{600} value reached nearly 3. The experimental procedure was repeated three times for each condition. The cultures under stress and non-stress conditions were incubated for 24 h at 150 rpm and 30°C and centrifuged at 5310 rpm (Rotor, Beckman Coulter JA-30.50i, USA) for 15 min. The supernatants were removed. In order to separate cells and the metal residues, the pellets were washed two times with distilled water. Pellets were dried at 110°C for 2 hours. Cells' dry weights were measured as described previously (Küçükgöze et al., 2013). They were then hydrolyzed for 2 h at 90°C with 10 M HNO_3 solution. Silver contents were detected by Varian AA 280FS (USA) model atomic absorption spectrophotometer equipped with deuterium background correction and air-acetylene flame burner. Silver content was measured at a wavelength and slit width of 328.1 nm and 0.5 nm, respectively.

2.2.11 Whole genome re-sequencing

Both reference and the evolved strains were subjected to the whole genome re-sequencing as described previously (Hacısalihoğlu et al., 2019). Variant Effect Predictor v.90, with latest gene build *S. cerevisiae* CEN.PK113-7D, ASM26988v1 was used for annotation of unique mutations of the evolved strain. The whole genome re-

sequencing data are available in the NCBI Sequence Read Archive (SRA) under BioProject PRJNA598433.

2.2.12 Lyticase sensitivity assay

The adapted version of the lyticase sensitivity assay (Kuranda et al. 2006) was applied. In this study, it was carried out as three biological replicates, as described previously (Balaban et al. 2020). First, the reference and evolved strain cultures were grown under both control and 200 µM $AgNO_3$ stress conditions, and 2 U/mL lyticase (Sigma-Aldrich, St. Louis, MO, USA) and 40 mM 2-mercaptoethanol (Merck, Hohenbrunn, Germany) were used. Absorbance (OD_{600}) were measured for every 20 min in order to detect cell lysis and divided to the initial OD_{600} value and multiplied by 100 to plot % lyticase resistance versus time.

2.2.13 Statistical analysis

All experiments were repeated at least three times and $n \geq 3$ for each biological replicate. Standard deviation and arithmetic mean were used as tool for data evaluation. Statistical analysis was performed by using 'Stats' package of R software ("*R software*", 2017). Except for the microarray analysis, at a significance level of $p<0.05$, statistical significance was performed by Student's test (two-way, unpaired) ("*R software*", 2017).

3. RESULTS

In all parts of this study, the results were obtained by comparison of the reference strain and the mutant strain. Selecting the silver-resistant mutant by evolutionary engineering, screening resistance against some stress conditions in addition to silver stress by using spot assay and MPN assay constitute the first part. The second part consists of the measurement of silver content, detection of cell wall integrity, and physiological characterization through analysis of growth as well as metabolites. The third part covers monitoring of differential gene expression by microarray analysis. Whole genome re-sequencing is the last part of this thesis study.

3.1 Selection of Silver-Resistant Mutant and Determination of its Silver Resistance

In the first part of the study, silver-resistant mutant 2E was selected by evolutionary engineering and its resistance against some stress conditions in addition to silver stress was screened by using spot assay and MPN assay.

3.1.1 Survival rate determination under silver-stress conditions

The non-mutagenized reference strain and the EMS-mutagenized initial population (906) of the reference strain were subjected to various silver stress levels in order to determine the starting silver stress concentration to be applied in the evolutionary selection experiment. To calculate the survival rates under each stress level, CFU method was used to calculate the viable cell numbers in the cultures. The non-mutagenized reference strain and the EMS-mutagenized cultures showed no difference in their results (data not shown).

As the stress levels and the range between them decreased, EMS-mutagenized culture (906) showed a noticable survival. The results indicated that the survival rate of the EMS-mutagenized culture was nearly 98% at 5 µM $AgNO_3$, but at 0.06 mM $AgNO_3$ concentration, it decreased to about 50%. It was observed that the survival rate was reduced significantly at 0.125 mM $AgNO_3$ concentration and further at 0.25 mM

$AgNO_3$. There was almost no survival at 0.5 mM $AgNO_3$ concentration (Figure 3.1). Finally, there was no survival for EMS-mutagenized culture (906) under the stress levels of 1-10 mM $AgNO_3$ (Figure 3.2).

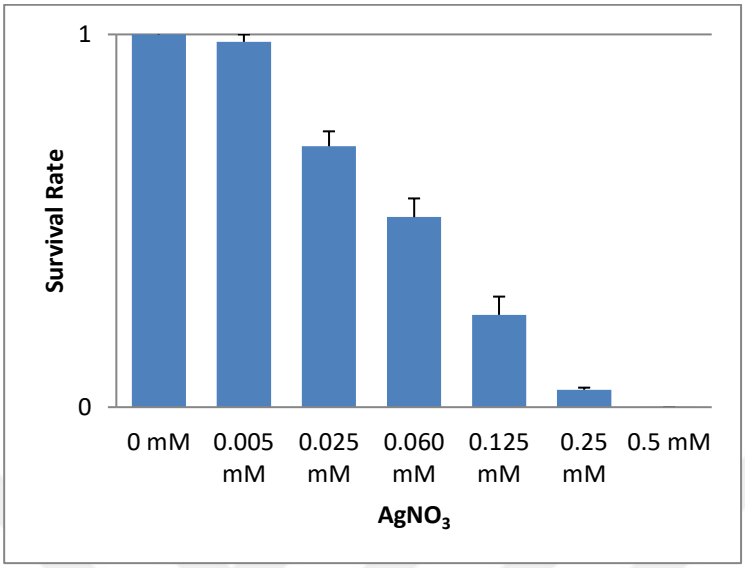

Figure 3.1 : Survival rate according to CFU values of the EMS-mutagenized initial *S. cerevisiae* culture under various silver stress levels ($AgNO_3$) for 24 h (Terzioglu et al., 2020).

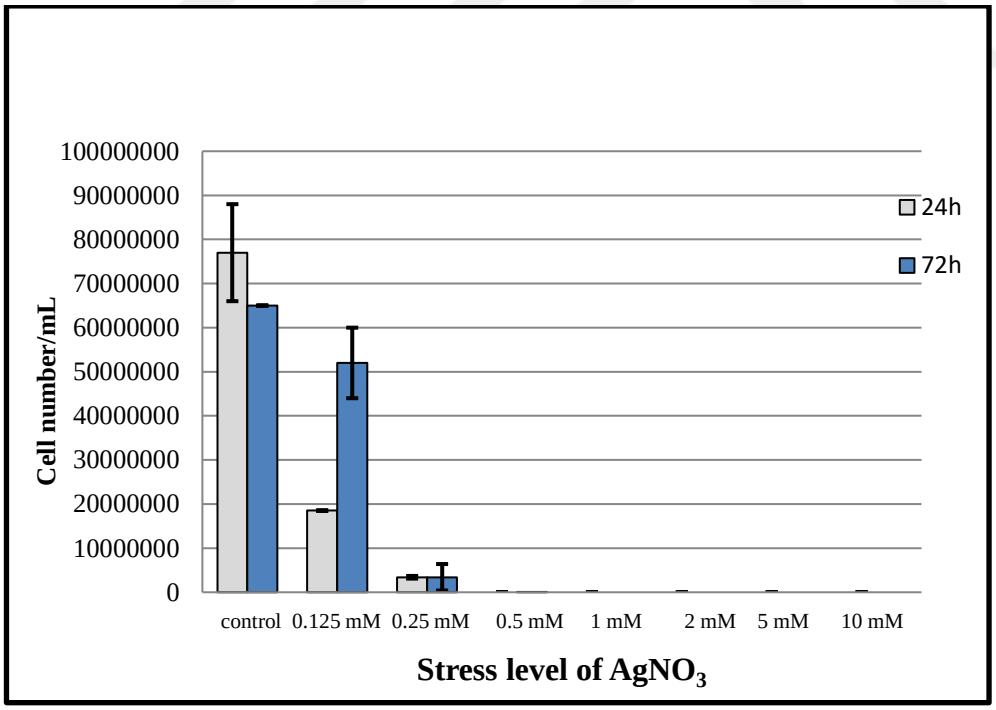

Figure 3.2 : CFU growth of 906 cells (24&72 h) upon various $AgNO_3$ stress levels.

Survival of 906 decreased in 72 h compared to 24 h in control condition, as expected. However, it showed a better or similar survival under silver stress conditions at 72 h which indicates that 906 cells adapted to the stress condition with time.

3.1.2 Increasing levels of silver for continuous selection strategy

According to data shown in Figure 3.1, 5 µM $AgNO_3$ was preferred as the initial silver stress concentration for silver-resistant population selection experiments. Because 5µM $AgNO_3$ inhibited growth slightly and let the cells have many generations or passages during selection. The silver concentration for each generation was increased gradually by 5µM or 10µM $AgNO_3$ and the culture was incubated for 24, 48, or 72 h, as shown in Table 3.1.

Table 3.1: Stress level and incubation time for every population of 905 and 906.

Population	Stress level ($AgNO_3$)	Incubation time (h)
1	5 µM	24
2	10 µM	24
3	15 µM	24
4	20 µM	24
5	25 µM	24
6	30 µM	24
7	35 µM	24
8	40 µM	48
9	50 µM	48
10	60 µM	48
11	70 µM	48
12	80 µM	48
13	90 µM	48
14	100 µM	48
15	110 µM	72
16	120 µM	48
17	130 µM	48
18	140 µM	48
19	150 µM	48
20	160 µM	48
21	170 µM	48
22	180 µM	48
23	190 µM	48
24	200 µM	48
25	210 µM	48
26	220 µM	48
27	230 µM	48
28	240 µM	48
29	250 µM	72

The evolutionary engineering strategy to obtain silver-resistant *S. cerevisiae* was carried out as the serial transfer of liquid batch cultures of the EMS-mutagenized (906) starting populations in control media (to compare and find survival rate) and in media containing gradually increasing $AgNO_3$ in each transfer. The determination of the

survival rates of each batch culture (each population) upon silver stress was done by viable cell counts on solid culture plates with and without $AgNO_3$. CFU values of each population with corresponding control culture were detected according to both control medium and medium with silver stress, and shown in Table 3.2 and Table 3.3, respectively.

Table 3.2: CFU of each population of non-treated EMS-mutagenized culture (906) populations (CFU_1, CFU_2, and CFU_3 correspond to three independent measurements of CFU).

Pop. Number	CFU/mL x 10^5 of Control Samples			Average	Standard Deviation
	1	2	3		
1st	840	870	1020	910	78
2nd	530	620	700	616	69
3rd	570	670	710	650	58
4th	940	1070	1190	1066	102
5th	730	930	980	880	108
6th	710	760	900	790	80
7th	640	670	770	693	55
8th	484	580	543	535	48
9th	230	270	290	263	24
10th	150	270	580	333	181
11th	150	230	240	206	40
12th	331	345	347	341	7
13th	320	400	430	383	46
14th	370	440	480	430	45
15th	170	210	270	216	41
16th	270	230	400	300	72
17th	290	330	460	360	72
18th	343	356	310	336	23
19th	332	341	299	324	22
20th	328	301	284	304	18
21st	328	334	344	335	6
22th	282	303	340	308	23
23th	460	480	656	532	88
24th	824	572	644	680	105

Table 3.2 (continued) : CFU of each population of non-treated EMS-mutagenised culture (906) populations (CFU_1, CFU_2, and CFU_3 correspond to three independent measurements of CFU).

Population Number	CFU/mL x 10^5 of Control Samples			Average	Standard Deviation
	1	2	3		
25th	788	804	836	809	19
26th	330	389	359	359	24
27th	419	411	522	450	50
28th	452	600	560	537	62
29th	347	353	365	355	7

Table 3.3: CFU of each population of stress-treated EMS-mutagenised culture (906) populations (CFU_1, CFU_2, and CFU_3 correspond to three independent measurements of CFU).

Population Number	Stress Level ($AgNO_3$)	CFU/mL x 10^5 of silver-treated samples			Average	Standard Deviation
		1	2	3		
1st	5 µM	830	1040	1180	1017	144
2nd	10 µM	780	950	1110	947	135
3rd	15 µM	460	540	620	540	65
4th	20 µM	840	940	970	917	56
5th	25 µM	940	1020	1030	997	40
6th	30 µM	640	740	810	730	70
7th	35 µM	640	760	790	730	65
8th	40 µM	245	275	264	261	12
9th	50 µM	630	700	760	697	53
10th	60 µM	360	400	490	417	54
11th	70 µM	390	460	690	513	128
12th	80 µM	448	452	462	454	6
13th	90 µM	230	310	340	293	46
14th	100 µM	290	330	430	350	59
15th	110 µM	120	140	180	147	25
16th	120 µM	10	30	40	27	12
17th	130 µM	210	250	420	293	91
18th	140 µM	690	850	790	777	66
19th	150 µM	430	420	440	430	8
20th	160 µM	209	164	210	194	21
21st	170 µM	100	100	200	133	47

Table 3.3 (continued) : CFU of each population of stress-treated EMS-mutagenised culture (906) populations (CFU_1, CFU_2, and CFU_3 correspond to three independent measurements of CFU).

Population Number	Stress Level ($AgNO_3$)	CFU/mL x 10^5 of silver-treated samples			Average	Standard Deviation
		1	2	3		
22th	180 µM	170	175	177	174	3
23th	190 µM	80	130	150	120	29
24th	200 µM	502	704	736	647	104
25th	210 µM	40	41	51	44	5
26th	220 µM	0.1	0.1	0.2	0.13	0.05
27th	230 µM	0.08	0.09	0.08	0.08	0.00
28th	240 µM	0.04	0.03	0.04	0.04	0.00
29th	250 µM	0.0022	0.0035	0.0049	0.004	0.001

Survival rates of 906 populations under silver stress conditions according to treated and non-treated 906 cultures' CFU values are shown in Figure 3.3. After the 25th serial batch culture, a significant decrease at the survival rates of the populations was observed. The stress concentration of 25th population culture was 210 µM $AgNO_3$. Evolutionary engineering selection was continued a few more passages to ensure that the 906 culture came up to the highest survival limit of the stress and the 29th population of selection was exposed to 0.25 mM $AgNO_3$ stress level, and it was called the last population of the selection experiment.

In order to control and ensure the consequence of the selection strategy, cultures indicated in Table 3.4 were grown in 50-mL culture tubes in the presence and absence of 220 µM $AgNO_3$ (the stress level applied to the 26th population) at 30°C and 150 rpm. Direct colony count (CFU/mL) values were measured at the end of 24th, 48th, and 72nd h of incubation and shown in Table 3.5 and Table 3.6. The survival rates according to CFU values of each culture based on time intervals are shown in Figure 3.4.

Table 3.4 : Four cultures tested to control selection strategy.

Culture	Code
26th population of reference strain	905-26
26th population of EMS-treated reference strain	906-26
29th population of reference strain	905-29
29th population of EMS-treated reference strain	906-29

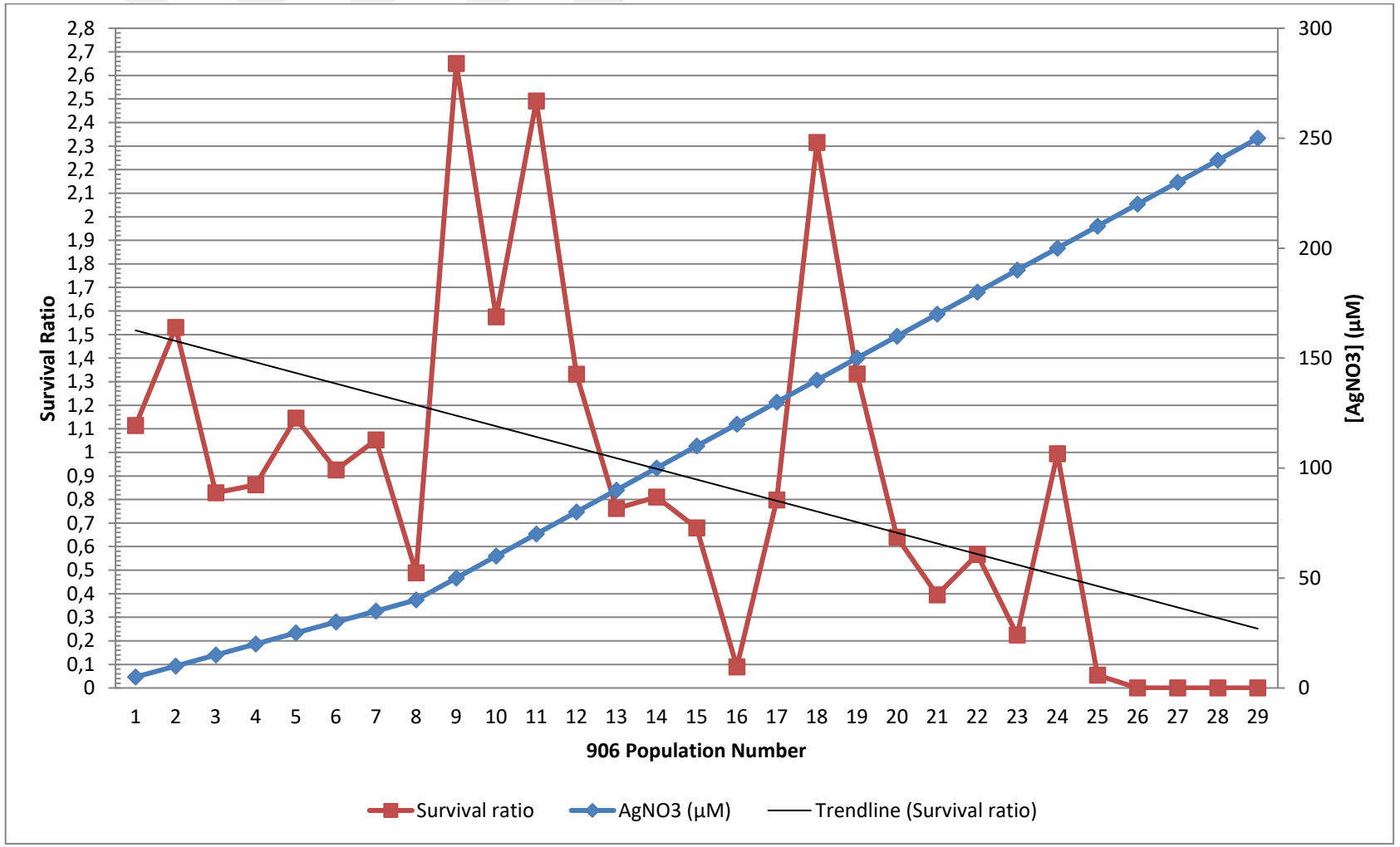

Figure 3.3 : Growth ratios of 906 populations at different stress levels during 29 passages of selection.

Table 3.5 : CFU/mL values of 905-26 and 906-26 at the end of 24th, 48th, and 72nd h of incubation under 220 µM $AgNO_3$.

(cells/mL x 10^4)	905-26			906-26		
Incubation time	24 h	48 h	72 h	24 h	48 h	72 h
Control	9300	3100	1410	7200	3520	2683
220 µM $AgNO_3$ applied	0	0	243	532	688	177
Survival ratio	0%	0%	2%	7%	20%	7%

Table 3.6 : CFU/mL values of 905-29 and 906-29 at the end of 24th, 48th, and 72nd h of incubation under 220 µM $AgNO_3$.

(cells/mL x 10^4)	905-29			906-29		
Incubation time	24 h	48 h	72 h	24 h	48 h	72 h
Control	6100	3656	3550	4050	2773	3850
220 µM $AgNO_3$ applied	0	0	417	1052	2028	1792
Survival ratio	0%	0%	1%	26%	73%	47%

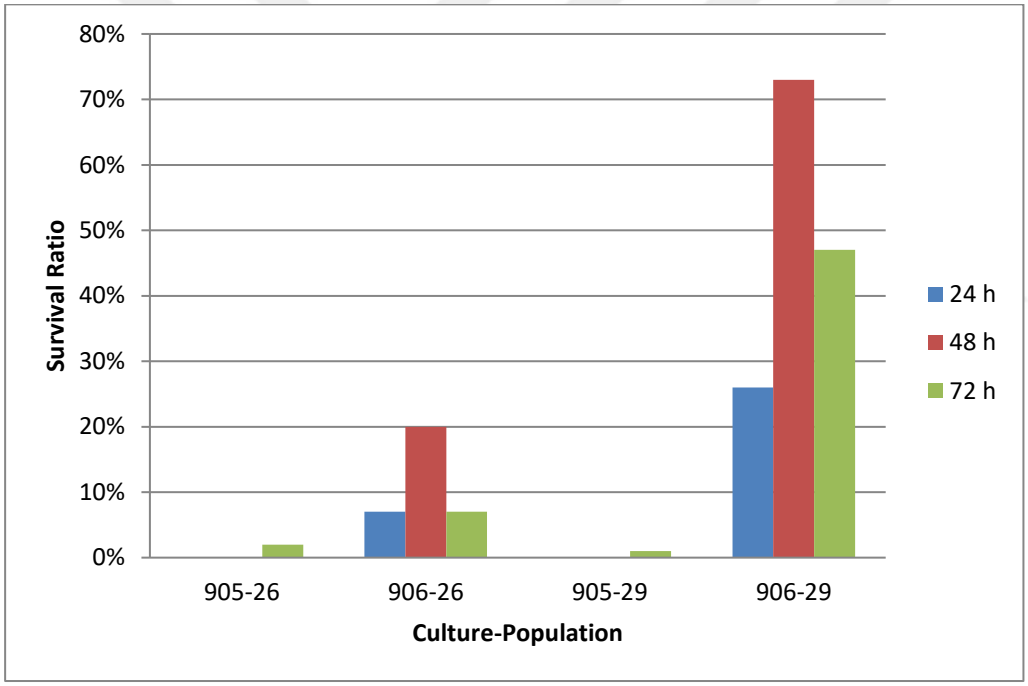

Figure 3.4 : Survival ratios of four cultures under 220 µM $AgNO_3$ stress.

It was observed that the 26th and 29th populations of the 905 culture showed no survival before 72 h. On the other hand, 26th and 29th populations of the 906 culture had noticeable survival under 220 µM $AgNO_3$ condition as a result of the selection. It was remarkable that the survival ratio of the last population was nearly 7 times higher than that of 906-26 at 72 h (Figure 3.4). .

3.1.3 Individual Mutant Selection

It was observed that there was nearly no survival of the 26th population of 906 at the stress level of 220 µM $AgNO_3$. On the other hand, 29th population had a better resistance compared to the 26th population at the stress level of 220 µM $AgNO_3$ (Table 3.4). Thus, the last population was chosen for selection of the individual mutants that had silver resistance.

The last population was spread onto solid YMM plates containing 0.2 mM $AgNO_3$ after it was diluted serially. Single colonies existed on plates after 72 h of incubation. In order to obtain the most resistant colony against silver, ten individual mutant colonies, named as 1E to 10E, were randomly picked for further investigation.

To compare the final population and the selected 10 individual colonies regarding their silver resistance, they were incubated in YMM without silver and with 220 µM $AgNO_3$ content. CFU values were measured and survival rates were calculated based on CFU values of the reference strain. The calculated survival rates are shown in Table 3.7 and Table 3.8, according to incubation times of 72 h and 144 h, respectively. They are also shown in Figure 3.5 and Figure 3.6, respectively.

Table 3.7 : CFU/mL values and survival ratios as fold of 905 for 29th population of 906 and ten individual mutants at the end of 72nd h of incubation under 200 µM $AgNO_3$.

72 h	Control samples (cells/mL)	Ag stress applied samples (cells/mL)	Survival Ratio (SR)	SR as fold of 905
905	3500000	2400	0.1%	-
29th pop.	2400000	92000	3.8%	55.9
1E	1600000	16000	1.0%	14.58
2E	1700000	240000	14.1%	205.88
3E	1400000	2400	0.2%	2.5
4E	3500000	9200	0.3%	3.83
5E	9200000	9200	0.1%	1.46
6E	2400000	5400	0.2%	3.28
7E	3500000	2400	0,1%	1
8E	1600000	24000	1.5%	21.88
9E	1700000	2400	0.1%	2.06
10E	16000000	5400	0.0%	0.49

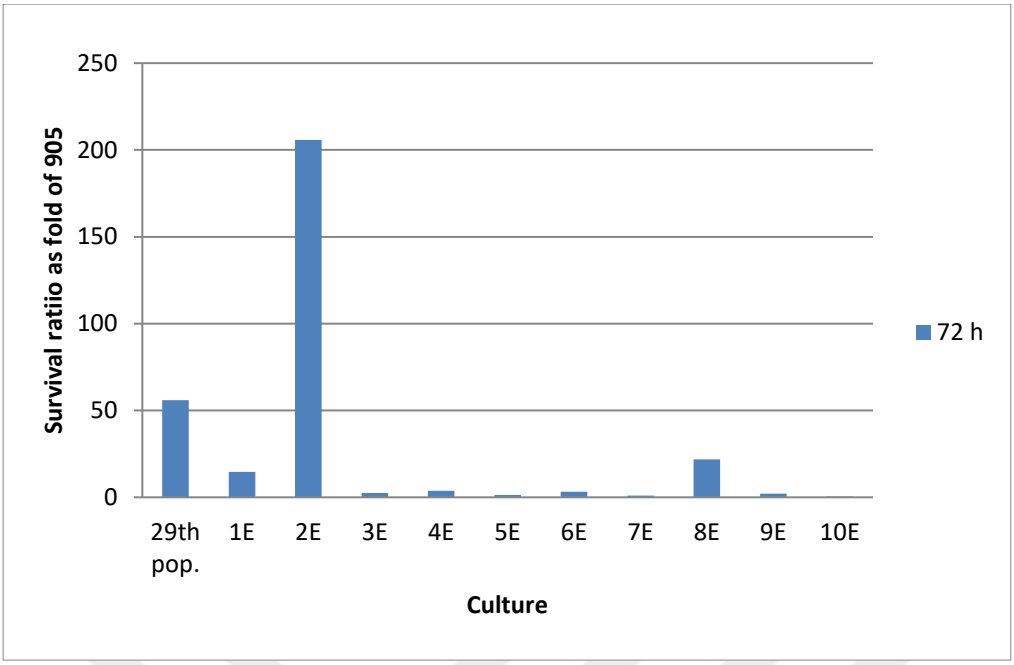

Figure 3.5 : Survival ratios as fold of 905 for 29th population of 906 and ten individual mutants at the end of 72nd h of incubation under 200 µM $AgNO_3$.

Regarding the 72 h incubation time results, the colonies named 2E and 8E showed differential growth under stress condition compared to other 8 colonies of the last population of 906 (Figure 3.5).

Table 3.8 : CFU/mL values and survival ratios as fold of 905 for 29th population of 906 and ten individual mutants at the end of 144th h of incubation under 200 µM $AgNO_3$.

144 h	Control samples (cells/mL)	Ag stress applied samples (cells/mL)	Survival Ratio (SR)	SR as fold of 905
905	3500000	170000	4.9%	-
29th pop.	2400000	350000	14.6%	3
1E	1600000	28000	1.8%	0.36
2E	1700000	350000	20.6%	4.24
3E	1400000	54000	3.9%	0.79
4E	3500000	92000	2.6%	0.54
5E	9200000	92000	1.0%	0.21
6E	2400000	160000	6.7%	1.37
7E	3500000	35000	1.0%	0.21
8E	1600000	280000	17.5%	3.6
9E	1700000	17000	1.0%	0.21
10E	16000000	24000	0.2%	0.03

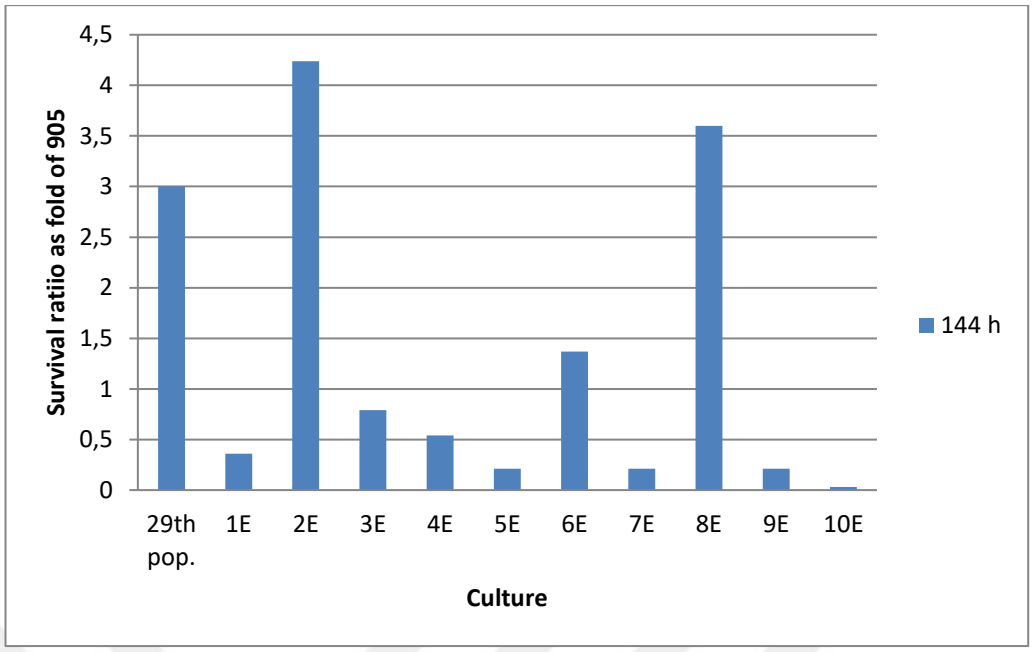

Figure 3.6 : Survival ratios as fold of 905 for 29th population of 906 and ten individual mutants at the end of 144th h of incubation under 200 µM $AgNO_3$.

Again, the colonies named 2E and 8E showed differential growth under the stress condition of 200 µM $AgNO_3$ for the incubation time of 144 h. All the colonies improved their growth during this period of time (Figure 3.6).

The mutant strains 1E, 2E, 3E, 4E, 5E, 6E, 7E, 8E, 9E, and 10E, the reference strain, and the last population were incubated on YMM plates containing 100 µM, 250 µM and 500 µM $AgNO_3$ in order to determine the silver stress resistance levels of these mutant colonies. As shown in Figure 3.7, 2E and 8E mutants had higher silver resistance than the other colonies.

The results obtained from survival rate comparison between the reference strain and the mutant colonies exposed to 200 µM $AgNO_3$ and the spot assay with 100 µM, 250 µM and 500 µM $AgNO_3$ were all parallel and indicated that 2E and 8E were much more resistant to silver even at higher concentrations. 2E showed slightly better survival and growth than 8E according to the results indicated in Figure 3.6. At this point of the study, detailed analyses consisting of estimation of stress resistance level by spot assay and MPN were required to decide which one of the 2E and 8E to choose for physiological characterization, transcriptomic analysis and whole genome re-sequencing.

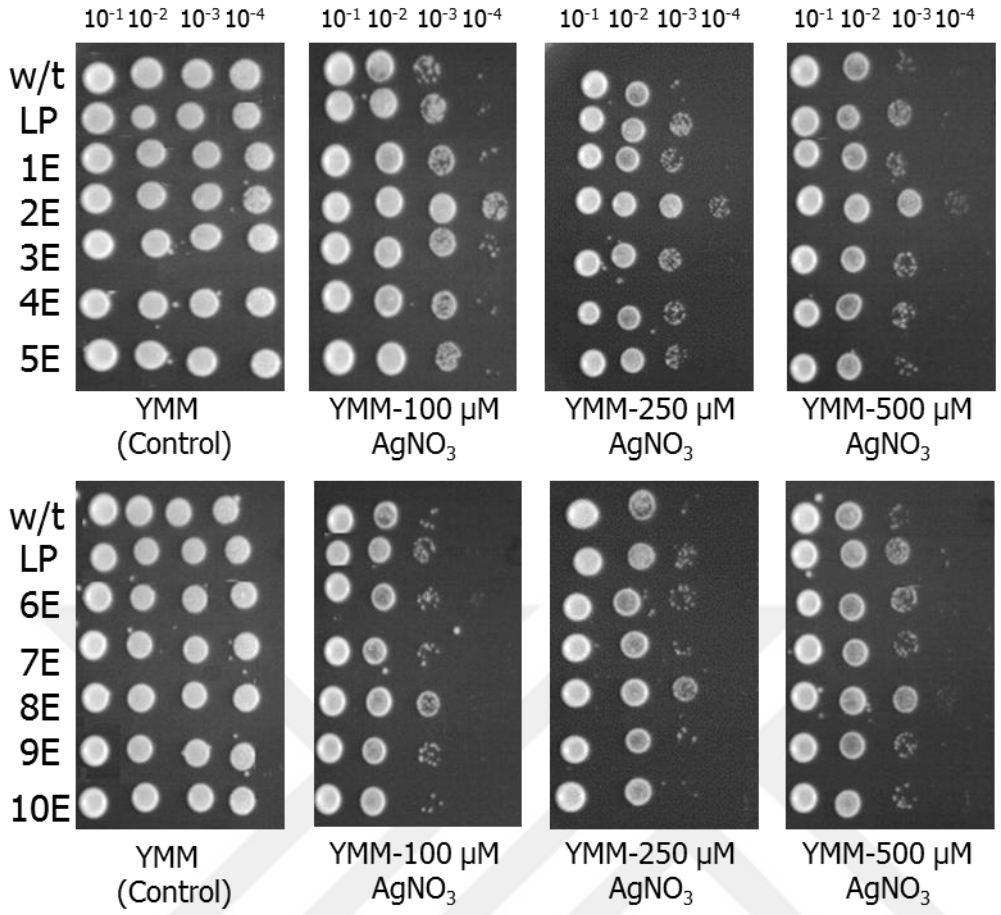

Figure 3.7 : Spot assay results under control conditions and in the presence of different silver levels (100 µM, 250 µM and 500 µM $AgNO_3$) for ten individual colonies (w/t as reference strain, LP as last population of 906) (Terzioğlu et al., 2020).

3.1.4 Phenotypes of the individual mutants

Phenotypic properties of the two individual mutants 2E and 8E were investigated. Stress resistance levels of these two mutants against various stress factors were determined by using spot assay and MPN methods, then also compared to the 29th population of 906.

3.1.4.1 Spot test to determine stress resistance

Possible cross-resistance of 2E, 8E, and the 29th population of 906 to various stress types were tested in solid media. The three cultures were grown until their exponential phase in YMM and then diluted in four ranges. The samples were dropped serially to the solid media containing copper (0.3 mM $CuSO_4$), hydrogen peroxide (1 mM H_2O_2), cobalt (3 mM $CoCl_2$), chromium (2 mM $CrCl_3$), aluminium (7.5 mM $AlCl_2$), ethanol (8% v/v), manganese (2 mM $MnCl_2$), nickel (0.25 mM $NiCl_2$), lithium (10 mM $LiCl_2$),

zinc (10 mM $ZnCl_2$), and iron (25 mM and 50 mM $(NH_4)_2Fe(SO_4)_2$) and the results are shown in Figure 3.8.

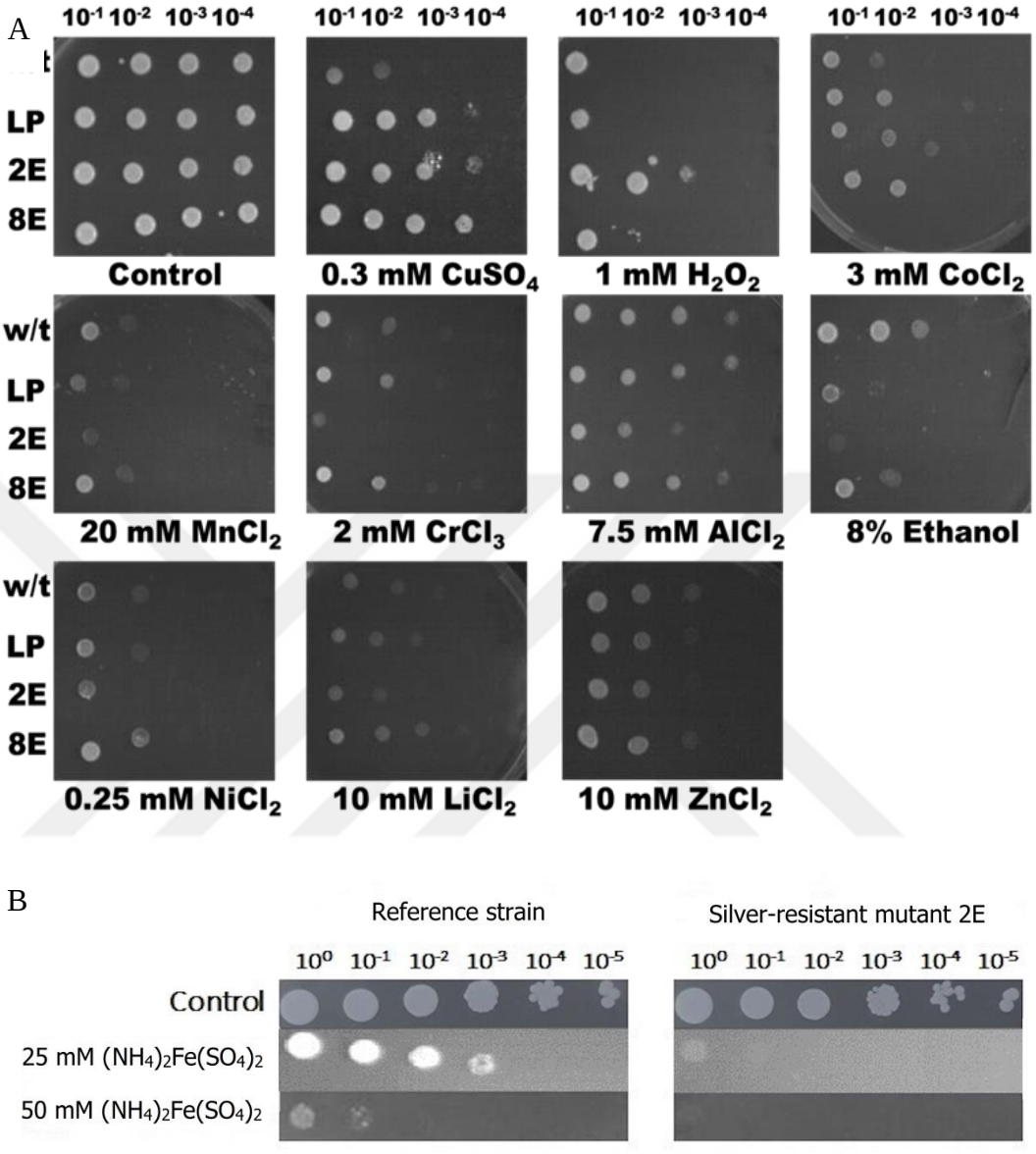

Figure 3.8 : Spot assay results under control conditions and in the presence of (A) various stress factors for w/t, LP, 2E, and 8E (w/t as reference strain, LP as last population of 906) and (B) iron stress for w/t and 2E (Terzioğlu et al., 2020).

Figure 3.8 indicated that the last population, 2E, and 8E were highly resistant against copper, but the reference strain was highly sensitive. 2E was the only strain that had resistance against hydrogen peroxide and it also resisted against cobalt stress. On the other hand, 2E was very sensitive to manganese, chromium, nickel, and ethanol stress. All three cultures had the same resistance or sensitivity level as the reference strain for

aluminium, lithium, and zinc. They were also more sensitive to ethanol stress, compared to the reference strain.

3.1.4.2 MPN Method to determine stress resistance

Possible cross-resistance of 2E, 8E, and the 29th population of 906 to various stress types were also tested by MPN method. CFU values were determined and survival rates were calculated for each strain and stress factor. Finally, survivals as fold of the reference strain survival upon every stress factor such as copper (0.5 mM $CuSO_4$), hydrogen peroxide (1 mM H_2O_2), cobalt (2 mM $CoCl_2$), chromium (2 mM $CrCl_3$), aluminium (10 mM $AlCl_2$), ethanol (8% v/v), manganese (15 mM $MnCl_2$), nickel (0.25 mM $NiCl_2$), lithium (5 mM $LiCl_2$), zinc (10 mM $ZnCl_2$) were determined and are shown in Figure 3.9.

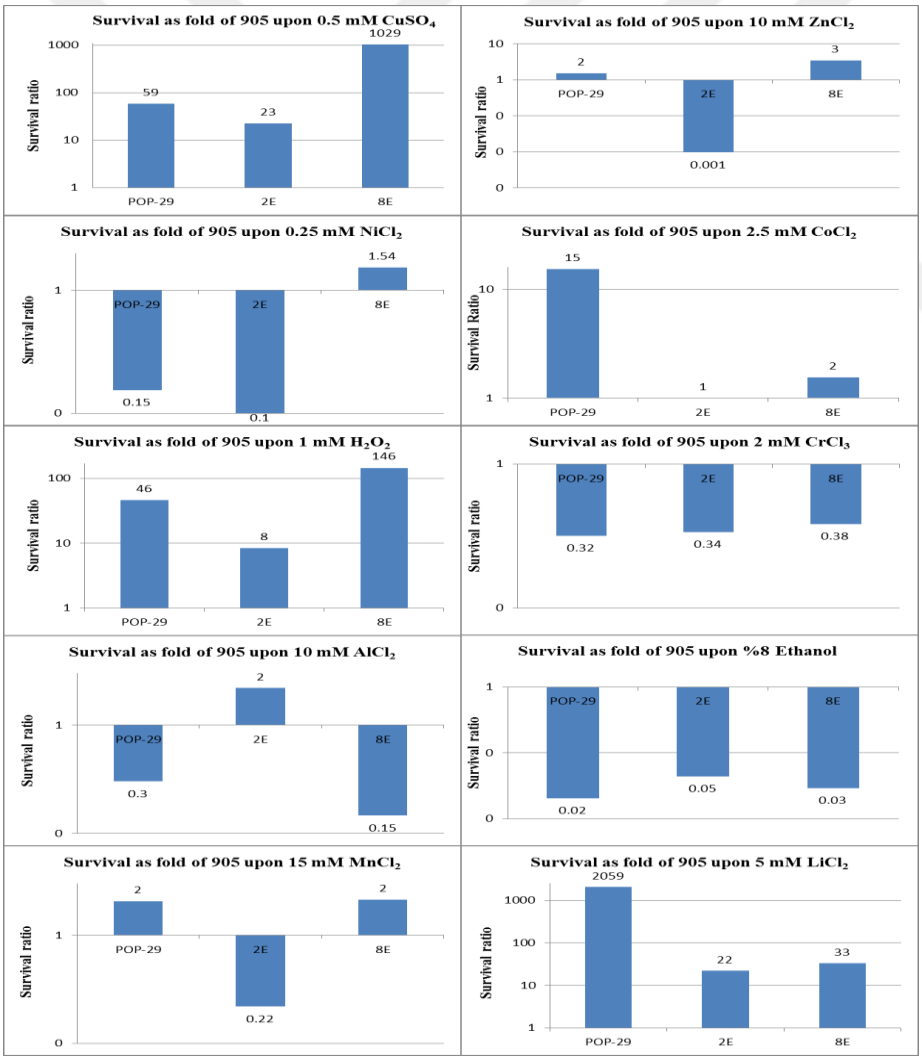

Figure 3.9 : Survival rates of 29th population of 906, 2E, and 8E as fold of reference strain in the presence of various stress factors.

Spot assay and the MPN method were both used for cross-resistance analysis to determine whether 2E and 8E became sensitive or resistant to other stress factors. The results of both methods showed that 2E and 8E were cross-resistant against copper stress. On the other hand, while spot assay indicated that 2E was cross-resistant to oxidative stress, it was detected by MPN that 8E was also cross-resistant. Ethanol, manganese, and chromium sensitivities were observed by both methods in 2E, but aluminium sensitivity was not observed in MPN. Resistance or sensitivity against zinc, lithium, and nickel in 2E and 8E were similar according to both results.

3.1.5 Genetic stability test for 2E and 8E

Spot assay and MPN analyses results revealed the resistance of the mutants 2E and 8E against silver and some other stress factors. In order to determine whether 2E and 8E were genetically stable or not, both mutants were batch cultivated in the absence of silver stress for 5 successive passages. They were then subjected to 200 µM $AgNO_3$. Their survival ratios as fold of the reference strain survival ratio are shown in Figure 3.10.

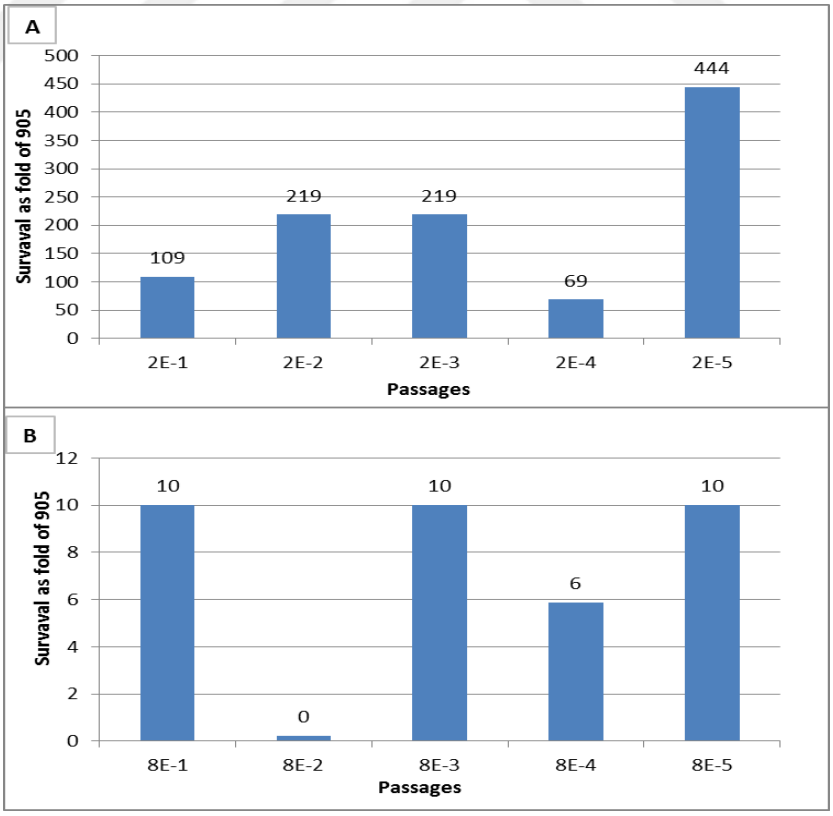

Figure 3.10 : Genetic stability test results of (A) 2E & (B) 8E after 5 passages in nonselective medium followed by growth in the presence of 200 µM $AgNO_3$.

The results showed that the silver resistance in both 2E and 8E were genetically stable traits, but 2E showed significantly higher survival under 200 µM $AgNO_3$ condition. Even though 8E had higher cross-resistance levels than 2E against copper and hydrogen peroxide stresses, 2E was chosen for further investigations due to its highest silver resistance and genetic stability.

3.2 Physiological Analyses of 2E

In order to determine the physiological characteristics of the mutant 2E, six different types of analyses were performed, including growth, cell dry weight, metabolites (by HPLC), silver content (by F-AAS), cell wall integrity, and trehalose content.

3.2.1 Analysis of growth

Reference strain (905) and the mutant 2E were cultivated in YMM in the presence and absence of 200 µM $AgNO_3$. Cultures were grown in 2-L flasks with 400 mL culture volume at 150 rpm and 30°C. Samples were collected in triplicate from each culture at 10 different time points.

The growth of the reference strain and the mutant 2E were measured by spectrophotometric OD_{600} values (shown in Table 3.9). OD_{600} values versus time graph was plotted and shown in Figure 3.11. The results revealed that the growth behavior of the reference strain was negatively affected by the presence of silver stress, but the growth of the mutant 2E was not affected by the presence of silver.

Table 3.9 : Average and standard deviation of OD_{600} values of the mutant 2E and reference strain (905) cultures in the presence and absence of 200 µM $AgNO_3$.

Incubation Time (h)	905 Control	905 Stress	2E Control	2E Stress
0	0.358 ± 0.88	0.282 ± 0.007	0.272 ± 0.001	0.329 ± 0.004
1.5	0.466 ± 0.004	0.295 ± 0.004	0.397 ± 0.004	0.410 ± 0.009
3	0.917 ± 0.010	0.390 ± 0.012	0.719 ± 0.013	0.620 ± 0.007
4.5	1.767 ± 0.097	0.452 ± 0.110	1.193 ± 0.009	0.948 ± 0.040
6	3.138 ± 0.028	0.275 ± 0.014	2.209 ± 0.035	0.997 ± 0.011
7.5	3.962 ± 0.160	0.667 ± 0.032	3.037 ± 0.271	1.910 ± 0.134
9	4.563 ± 0.029	0.853 ± 0.087	4.105 ± 0.115	2.330 ± 0.059
10.5	5.143 ± 0.009	1.007 ± 0.022	4.791 ± 0.201	3.209 ± 0.196
12	5.555 ± 0.098	1.415 ± 0.082	4.885 ± 0.062	3.545 ± 0.149
24	5.963 ± 0.143	6.150 ± 0.062	5.477 ± 0.136	5.691 ± 0.006

According to the data in Table 3.9, the graph of OD_{600} values versus time was plotted for the reference strain and 2E, and is shown in Figure 3.11.

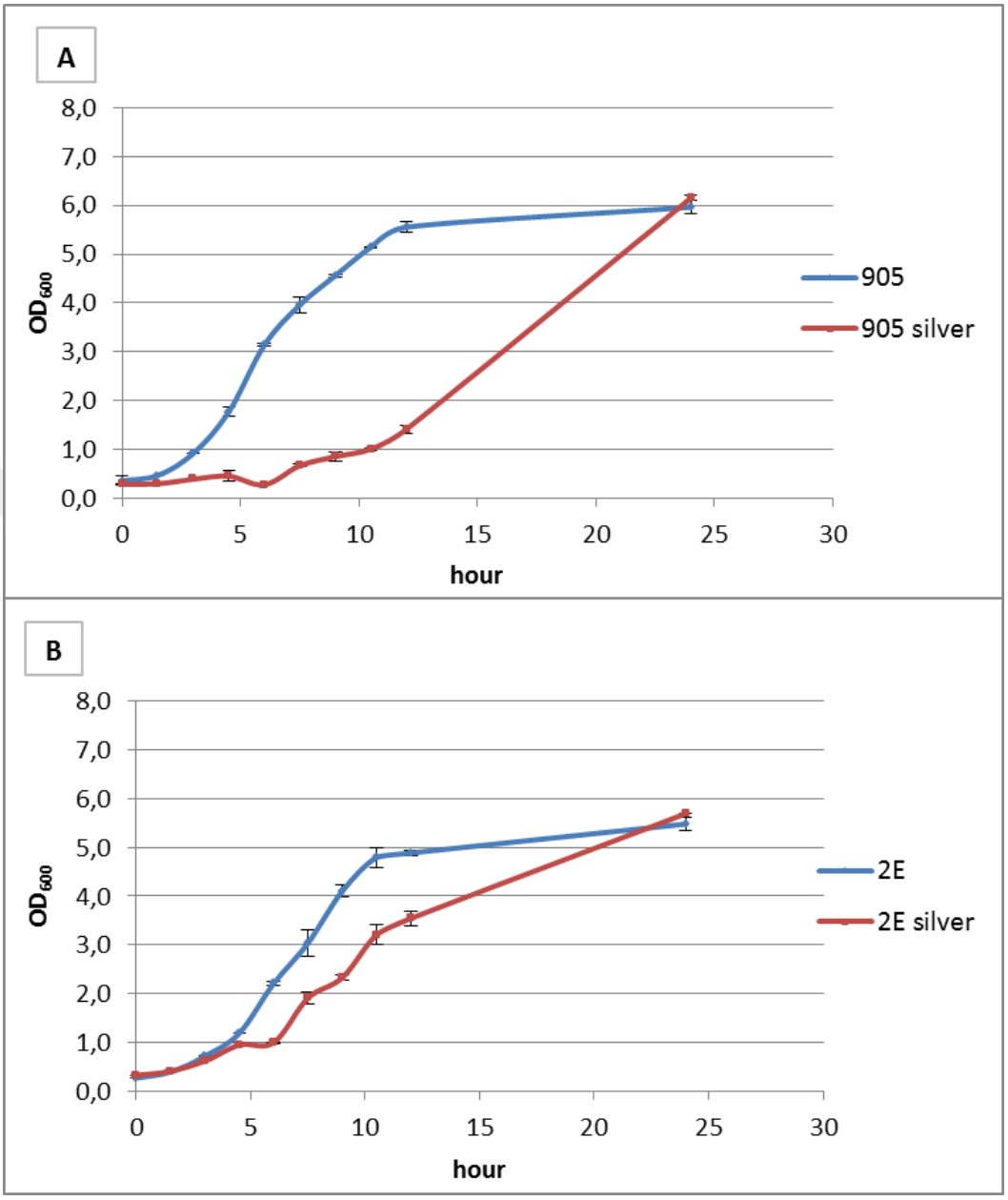

Figure 3.11 : Growth curve according to the spectrophotometric (OD_{600}) measurement of (A) the reference strain (905) and (B) the mutant 2E, with and without 200 µM $AgNO_3$.

The maximum specific growth rates of the reference strain and the mutant 2E are shown in Table 3.10. According to these data, 2E had 0.37 h^{-1} of maximum specific growth rate (μ_{max}) under control conditions, slightly lower than that of the reference strain which was 0.42 h^{-1}. On the other hand, the μ_{max} was only reduced by about 22% and came to 0.29 h^{-1} for the mutant 2E under silver stress conditions. The μ_{max} of the reference strain reduced sharply by about 74% and calculated as 0.11 h^{-1}.

Table 3.10 : Maximum specific growth rate (μ_{max}, h^{-1}) of the cultures 905 and 2E in the presence and absence of 200 µM $AgNO_3$.

Cultures	μ_{max} h^{-1}	μ_{max} ratio of stress treated cultures to that of control
905	0.42	0.26
905 - 200 µm $AgNO_3$	0.11	
2E	0.37	0.78
2E - 200 µm $AgNO_3$	0.29	

The exponential phase growth behavior of the reference strain and the mutant 2E in the absence and presence of 200 µM $AgNO_3$ is shown in Figure 3.12, Figure 3.13, and Figure 3.14, together for comparison (in Figure 3.12) and separately for 905 and 2E in detail (in Figures 3.13 and 3.14), including four data points during their exponential phase of growth.

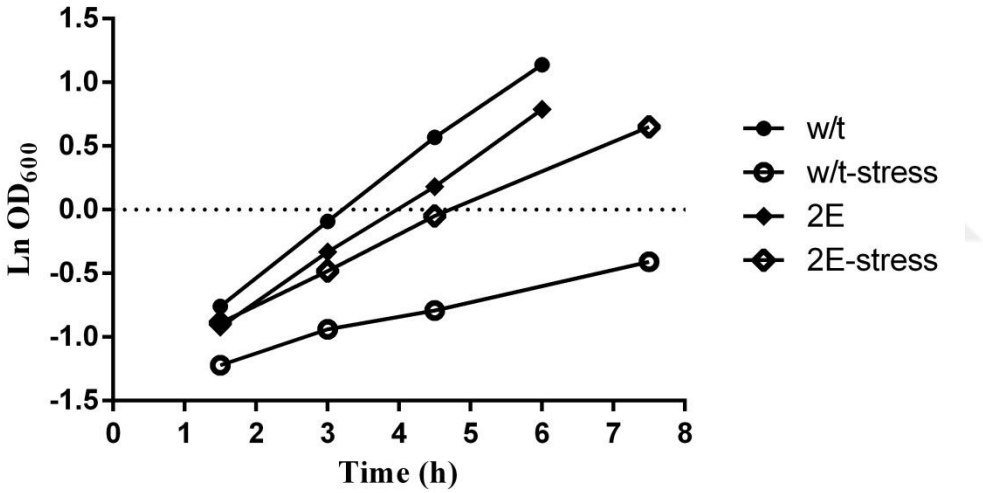

Figure 3.12 : Exponential phase growth behavior of the reference strain (w/t) and the mutant 2E in the absence and presence of 200 µM $AgNO_3$.

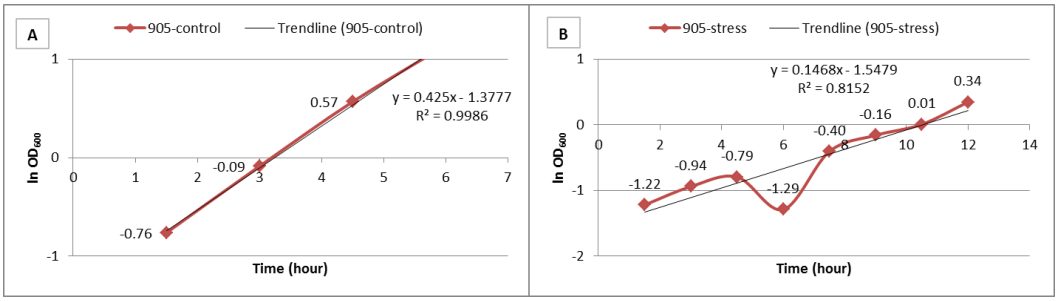

Figure 3.13 : Exponential phase growth behavior of the reference strain (905) (A) in the absence and (B) presence of 200 µM $AgNO_3$.

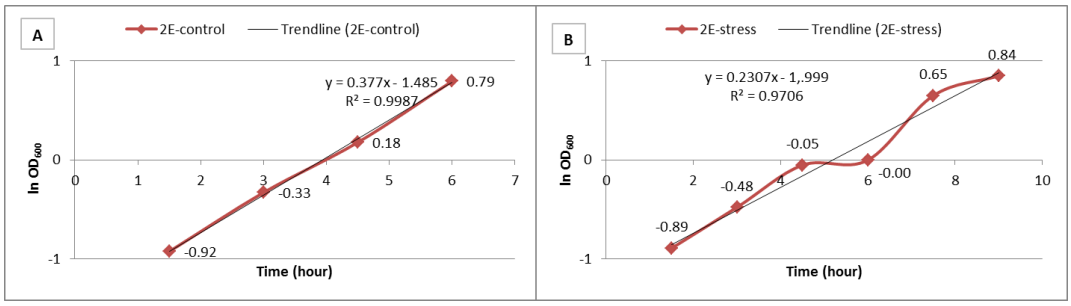

Figure 3.14 : Exponential phase growth behavior of the mutant 2E (A) in the absence and (B) presence of 200 µM $AgNO_3$.

3.2.2 Analysis of cell dry weight (CDW)

The biomass production of the reference strain and the mutant 2E were measured by CDW analysis. First, samples were taken during the growth of the cultures for determined time intervals and put into the tubes that had been dried and preweighed before. Second, supernatant was removed after the centrifugation of the tubes. The tubes containing pellets were then dried in an oven with their caps open to get dry pellets. Finally, after being weighed, the difference between the weights of the tubes was used to determine the cultures' CDW per mL and the values are shown in Table 3.11.

Table 3.11 : Biomass production as CDW (mg/mL) values of the cultures 905 and 2E in the presence and absence of 200 µM $AgNO_3$.

Incubation Time (h)	905 Control	905 Stress	2E Control	2E Stress
4.5	0.617 ± 0.161	0.300 ± 0.354	0.625 ± 0.035	0.350 ± 0.050
6	0.717 ± 0.153	0.267 ± 0.076	0.717 ± 0.104	0.675 ± 0.106
7.5	1.200 ± 0.218	0.233 ± 0.153	1.033 ± 0.104	0.817 ± 0.202
11	1.583 ± 0.029	0.733 ± 0.029	1.717 ± 0.252	1.250 ± 0.265
23	1.917 ± 0.115	1.600 ± 0.132	1.817 ± 0.355	1.833 ± 0.076

Biomass production of the reference strain and the mutant 2E in the presence and absence of 200 µM $AgNO_3$ are also shown in Figure 3.15. According to CDW values, 2E was faster than the reference strain in biomass production under control conditions during the exponential growth phase and it reached the stationary phase earlier. On the other hand, there was a similar biomass production level of the mutant 2E in stress condition, but it reached the stationary phase in about 23 hours. The reference strain, however, showed a significant decrease in biomass production under stress condition than the one under control condition, indicating that the reference strain was inhibited by the silver stress.

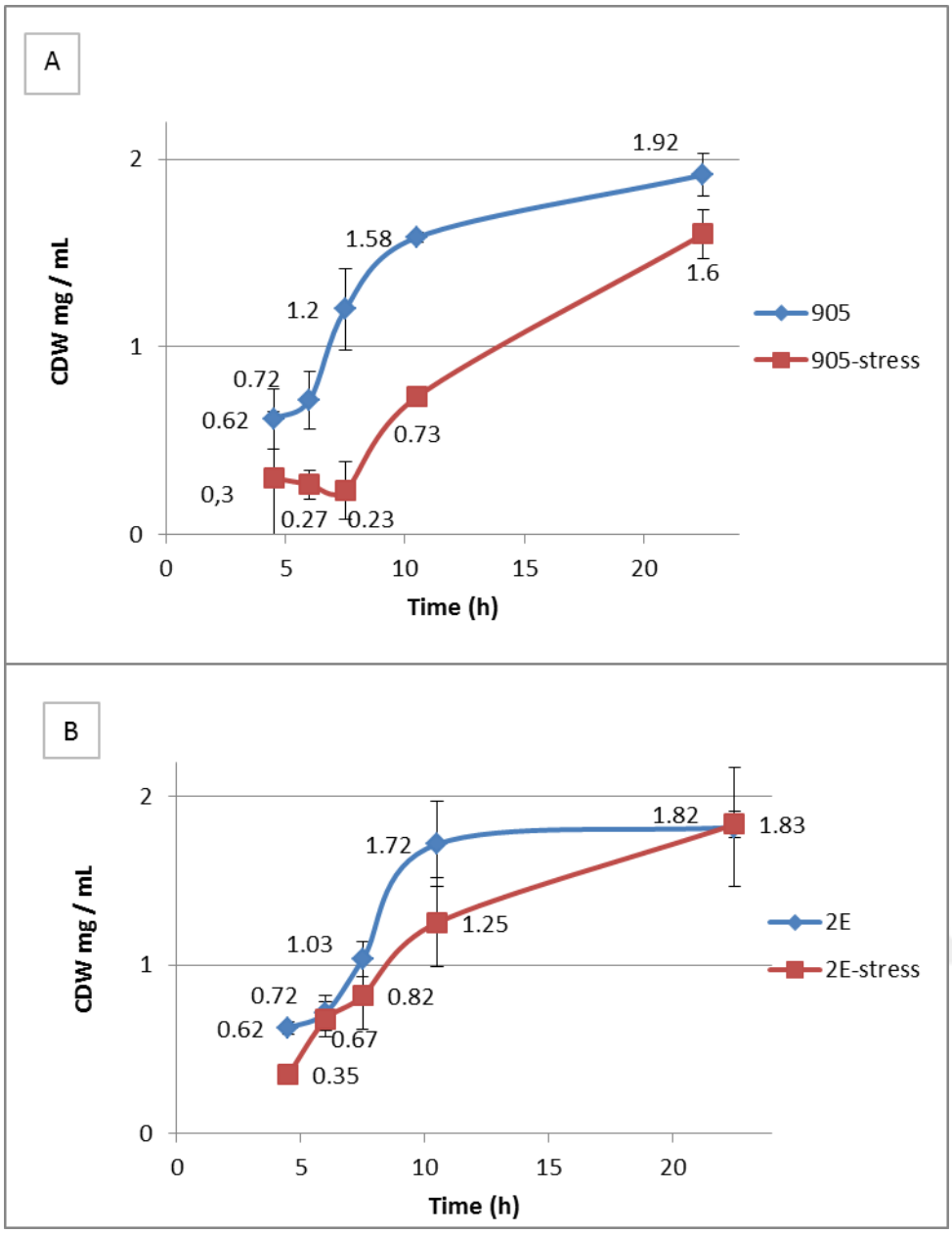

Figure 3.15 : Biomass production as CDW values of the cultures (A) 905 and (B) 2E in the presence and absence of 200 µM $AgNO_3$.

To further analyse the physiological differences between the reference strain and the mutant 2E, their glucose consumption and metabolite production were investigated by high performance liquid chromatography method (HPLC).

3.2.3 Analysis of metabolites by HPLC

Metabolite profiles of the reference strain and the mutant 2E were determined by using HPLC analysis. First, standard curves of ethanol, glucose, acetate, and glycerol were plotted by using known standards and the results are shown in Figure 3.16 and 3.17, respectively.

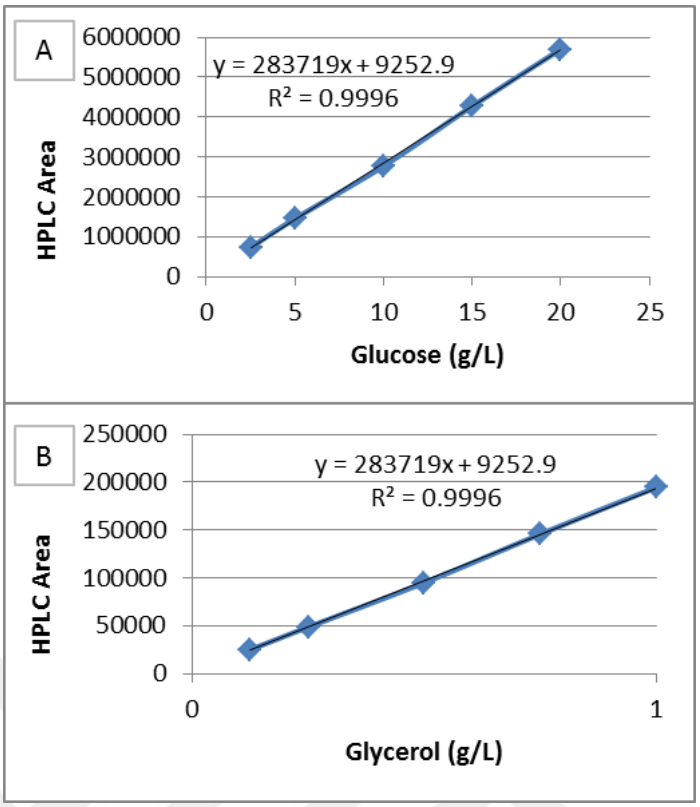

Figure 3.16 : Standard HPLC curves of (A) glucose and (B) glycerol.

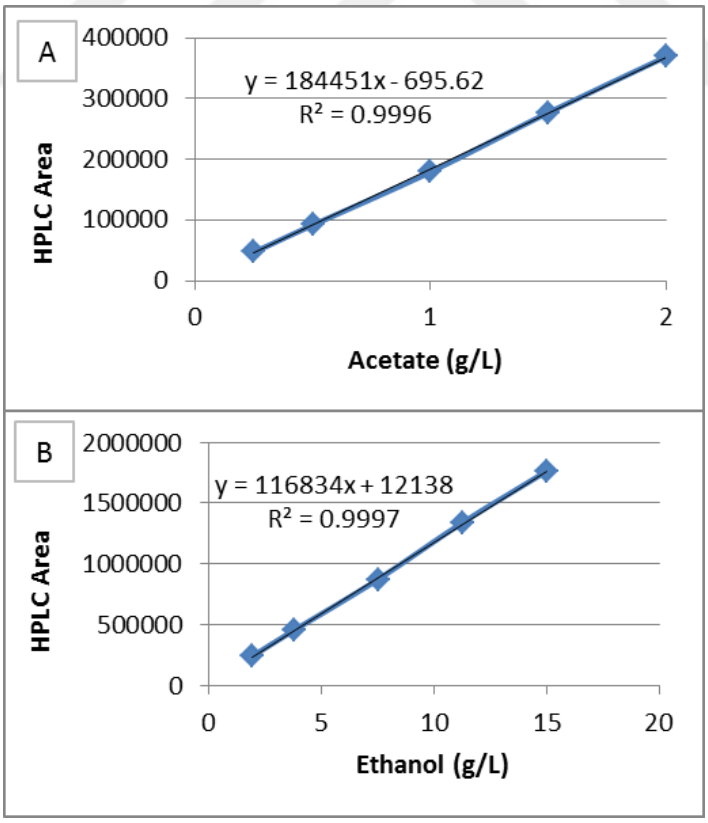

Figure 3.17 : Standard HPLC curves of (A) acetate and (B) ethanol.

The amount of each metabolite in culture was measured by using the standard curves in Figure 3.16 and Figure 3.17. Measured data of glucose, glycerol, acetate, and ethanol for the reference strain and the mutant 2E are shown in Table 3.12 and Table 3.13, respectively.

Table 3.12 : Metabolite values of the reference strain in control culture for an incubation of 25 h.

Time (h)	Glucose (g/l)	Ethanol (g/l)	Glycerol (g/l)	Acetate (g/l)
0	19.25 ± 0.85	0.14 ± 0	0 ± 0	0 ± 0.09
1.5	18.93 ± 0.55	0.28 ± 0.06	0.00 ± 0	0.01 ± 0.1
3	18.31 ± 0.39	0.45 ± 0.11	0.02 ± 0	0.02 ± 0.06
4.5	15.32 ± 0.88	1.04 ± 0.06	0.05 ± 0	0.04 ± 0
6				
7.5	9.46 ± 0.04	2.42 ± 0.28	0.11 ± 0	0.08 ± 0.12
9	8.27 ± 0.25	3.54 ± 0.12	0.21 ± 0.06	0.14 ± 0.1
10.5	4.86 ± 0.16	4.73 ± 0.22	0.32 ± 0	0.19 ± 0.05
12	2.46 ± 0.07	5.20 ± 0.25	0.40 ± 0.07	0.28 ± 0.11
25	0 ± 0	5.40 ± 0.18	0.44 ± 0	0.41 ± 0

Table 3.13 : Metabolite values of the mutant 2E in control culture for an incubation of 25 h.

Time (h)	Glucose (g/l)	Ethanol (g/l)	Glycerol (g/l)	Acetate (g/l)
0	18.85 ± 0.85	0.23 ± 0	0 ± 0	0 ± 0.09
1.5	18.74 ± 0.2	0.32 ± 0	0.00 ± 0	0.01 ± 0.01
3	17.9 ± 0.13	0.48 ± 0.07	0.01 ± 0	0.03 ± 0.1
4.5	16.58 ± 0.62	0.93 ± 0.34	0.03 ± 0	0.05 ± 0.04
6		1.06 ± 0.41	0.03 ± 0.06	0.05 ± 0.18
7.5	11.97 ± 0.03	1.44 ± 0.05	0.04 ± 0	0.07 ± 0
9	10.33 ± 0	3.04 ± 0.12	0.12 ± 0.07	0.12 ± 0.08
10.5	7.47 ± 0	3.68 ± 0.06	0.19 ± 0	0.13 ± 0.21
12	5.51 ± 0	4.53 ± 0.27	0.29 ± 0.09	0.24 ± 0.34
25	0 ± 0	6.17 ± 0.26	0.42 ± 0	0.44 ± 0.21

According to the HPLC data, glucose consumption behaviour of the reference strain and the mutant 2E were similar during growth in the media without silver stress. Glucose consumption under control condition is also shown in Figure 3.18. The reference strain consumed glucose nearly at same rate with 2E during the first 5 h. After 10 h of incubation, reference strain glucose consumption rate increased and glucose was depleted earlier than 2E in accordance with Figure 3.15 that shows the CDW values of both cultures in control conditions.

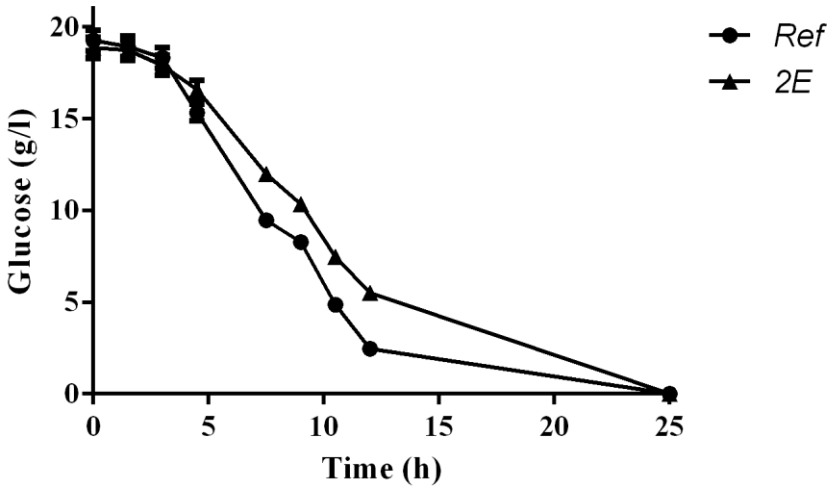

Figure 3.18 : Glucose consumption of 905 (Ref) and 2E grown in control media without silver stress (Terzioğlu et al., 2020).

In the media without silver stress, reference strain produced ethanol more than the mutant 2E until the mid-stationary phase of the reference strain (approximately 17th hour of incubation), as shown in Figure 3.19. However, the ethanol production of 2E continued until the 25th hour of cultivation and the final ethanol concentrations of 2E and the reference strain were 6.17 g/L and 5.40 g/L, respectively, at the end of the 25 h of cultivation.

Glycerol production of the reference strain and the mutant 2E under control conditions is shown in Figure 3.20. 2E generally produced less glycerol throughout the cultivation, but the final glycerol concentrations of both strains were similar. Glycerol data at 25 h supported the faster growth and earlier arrival at the stationary phase of the reference strain compared to 2E. 2E had a lower rate of growth under control condition and lower metabolite production than the reference strain.

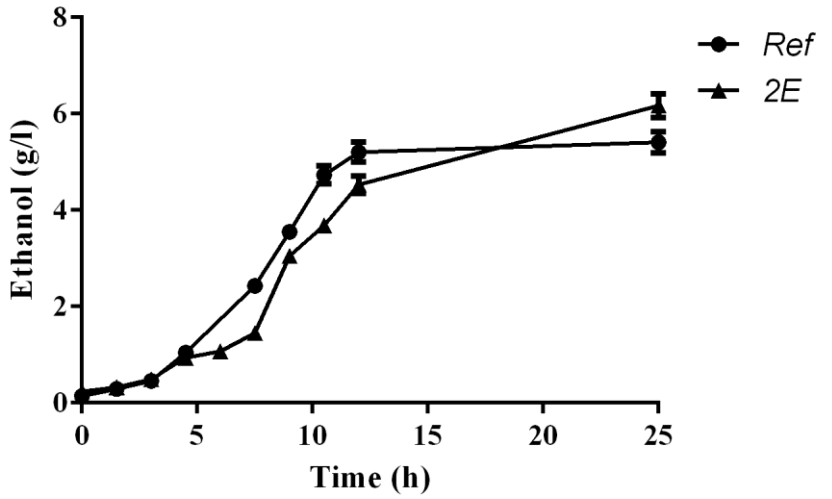

Figure 3.19 : Ethanol production behavior of 905 (Ref) and 2E grown in control media without silver stress (Terzioğlu et al., 2020).

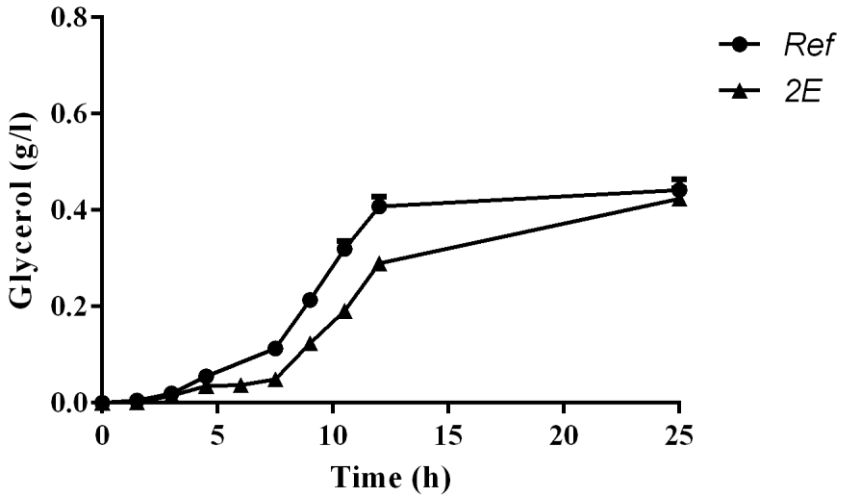

Figure 3.20 : Glycerol production behavior of 905 (Ref) and 2E grown in control media without silver stress (Terzioğlu et al., 2020).

Acetate producttion of the reference strain and the mutant 2E are shown in Figure 3.21. Acetate profiles for both reference strain and 2E were similar to their ethanol profiles. While both strains had the same amount of acetate production until the 7th h of incubation, the reference strain started then to produce more acetate compared to 2E. Between the 10th and 12th h of incubation, 2E produced less acetate than the reference strain, but it could reach acetate production levels similar to those of the reference strain, by the end of the 25th hour of cultivation, (0.44 g/L and 0.41 g/L for 2E and the reference strain, respectively).

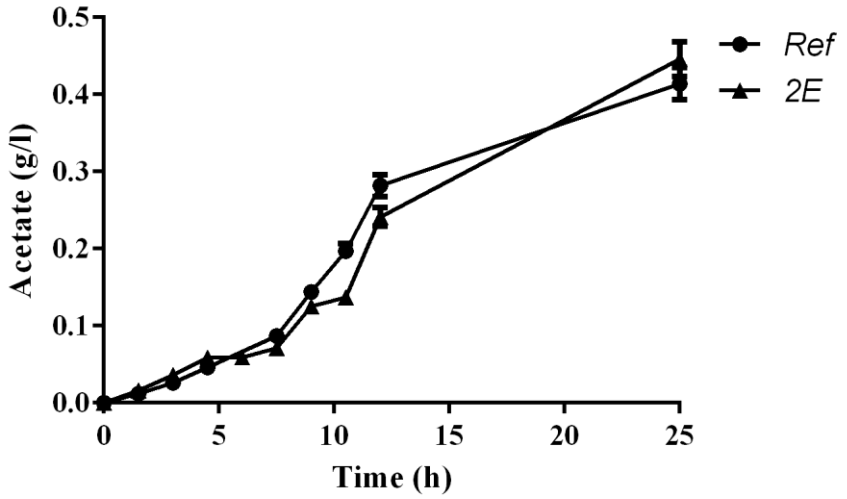

Figure 3.21 : Acetate production behavior of 905 (Ref) and 2E grown in control media without silver stress (Terzioğlu et al., 2020).

In order to get detailed information about the metabolism of the reference strain and the mutant 2E under silver stress condition, HPLC method was applied again. The measurements were done at ten different time points during 25-hour long cultivation. Measured data for glucose, glycerol, acetate, and ethanol (in g/L) for the reference strain in the media containing 200 µM $AgNO_3$ are shown in Table 3.14.

Table 3.14 : Metabolite values of the reference strain in the media containing 200 µM $AgNO_3$ culture for an incubation of 25 h.

Time (h)	Glucose (g/l)	Ethanol (g/l)	Glycerol (g/l)	Acetate (g/l)
0	19.71 ± 0.89	0.13 ± 0.0	0 ± 0	0 ± 0
1.5	19.51 ± 0.51	0.14 ± 0.05	0.00 ± 0	0 ± 0
3			0.00 ± 0	0 ± 0
4.5			0.00 ± 0	0 ± 0
6			0.00 ± 0	0 ± 0
7.5	17.63 ± 0.44	0.36 ± 0.07	0.04 ± 0.00	0.03 ± 0.01
9		0.40 ± 0.08	0.07 ± 0.01	0.04 ± 0.03
10.5	17.14 ± 0.36	0.64 ± 0.09	0.11 ± 0.00	0.05 ± 0.02
12	16.69 ± 0.27	0.93 ± 0.14	0.16 ± 0.06	0.06 ± 0.01
25	0.29 ± 0.06	4.88 ± 0.19	0.73 ± 0.04	0.17 ± 0.03

Measured data of glucose, glycerol, acetate, and ethanol in g/L for the mutant 2E in the media containing 200 µM $AgNO_3$ are shown in Table 3.15.

Table 3.15 : Metabolite values of the mutant 2E in the media containing 200 µM $AgNO_3$ culture for an incubation of 25 h.

Time (h)	Glucose (g/l)	Ethanol (g/l)	Glycerol (g/l)	Acetate (g/l)
0	19.22 ± 0.87	0.21 ± 0.00	0 ± 0	0 ± 0
1.5	19.01 ± 0.69	0.26 ± 0.00	0.00 ± 0	0.01 ± 0.00
3	18.18 ± 0.54	0.29 ± 0.04	0.01 ± 0	0.03 ± 0.01
4.5				
6	16.81 ± 0.45	0.83 ± 0.22	0.07 ± 0.04	0.07 ± 0.02
7.5	15.53 ± 0.34	1.17 ± 0.16	0.11 ± 0.00	0.09 ± 0.02
9	14.19 ± 0.29	1.69 ± 0.11	0.17 ± 0.06	0.11 ± 0.03
10.5	11.81 ± 0.22	2.33 ± 0.09	0.25 ± 0.05	0.13 ± 0.04
12	10.07 ± 0.19	3.03 ± 0.18	0.36 ± 0.10	0.23 ± 0.07
25	0 ± 0	6.15 ± 0.27	0.59 ± 0.03	0.38 ± 0.05

The growth behaviour of the cultures were mostly in line with their metabolite profiles. Strong inhibition of the reference strain under silver stress condition was observed. During the first 10 hours of the cultivation, the inhibition of the reference strain was more clear.

Glucose consumption of the reference strain and 2E grown in media with silver stress is shown in Figure 3.22. Glucose was slightly consumed by the reference strain in the first half of the 25-hour cultivation with 200 µM $AgNO_3$. This slow glucose consumption was significant compared to the glucose consumption profile under control condition. On the other hand, 2E showed no noticable change in glucose consumption under control and stress conditions.

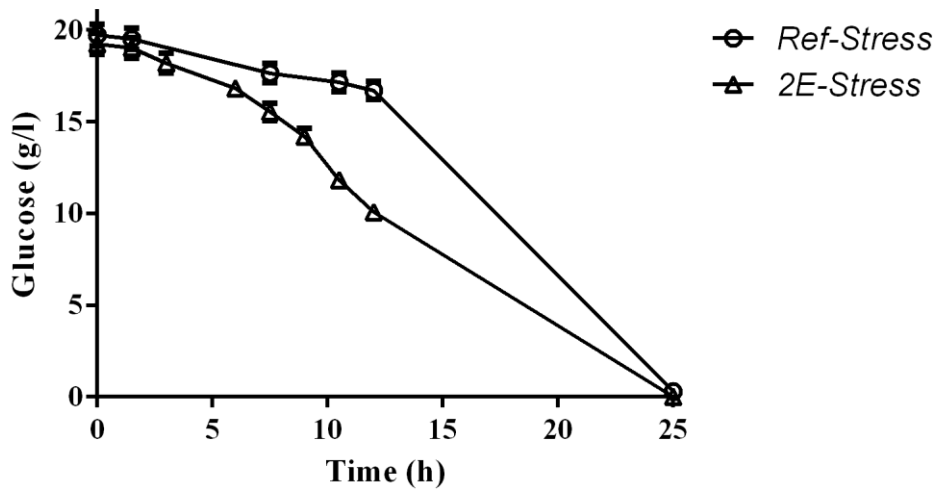

Figure 3.22 : Glucose consumption of 905 (Ref) and 2E grown in media with silver stress (200 µM $AgNO_3$) (Terzioğlu et al., 2020).

Ethanol production of the reference strain and 2E grown in media with silver stress is shown in Figure 3.23. It was observed that the mutant 2E produced more ethanol than the reference strain throughout the 25-hour cultivation up to a maximum level of of 6.15 g/L, which was 4.88 g/L for the reference strain. Higher glucose consumpiton and so growth rates of 2E in stress condition were the reason of high ethanol production.

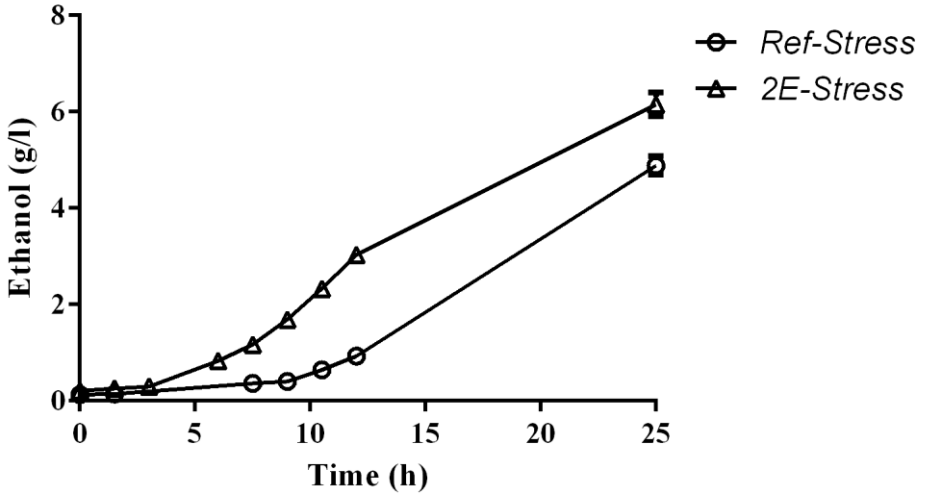

Figure 3.23 : Ethanol production of 905 (Ref) and 2E grown in media with silver stress (200 µM $AgNO_3$) (Terzioğlu et al., 2020).

Glycerol production of the reference strain and 2E grown in media with silver stress is shown in Figure 3.24.

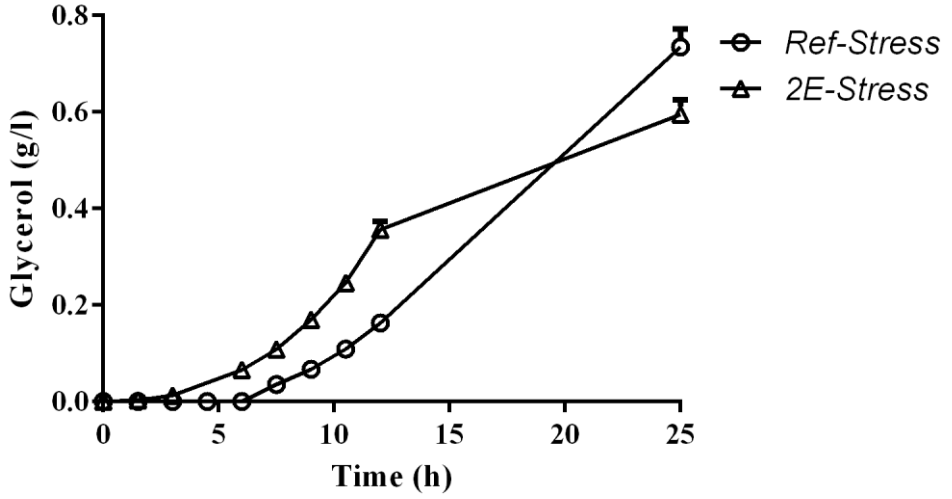

Figure 3.24 : Glycerol production of 905 (Ref) and 2E grown in media with silver stress (200 µM $AgNO_3$).

Glycerol production of 2E under silver stress condition was higher until about the 12th h of the cultivation. However, the reference strain's final glycerol concentration was higher than that of 2E and it reached 0.73 g/L.

Acetate production of the reference strain and 2E grown in media with silver stress is shown in Figure 3.25. While their acetate production behavior were nearly the same under control conditions, the mutant 2E produced 2-fold higher acetate than the reference strain (0.38 and 0.17 g/L, respectively) under stress conditions. Ethanol and acetate profiles of both strains were similar under stress conditions.

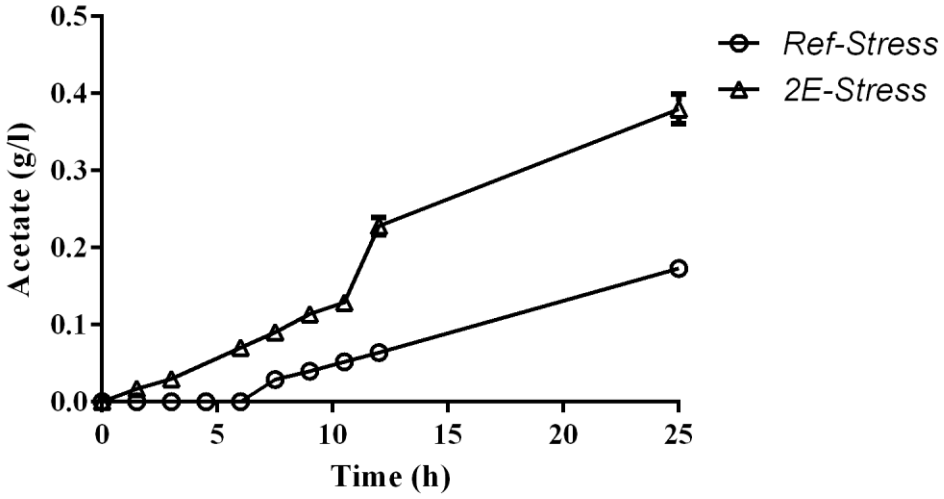

Figure 3.25 : Acetate production of 905 (Ref) and 2E grown in media with silver stress (200 µM $AgNO_3$).

Regarding all four metabolites, the reference strain's rates of glucose consumption, ethanol and acetate production were the lowest, under silver stress conditions. On the other hand, the reference strain produced the highest level of glycerol under silver stress condition, at the 25th hour of the cultivation.

3.2.4 Flame – atomic absorption spectrophotometry (F-AAS) analysis

In order to determine the silver ion concentrations associated with the mutant 2E and the reference strain, flame – atomic absorption spectrophotometry (F-AAS) method was used. The silver absorbance standard curve is shown in Figure 3.26. The cultures were cultivated at silver stress levels of 50, 100, and 250 µM $AgNO_3$ and their silver content was measured by comparing CDW values with AAS values. The comparison of the silver content of the reference strain and the mutant 2E is shown in Figure 3.27.

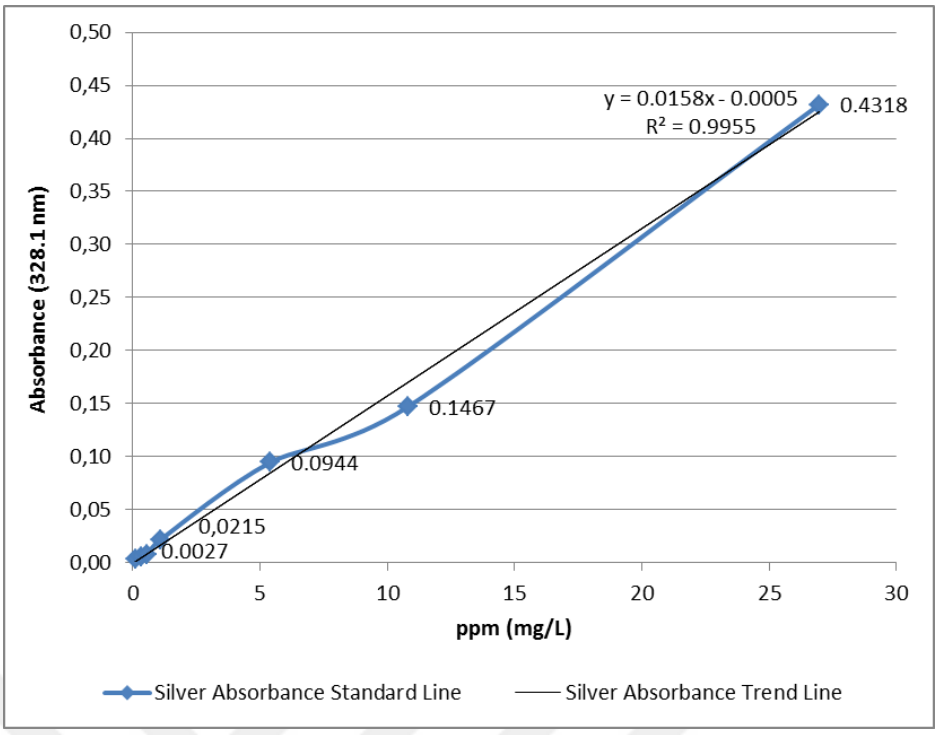

Figure 3.26 : Silver absorbance standard curve measured and used for silver absorbance of 905 and 2E by F-AAS.

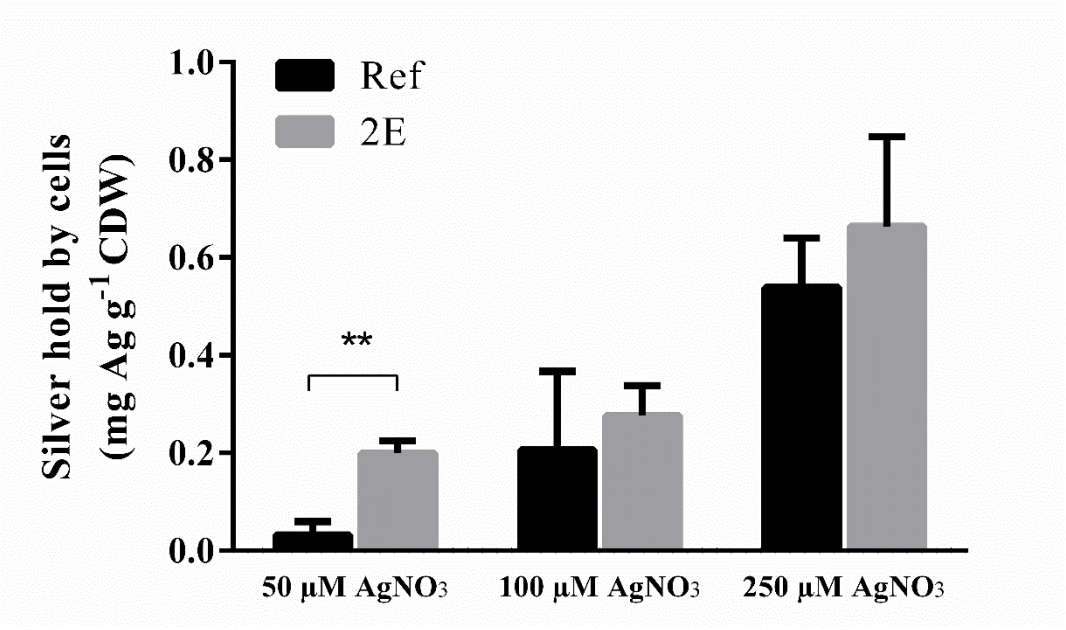

Figure 3.27 : The average mg silver per CDW values for 905 (Ref)and 2E at different incubation conditions with 50 µM $AgNO_3$, 100 µM $AgNO_3$, and 200 µM $AgNO_3$ (Terzioğlu et al., 2020).

The silver-resistant strain 2E had a higher amount of silver ions associated with the cells than the reference strain, in the media containing 50 µM $AgNO_3$. On the other hand, while both strains could hold increased amount of silver at higher concentrations

of $AgNO_3$, the significant difference between them at lower concentrations was not observed at higher concentrations.

3.2.5 Analysis for cell wall integrity

The lyticase sensitivity assay (Kuranda et al., 2006; Balaban et al., 2020) was performed for the reference strain and the mutant 2E in the absence and presence of 200 µM $AgNO_3$ in order to detect differences between both strains in cell wall integrity. The cell wall β-1,3-glucan-degrading enzyme lyticase was used and cell wall integrity comparison is shown in Figure 3.28.

It was observed that the lyticase resistance of the mutant 2E was significantly higher than the reference strain. As a result, the cell wall integrity or the robustness of 2E was higher than the reference strain. These results were compared with whole-genome resequencing and transcriptomic results of the mutant 2E and the reference strain in order to identify differential expression or mutation of genes associated with cell wall integrity and biogenesis.

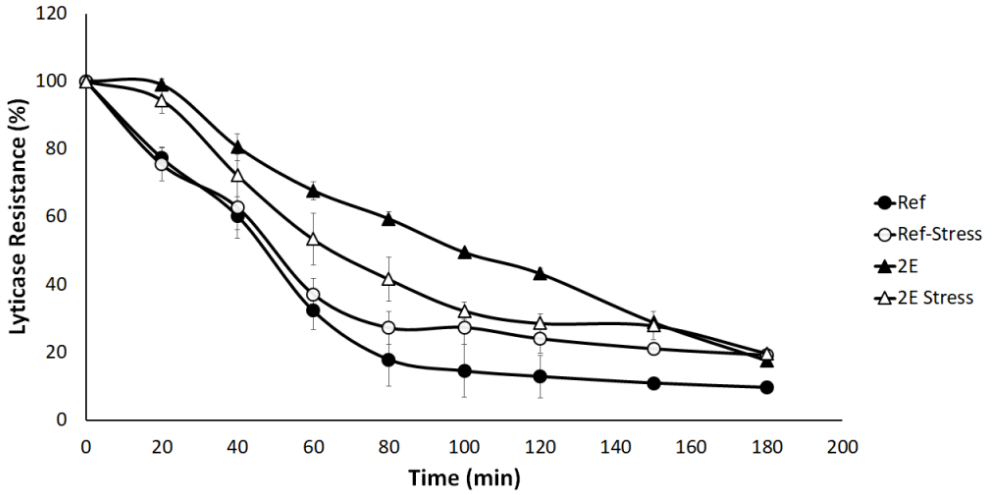

Figure 3.28 : Lyticase resistance of 905 (Ref) and 2E under control and silver stress (200 µM $AgNO_3$) conditions (Terzioğlu et al., 2020).

3.2.6 Analysis of trehalose content

Glucose standard curve for trehalose content determination was obtained first and it is shown in Figure 3.29.

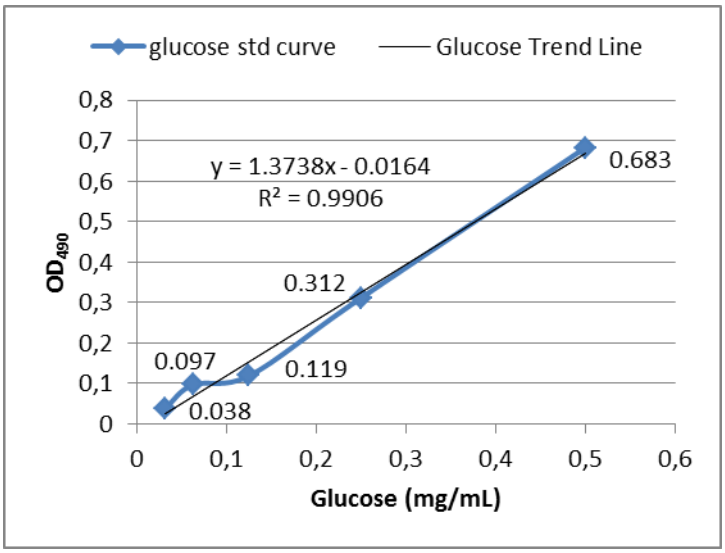

Figure 3.29 : Glucose standard curve for trehalose content determination.

After cultivation of the reference strain and the mutant 2E in YMM in the presence and absence of 200 µM $AgNO_3$ stress, each culture was sampled at two different time intervals. The OD_{490} values were then measured for 905 and 2E and are shown in Table 3.16.

Table 3.16 : OD_{490} results of 905 and 2E in control media and the media containing 200 µM $AgNO_3$ at 25th h and 30th h.

Time (h)	905-control	905-stress	2E-control	2E-stress
25	0.007	0.035	0.000	0.016
30	0.000	0.033	0.000	0.031

Calculated trehalose concentration of the samples in terms of glucose content for 905 and 2E in control media and media containing 200 µM $AgNO_3$ at 25th and 30th h are shown in Table 3.17. The glucose standard curve shown in Figure 3.28 was used for calculations.

Table 3.17 : Calculated trehalose content (mg/mL) in terms of glucose content for 905 and 2E in control media and media containing 200 µM $AgNO_3$ at 25th and 30th h.

Time (h)	905-control	905-stress	2E-control	2E-stress
25	0.017	0.037	0.000	0.024
30	0.000	0.036	0.000	0.035

CDW were determined by sampling 1 mL of each culture at two corresponding time points. After pellets were obtained by centrifugation, they were washed twice with ddH_2O, and the pre-weighed microcentrifuge tubes containing cell pellets were dried at 80^{o}C for 24 h and weighed. Trehalose content per CDW was calculated by dividing

the trehalose content in terms of glucose to the corresponding cell dry weight values. The results are shown in Table 3.18.

Table 3.18 : Trehalose content per CDW (mg/mg) for 905 and 2E in control media and media containing 200 µM $AgNO_3$ at 25^{th} & 30^{th} h.

Time (h)	905-control	905-stress	2E-control	2E-stress
25	0.009	0.023	0.000	0.013
30	0.000	0.021	0.000	0.018

Under control conditions, both reference strain and the mutant 2E nearly did not continue to produce trehalose during the last hours of the 30-h cultivation. On the other hand, both of them produced muchmore trehalose under silver stress conditions. Particularly the mutant 2E seemed to continue producing trehalose until the 30^{th} hour of cultivation.

3.3 Global Transcriptomic Analysis of the Silver-Resistant Strain

The mutant 2E was investigated using whole genome transcriptomic analysis in order to investigate the molecular mechanisms of silver resistance. The expression profiles of approximately 6000 genes that make up the yeast genome were compared between the reference strain and the mutant 2E in the absence and presence of 75 µM $AgNO_3$ by using DNA microarray technology (Agilent, USA). First, overnight precultures were incubated in fresh medium (2% YMM) until mid-exponential phase of growth. After RNA isolation was performed by using RNeasy Mini Kit (Qiagen, Germany) with 1 ml samples withdrawn from the cultures at 1 OD_{600} unit of cells, spectrophotometrical (Nanodrop 2000) determination of purified total RNA concentration was done and the results are shown in Table 3.19. RNA integrity number (RIN) of the samples with RNA concentrations higher than 150 ng/µl was determined by using Agilent 2100 BioAnalyzer and the results are shown in Table 3.20. For microarray analysis, RNA samples with RIN values higher than 9 were included.

Table 3.19 : RNA concentrations (ng/µL) of 905 and 2E in control and 75 µM $AgNO_3$ conditions.

Culture	Replicate 1	Replicate 2	Replicate 3
905-control	625	455	595
905-stress	494	665	633
2E-control	380	259	369
2E-stress	506	724	673

Table 3.20 : RIN values of 905 and 2E in control and 75 µM $AgNO_3$ conditions.

Culture	Replicate 1	Replicate 2	Replicate 3
905-control	9.9	10.0	9.7
905-stress	9.2	9.1	9.1
2E-control	9.8	9.4	9.7
2E-stress	9.1	9.1	9.5

GeneSpring software was used for microarray signal analysis. Genes with more than 2-fold change in expression were included in the data analysis.

Gene expression profiles were detected in three segments; 2E as fold of reference strain in control condition, 2E as fold of reference strain in stress conditions, and 2E in stress condition as fold of 2E in control condition. Classification of upregulated and downregulated genes were done in three parts, according to biological process, molecular function, and cellular component by using Slim Mapper in Yeast Genome Database (URL-2). The complete microarray data are available at GEO repository under the accession number GSE143335 (Terzioğlu, Arslan, Kısakesen, Çakar, 2020).

3.3.1 Gene expression profile of 2E under non-stress condition

Microarray analysis revealed that 1657 genes of the mutant 2E had expression changes compared to the reference strain under non-stress condition. 109 of these genes were unknown or dubious open reading frame unlikely to encode a functional protein or a protein, based on the available experimental and comparative sequence data source SGD (URL-2).

3.3.1.1 Induced genes of 2E as fold of 905 under non-stress condition

781 genes were upregulated in silver resistant mutant 2E compared to the reference strain under control conditions. 52 of these upregulated genes were unknown or dubious open reading frame unlikely to encode a functional protein or a protein, based on available experimental and comparative sequence data source SGD. Five-fold and higher upregulated genes are shown in Table 3.21. The genes that were upregulated by less than 5-fold and more than 2-fold are not shown. The genes named *YMR206W*, *HXK1*, and *YNL194C* were the most upregulated genes with fold changes of 246, 113, and 100, respectively.

Table 3.21 : Upregulated genes in 2E by more than 5-fold compared to 905 under control conditions.

Fold (Up) Change	Systematic / Gene Name
>100	*YMR206W, HXK1, YNL194C*
50 - 100	*TMA10, ISF1, GPH1, HXT6, SPG4, MAL12*
20 - 50	*HXT7, CYC7, MRK1, MAL32, HXT2, YFL052W, SLZ1, RGI1, ALD4, YBR285W, TSL1, GSY1, PGM2, BDH2, GLC3, EMI2, YKR075C*
10 - 20	*RTN2, YPT53, MAL11, GPM2, GAC1, YLR149C, YGL258W-A, DDR2, SUE1, YPS5, RGI2, LEE1, NCE103, OM14, IGD1, SOL4, CAR1, DSF1, ATO2, FMP43, MTH1, YER121W, YNR034W-A, SRX1, RTS3, YLR312C, STF1, HSP12, CRC1, CLD1, MSC1, YNR073C, YHR097C, YDR379C-A, ATG15, AIM17, GUT2, SYM1, YER079W, YJL144W, YJR115W, ECM8, SDS24*
5 - 10	*HSP26, PUT1, AGP2, YDR034W-B, CAT8, DCS2, YDR018C, JEN1, UIP4, YGR050C, YFL054C, EMP46, GLK1, IME4, YPR015C, RRT6, ATG8, TFS1, ZTA1, UGX2, RIM4, YPL113C, FMP45, XBP1, RTC3, ATG36, PAI3, CIN5, PRR2, YPK2, YJL163C, SIP2, HXT5, FMT1, USV1, AMS1, ALD3, NQM1, STF2, YNR014W, YML003W, TSA2, XKS1, YKL107W, RRT8, PYK2, ETR1, SFC1, RNY1, AAD15, YPS6, YGL262W, PBI2, RMD5, YPT35, COX5B, FMP46, ECM4, TPS2, FMP16, HSP78, TDA10, YML083C, GCY1, GRX1, YMR084W, YKL091C, CYB2, PCD1, TMA17, GIP2, KIN82, NDE2, YOR289W, SNA2, GAD1, ACH1, IMA1, UGP1, YGR053C, GTO1, PIN3, TDA1, XYL2, YGR066C, RMR1, IME1, URA10, YLR415C, ATG29, HSP42, GIS1, OM45, GSY2, YJR096W, AIM19, YMR196W, GDH3, YSC84, YNL092W, TPK2, YBR053C, OSW2, BXI1, PDC6, GAL7, YAP5*

The analysis of the upregulated genes based on biological process revealed that 90 processes were induced in the silver-resistant mutant 2E under non-stress conditions and the first 20 of them are shown in Figure 3.30. It was observed that response to chemical and carbohydrate metabolic process was significantly induced in the silver-resistant mutant 2E under non-stress conditions. Mitochondrion organization, transcription by RNA polymerase II, transmembrane transport, ion transport, response to oxidative stress, proteolysis involved in cellular protein catabolic process, meiotic cell cycle, generation of precursor metabolites and energy, monocarboxylic acid metabolic process, lipid metabolic process, protein targeting, regulation of organelle organization, protein phosphorylation, protein modification by small protein conjugation or removal, nucleobase-containing small molecule metabolic process, cellular respiration, cellular amino acid metabolic process, cell wall organization or biogenesis were the biological processes constituting the top 20 upregulated processes list.

The analysis of the upregulated genes based on molecular function revealed that 38 functions were induced in the silver-resistant mutant 2E under non-stress conditions and the first 20 of them are shown in Figure 3.31.

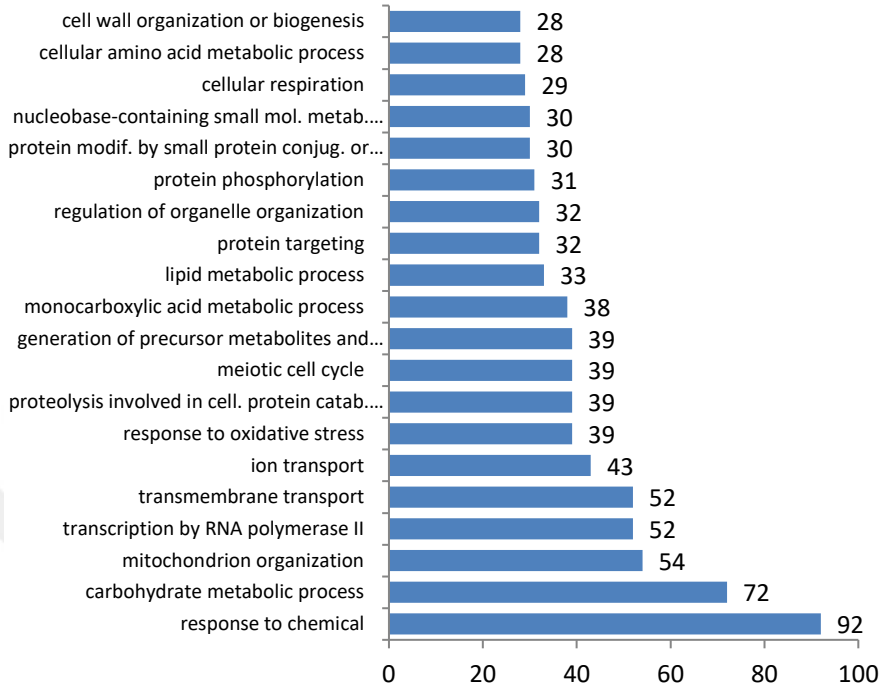

Figure 3.30 : The first 20 biological processes with the highest number of induced genes in 2E compared to 905 under non-stress condition.

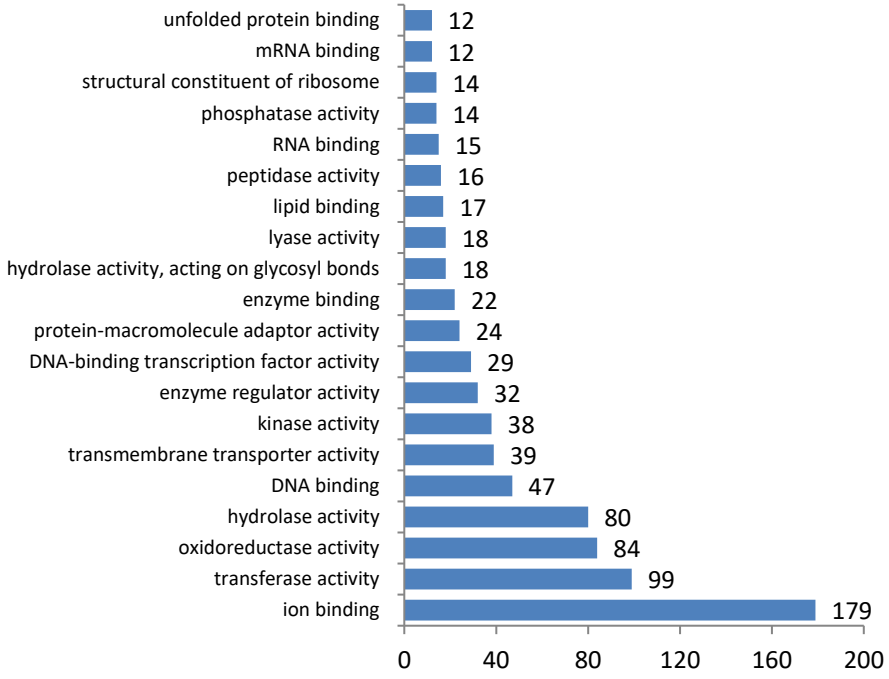

Figure 3.31 : The first 20 molecular functions with the highest number of induced genes in 2E compared to 905 under non-stress condition.

Ion binding was significantly induced in 2E compared to reference strain under non-stress conditions. Transferase, oxidoreductase, and hydrolase activities were also highly induced molecular functions. Other most induced molecular functions were DNA binding, transmembrane transporter activity, kinase activity, enzyme regulator activity, DNA-binding transcription factor activity, protein-macromolecule adaptor activity, enzyme binding, hydrolase activity acting on glycosyl bonds, lyase activity, lipid binding, peptidase activity, RNA binding, phosphatase activity, structural constituent of ribosome, mRNA binding, unfolded protein binding.

The analysis of the upregulated genes based on cellular component revealed that genes belonging to 21 cellular components were induced in the silver-resistant mutant 2E under non-stress conditions and they are shown in Figure 3.32. A significant number of genes related to cytoplasm were also induced. The genes associated with the membrane, nucleus, and mitochondrion were also highly induced.

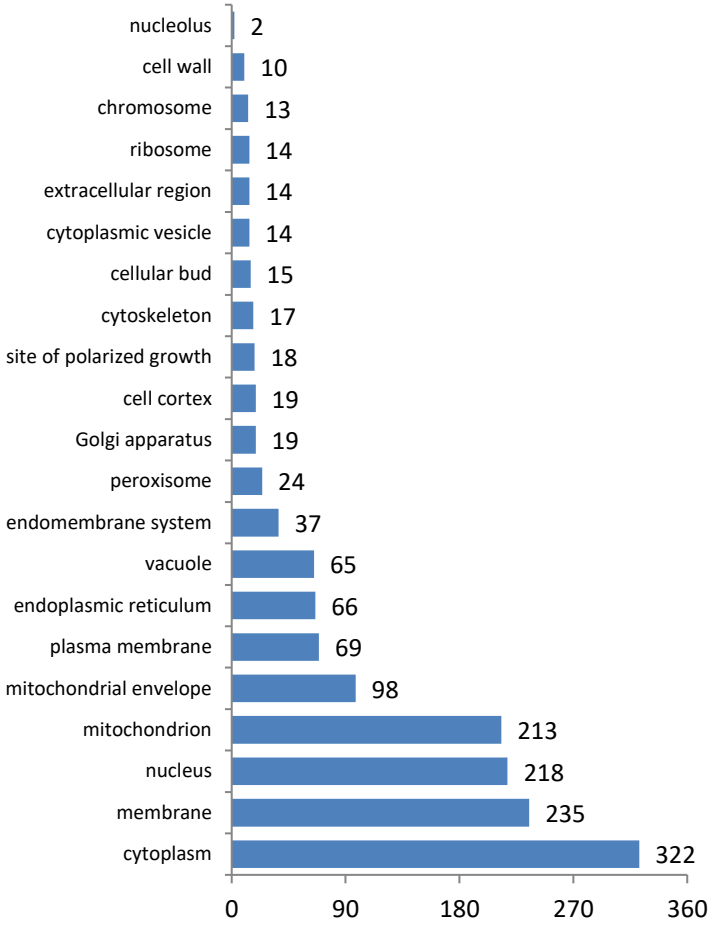

Figure 3.32 : Cellular components with the number of induced genes in 2E compared to 905 under non-stress condition.

3.3.1.2 Repressed genes of 2E as fold of 905 under non-stress condition

876 genes were downregulated in 2E compared to the reference strain under control conditions. 57 of these downregulated genes were unknown or dubious open reading frame unlikely to encode a functional protein or a protein, based on available experimental and comparative sequence data source SGD. Five-fold and higher downregulated genes are shown in Table 3.22. The genes that were downregulated by less than 5-fold and more than 2-fold are not shown. The genes named *ARO3*, *BI2*, *PHO84*, and *ERG20* were the most downregulated genes with fold changes of 76, 74, 68, and 64, respectively.

Table 3.22 : Downregulated genes by at least 5-fold of 2E compared to 905 under control conditions.

Fold (Down) Change	Systematic / Gene Name
50 - 100	*ARO3, BI2, PHO84, ERG20*
20 - 50	*ADH4, SET6, AI3*
10 - 20	*PCS60, SDA1, GRC3, EHD3, EEB1, PDC5, AI5_BETA, HMS1, PRP24, PRM7, PHM6, RNA14, RSA4, TPO2, FUI1, YNL024C, NSR1, TIR2, AAT1, SPO19, AI1, YGR079W, YGR035C, YBR255C-A, ATF2*
5 - 10	*GFD2, NCA3, AQR1, RCL1, RRT5, DBP2, RGS2, RRN11, TIR1, SEO1, YJR124C, KRE33, PRM7, YDR222W, NRP1, NOG2, RLP24, RPC53, KRE29, RPS28B, AAH1, EFM2, CLN1, VTS1, BFR2, HMT1, YLR297W, EKI1, FUR4, AIR1, PCL1, MTC3, HO, ATR1, ALB1, DAD2, TRM13, UTP23, MCH5, ECM1, IRC7, RPC17, BDF2, RIX7, TRM44, SAD1, RKI1, KIN4, DHR2, EFM1, MAK16, KCH1, FAR3, CBF5, TIP1, SNU13, RPA12, HES1, YBR219C, RFU1, PNO1, DBP8, UBP12, IMD4, ATC1, WSC4, NIP7, SPS4, KAP123, YBL081W, YCR087C-A, IPI1, SFG1, IPI3, RRS1, UTP9, YHP1, DRS1, CGR1, FAR1, RPB5, TSR2, RED1, SUI1, NOG1, BAP3, SEE1, YJL193W, YHL050C, FCY22, DBP7, FAA3, URA7, YIL096C, MAK21, CDC6, NOP4, IMP4, HLR1, YAR029W*

The analysis of downregulated genes based on biological process revealed that 93 processes were repressed in the silver-resistant mutant 2E under non-stress conditions and the first 20 of them are shown in Figure 3.33. It was observed that rRNA processing was significantly downregulated in the silver-resistant mutant 2E under non-stress conditions. Ribosomal small subunit biogenesis, ribosomal large subunit biogenesis, transmembrane transport, transcription by RNA polymerase II, ion transport, RNA modification, cytoplasmic translation, response to chemical, mitotic

cell cycle, tRNA processing, regulation of cell cycle, ribosome assembly, peptidyl-amino acid modification, cellular amino acid metabolic process, regulation of translation, nucleobase-containing compound transport, DNA repair, cell wall organization or biogenesis, and nucleobase-containing small molecule metabolic were biological processes constituting top 20 downregulated processes list.

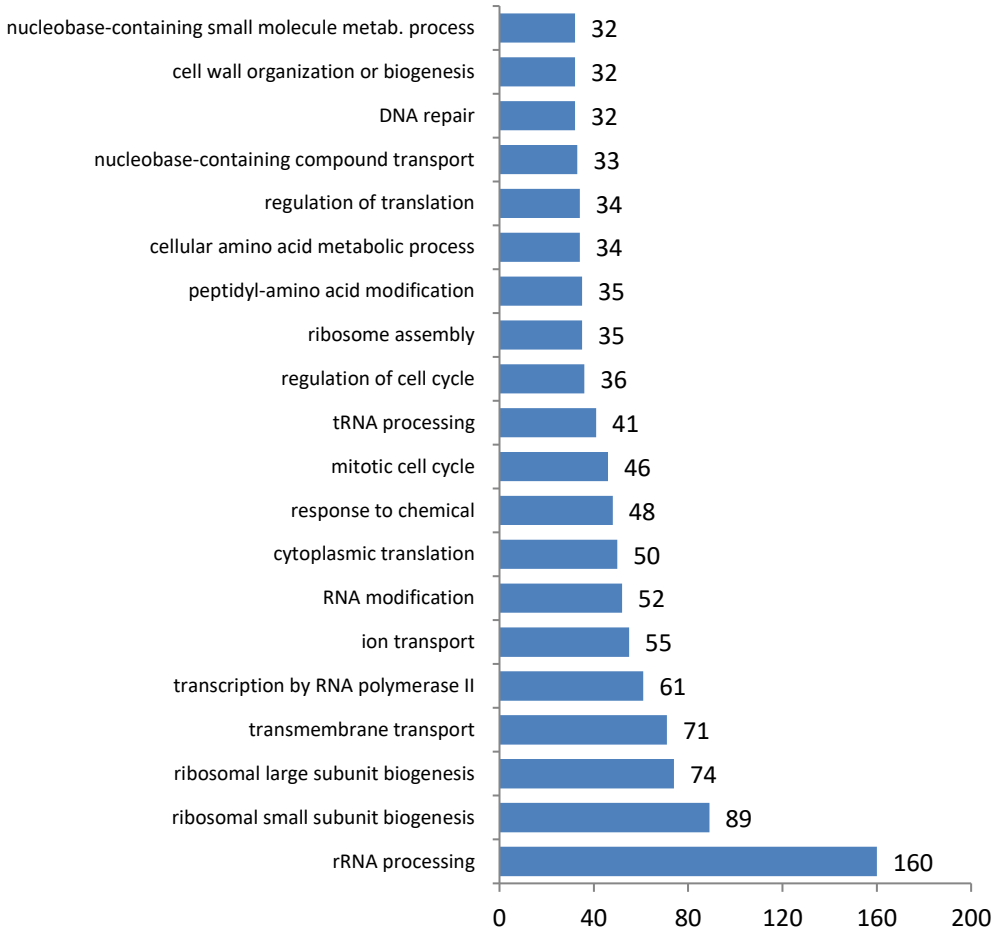

Figure 3.33 : The first 20 biological processes with the highest number of repressed genes in 2E compared to 905 under non-stress condition.

The analysis of downregulated genes based on molecular function revealed that 38 functions were repressed in the silver-resistant mutant 2E under non-stress conditions and the first 20 of them are shown in Figure 3.34. Ion binding was significantly repressed in 2E compared to reference strain under non-stress conditions. RNA binding and transferase activities were also highly repressed molecular functions. Other most repressed molecular functions were hydrolase activity, DNA binding, transmembrane transporter activity, mRNA binding, methyltransferase activity, oxidoreductase activity, structural constituent of ribosome, ATPase activity, rRNA binding, enzyme regulator activity, nucleotidyltransferase activity, helicase activity,

kinase activity, nuclease activity, transferase activity transferring glycosyl groups, DNA-binding transcription factor activity, and chromatin binding.

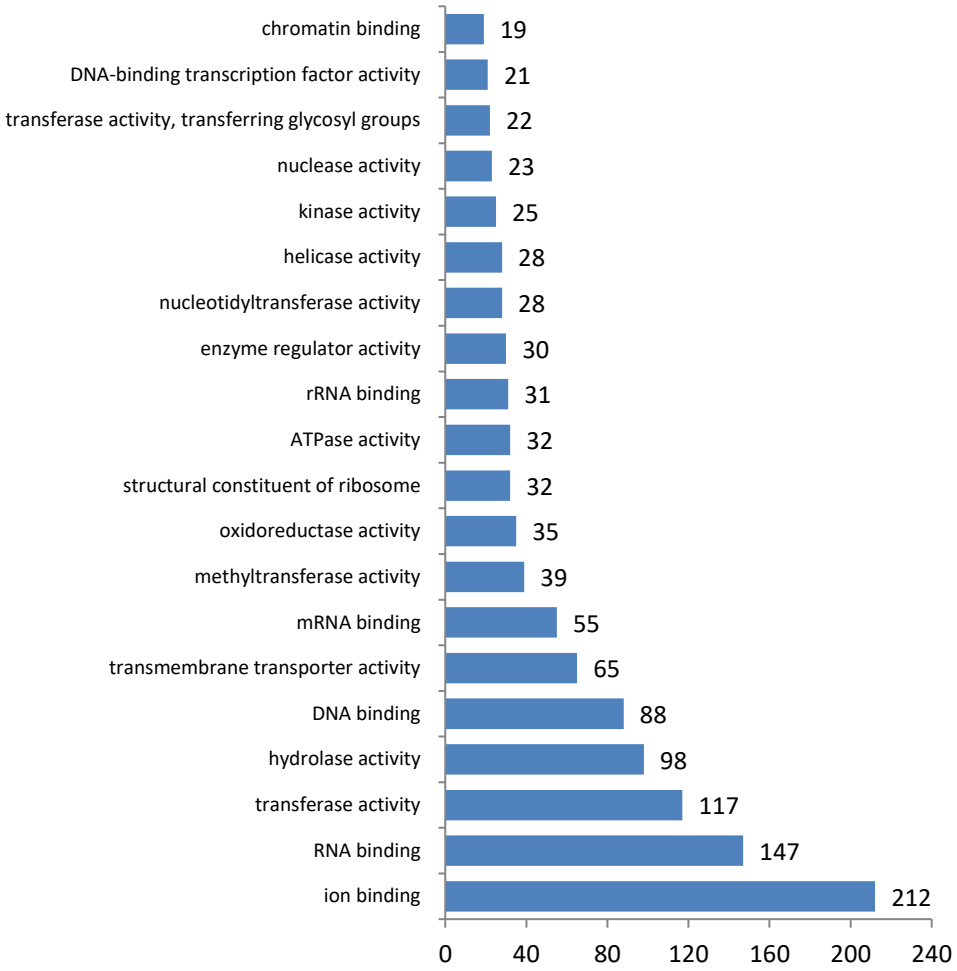

Figure 3.34 : The first 20 molecular function with the highest number of repressed genes in 2E compared to 905 under non-stress condition.

The analysis of the downregulated genes based on cellular component revealed that many genes associated with 21 cellular components were repressed in the silver-resistant mutant 2E under non-stress conditions and they are shown in Figure 3.35. A significant number of genes related to nucleus were repressed. The genes in cytoplasm, membrane, and nucleolus were also highly repressed.

Prominent functional categories of upregulated and downregulated genes in 2E that were found to be directly related to silver resistance and discussed in this study are shown in Table A.1.

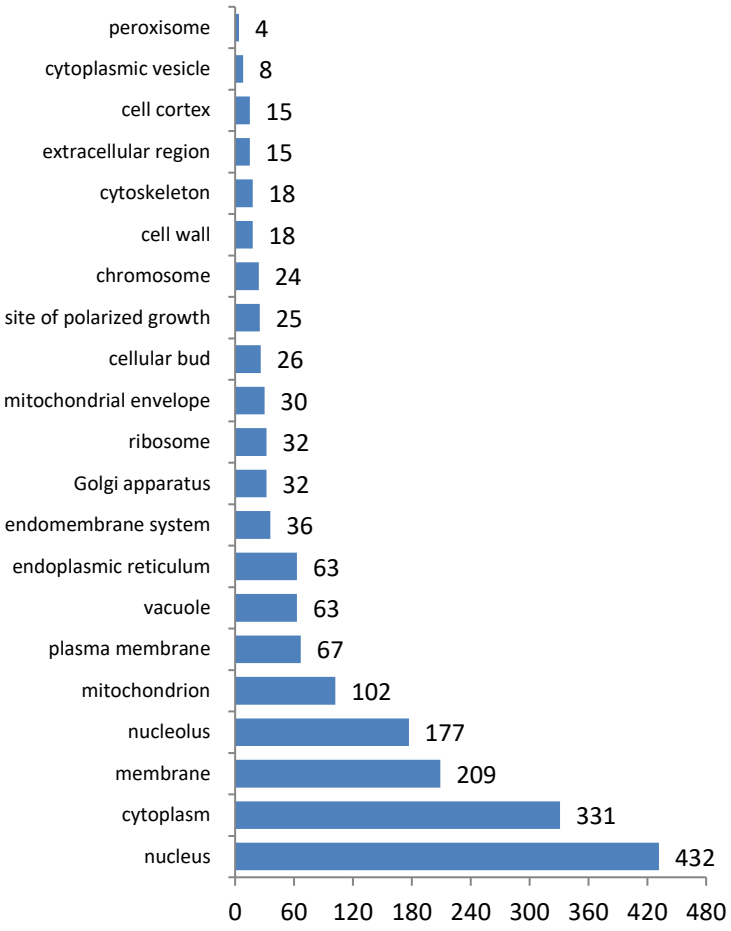

Figure 3.35 : Cellular components with the number of repressed genes in 2E compared to 905 under non-stress condition.

3.3.2 Gene expression profile of 2E under silver stress condition

Microarray analysis results revealed that 8 genes of the mutant 2E had expression changes compared to the reference strain under stress condition (75 µM $AgNO_3$). One of these genes was dubious open reading frame unlikely to encode a functional protein, based on available experimental and comparative sequence data source SGD.

3.3.2.1 Induced gene of 2E as compared to 905 under silver stress condition

Only one gene, *YDR366C*, was 22.22-fold upregulated in 2E compared to the reference strain, under stress condition. It encodes a predicted integral membrane protein whose biological role is unknown.

3.3.2.2 Repressed genes of 2E as compared to 905 under silver stress condition

Seven genes were downregulated in 2E compared to the reference strain under stress condition. One of these genes was dubious open reading frame unlikely to encode a

functional protein, based on available experimental and comparative sequence data source SGD. The downregulated genes are shown with their fold-change, biological process, molecular function, and cellular component in Table 3.23.

Table 3.23 : Downregulated genes of 2E compared to 905 , under stress condition.

Fold Down Change	Systematic / Gene Name	Biological Process	Molecular Function	Cellular Component
8.65	*TIP1*	Fungal-type cell wall organization.	Lipase activity, structural constitute of cell wall.	Fungal-type cell wall, cell periphery, cytosol.
8.08	*YOR008C-A*	Unknown.	Unknown.	Membrane.
7.16	*HO*	DNA recombination, protein maturation.	Ion binding, hydrolase activity, nuclease activity, DNA binding.	Nucleus
4.17	*ATF2*	Response to chemical, lipid metabolic process, generation of precursor metabolites and energy.	Transferase activity.	Membrane, endoplasmic reticulum, cytoplasm, endomembrane system.
3.71	*YDL241W*	Unknown.	Unknown.	Endoplasmic reticulum.
3.42	*ARN1*	Ion transport, cellular ion homeostasis, transmembrane transport.	Transmembrane transporter activity.	Membrane, nucleus, cytoplasm, cytoplasmic vesicle, vacuole, plasma membrane.

3.3.3 Gene expression profile differences of 2E between non-stress and silver stress conditions

Microarray analysis results revealed that 17 genes of the mutant 2E grown under stress condition (75 µM $AgNO_3$) had expression changes compared to 2E grown under non-stress condition. Two of these genes were dubious open reading frame unlikely to encode a protein, based on available experimental and comparative sequence data source SGD.

3.3.3.1 Induced genes of 2E under silver stress condition compared to non-stress condition

Thirteen genes were upregulated in 2E under stres condition compared to control condition. The upregulated genes are shown in Table 3.24 with their fold-change value, the biological process they are associated with, their molecular function and cellular component.

Table 3.24 : Upregulated genes of 2E under silver stress condition compared to control condition.

Fold Up Change	Systematic / Gene Name	Biological Process	Molecular Function	Cellular Component
8.87	*YGP1*	Cell wall organization or biogenesis.	Unknown.	Extracellular region.
7.10	*SPI1*	Cell wall organization or biogenesis.	Structural molecule activity.	Membrane, cell wall, extracellular region.
6.27	*HSP26*	Response to heat, protein folding, response to chemical, response to osmotic stress.	Unfold protein binding, mRNA binding.	Cytoplasm, nucleus, mitochondrion.
6.10	*HSP12*	Response to heat, response to chemical, response to osmotic stress, response to oxidative stress.	Lipid binding.	Cytoplasm, nucleus, plasma membrane.
4.25	*HXT16*	Transmembrane transport, ion transport, carbohydrate transport.	Transmembrane transporter activity.	Membrane.
4.17	*ARN1*	Transmembrane transport, ion transport, cellular ion homeostasis.	Transmembrane transporter activity.	Cytoplasm, nucleus, plasma membrane, membrane, vacuole, cytoplasmic vesicle.
3.90	*IRC15*	Chromosome segregation, regulation of cell wall, meiotic cell cycle, mitotic cell cycle, organelle fission, DNA recombination, cytoskeleton organization.	Ion binding, oxidoreductase activity, cytoskeletal protein binding.	Cytoplasm, mitochondrion.
3.70	*VMR1*	Response to chemical, transmembrane transport.	Ion binding, Transmembrane transporter activity, ATPase activity.	Membrane, mitochondrion, vacuole.
3.57	*GND2*	Regulation of precursor metabolites and energy, monocarboxylic acid metabolic process, carbohydrate metabolic process.	Oxidoreductase activity.	Plasma membrane.
2.74	*SRD1*	rRNA processing.	Ion binding, DNA binding.	Cytoplasm, nucleus.
2.45	*SSE2*	Protein folding, proteolysis involved in cellular protein catabolic process.	Ion binding, enzyme regulator activity.	Cytoplasm, nucleus.
2.38	*AHA1*	Response to heat, protein folding.	Enzyme regulator activity.	Cytoplasm.
2.28	*HSP82*	Response to heat, protein folding, response to osmotic stress, protein targeting, protein maturating, telomere organization, regulation of DNA metabolic process, mitochondrion organization, regulation of organelle organization.	Ion binding, unfold protein binding.	Cytoplasm, plasma membrane, cell wall.

The genes participating in cell wall organization or biogenesis were among the most upregulated ones in 2E, under silver stress condition. The genes related to response to heat, response to chemical, response to osmotic stress, response to oxidative stress were also highly upregulated in 2E under silver stress condition compared to non-stress condition, as expected.

3.3.3.2 Repressed genes of 2E under silver stress condition compared to non-stress condition

Four genes were downregulated in 2E under silver stress condition compared to non-stress conditions. Two of these genes were dubious open reading frame unlikely to encode a protein, based on available experimental and comparative sequence data source SGD (URL-2). *TDR366C* encoding a putative protein whose biological role is unknown was 10-fold downregulated. *GRX4* encoding a glutathion-dependent oxidoreductase was 4-fold downregulated. *GRX4* is involved in actin cytoskeleton organization, cellular iron ion homeostasis, cellular response to oxidative stress, negative regulation of transcription regulatory region DNA binding, and positive regulation of histone deacetylation. It acts in nucleus and enables disulfide oxidoreductase activity, glutathione transferase activity, and RNA polymerase II activating transcription factor binding.

3.3.4 Gene expression profile differences of 905 between non-stress and silver stress conditions

Microarray analysis results revealed that 1467 genes of the reference strain 905 had expression changes under silver stress condition, compared to non-stress condition. Among these, 99 genes were unknown or dubious open reading frame unlikely to encode a functional protein or a protein, based on available experimental and comparative sequence data source SGD (URL-2).

3.3.4.1 Induced genes of 905 under silver stress condition compared to non-stress condition

700 genes were upregulated in 905 under silver stress condition, compared to the control condition. 37 of these upregulated genes were unknown or dubious open reading frame unlikely to encode a functional protein or a protein, based on available experimental and comparative sequence data source SGD. Five-fold and higher

upregulated genes are shown in Table 3.25. The genes that were upregulated by less than 5-fold and more than 2-fold are not shown. The genes named *FIT2*, *SPG4*, *YNL194C HXK1*, and *FIT3* were the most upregulated ones with fold changes of 270, 178, 137, 132, and 120, respectively.

Table 3.25 : Genes upregulated by at least 5-fold in 905 under silver stress condition, compared to control condition.

Fold (Up) Change	Systematic / Gene Name
>100	*FIT2, SPG4, YNL194C, HXK1, FIT3*
50 - 100	*HSP12, YMR206W, FRE5, HSP26, FMP45, GPH1, TIS11, ISF1, TMA10, SLZ1*
20 - 50	*TSL1, DIP5, HXT6, ARO10, HXT7, MRK1, BDH2, JEN1, YPT53, MAL12, YTP1, HXT2, PGM2, CTR3, MAL32, HXT5, DDR2, ALD4, NQM1, YBR285W, ATO2, PHM7, RGI2, RTN2, GSY1, SNO1, CYC7, SPI1, OSW2, SOL4, YKR075C, MTH1*
10 - 20	*RGI1, SUE1, GAC1, YGP1, FET3, ALD3, MAL11, YIL054W, SNZ1, PDC6, GPM2, GTO3, IGD1, FRE1, YLR149C, RTS3, DCS2, ADR1, YNR034W-A, GLC3, FDH1, TKL2, RSB1, SSA4, CCC2, YCR007C, GDH3, YJL144W, EMI2, GCY1, XBP1, GND2, PRM1, SIT1, GPG1, AMS1, ECM4, BTN2, HSP78, HSP82, UIP4, YDR034W-B, MSC1, YMR085W, ENB1, YNL195C, YOL047C, CLD1, GRE1*
5 - 10	*GUT2, YMR084W, HXT15, YER121W, CYB2, TFS1, RTA1, PRM10, ECM8, YKL107W, NCE103, CUP1-1, YHR097C, SDS24, BOP2, MEK1, VMR1, ARO9, BAP3, GRE3, SED1, YJR115W, JLP1, CUP1-2, AQY1, YMR196W, LEE1, PRM5, PIN3, YLR312C, RTC3, YDR379C-A, YNR014W, HBN1, GLK1, YGR066C, BAP2, CSR2, NCA3, YOR338W, GSC2, ATG15, PRB1, HMX1, AIM17, SSA1, YFL054C, FIT1, GIP2, GSY2, FMP40, GAD1, OYE3, PCA1, NDE2, CRC1, HBT1, IRC15, THI4, USV1, TPS2, STF1, CMK2, OM14, YJL163C, ECL1, CAR2, MGA1, CAT8, ARN1, PRM4, DIA3, GYP7, MOH1, AGP2, CTT1, FMP23, YHR022C, YIL169C, YIL055C, YBR085C-A, HPF1, YKL091C, SFC1, YGL081W, RRT6, PRR2, MPH3, YAP5, HSP32, APJ1, IMA1, XKS1, STB2, DDR48, ATH1, MTL1, OPI10, TSA2, YDR018C, YNR064C, UBI4, RIM4, IDH2, CRR1, HSP42, YKL151C, RRT8, PDH1, YAR068W, ATG36, GRX1, YLR030W, YCT1, SYM1, UGP1, VPS73, PIR3, YAR068W, PUN1, YJL213W*

The analysis of the upregulated genes based on biological process revealed that 91 processes were induced in the reference strain under stress conditions and the first 20 of them are shown in Figure 3.36. It was observed that response to chemical was the most upregulated biological process in the reference strain under silver stress condition. Transmembrane transport, carbohydrate metabolic process, ion transport, cell wall organization or biogenesis, monocarboxylic acid metabolic process,

transcription by RNA polymerase II, generation of precursor metabolites and energy, meiotic cell cycle, protein phosphorylation, lipid metabolic process, sporulation, response to oxidative stress, cellular ion homeostasis, endocytosis, proteolysis involved in cellular protein catabolic process, nucleobase-containing small molecule metabolic process, protein targeting, regulation of organelle organization, protein modification by small protein conjugation or removal were the other biological processes constituting the 20 most upregulated biological processes list.

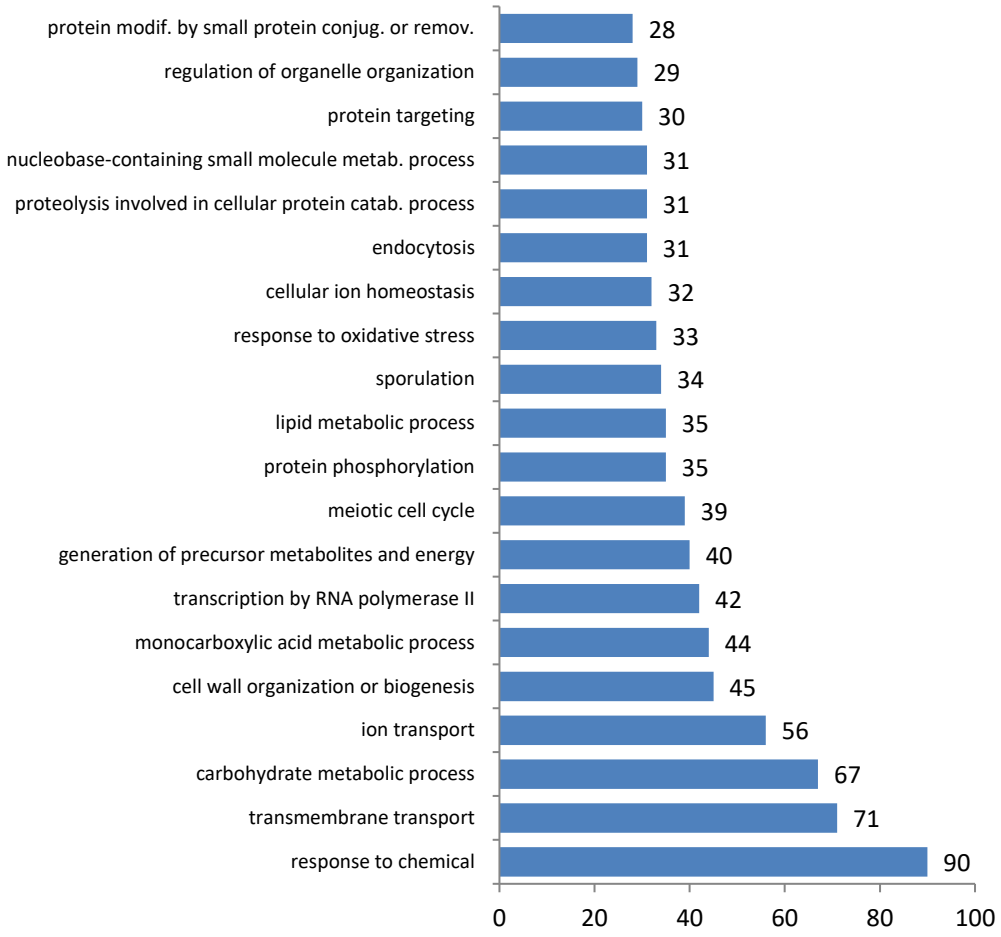

Figure 3.36 : The first 20 biological processes with the highest number of induced genes in 905 under silver stress condition compared to non-stress condition.

The analysis of the upregulated genes based on molecular function revealed that 35 functions were induced in reference strain under stress condition and the first 20 of them are shown in Figure 3.37. Ion binding was the most upregulated molecular function in the reference strain under stress conditions. Transferase activity was also a highly induced molecular function. Other most induced molecular functions were oxidoreductase activity, hydrolase activity, transmembrane transporter activity, kinase activity, DNA binding, enzyme regulator activity, DNA-binding transcription factor

activity, enzyme binding, lyase activity, protein-macromolecule adaptor activity, lipid binding, ATPase activity, transferase activity transferring glycosyl groups, peptidase activity, hydrolase activity acting on glycosyl bonds, RNA binding, phosphatase activity, cytoskeletal protein binding.

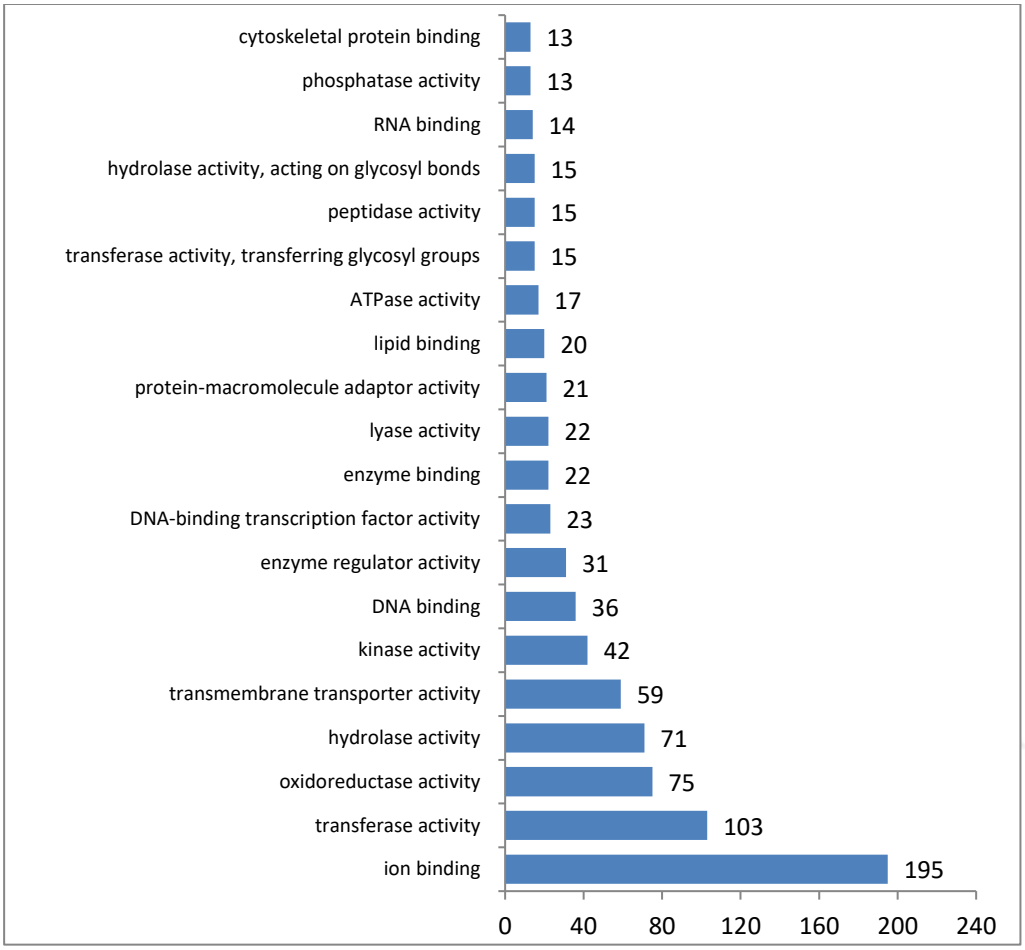

Figure 3.37 : The first 20 molecular function with the highest number of induced genes in 905 under stress condition, compared to non-stress condition.

The analysis of upregulated genes based on cellular component revealed that several genes belonging to 21 cellular components were induced in the reference strain 905 under silver stress conditions and they are shown in Figure 3.38. A significantly high number of genes related to cytoplasm were induced in 905. The genes associated with the membrane, nucleus, and mitochondrion were also highly induced.

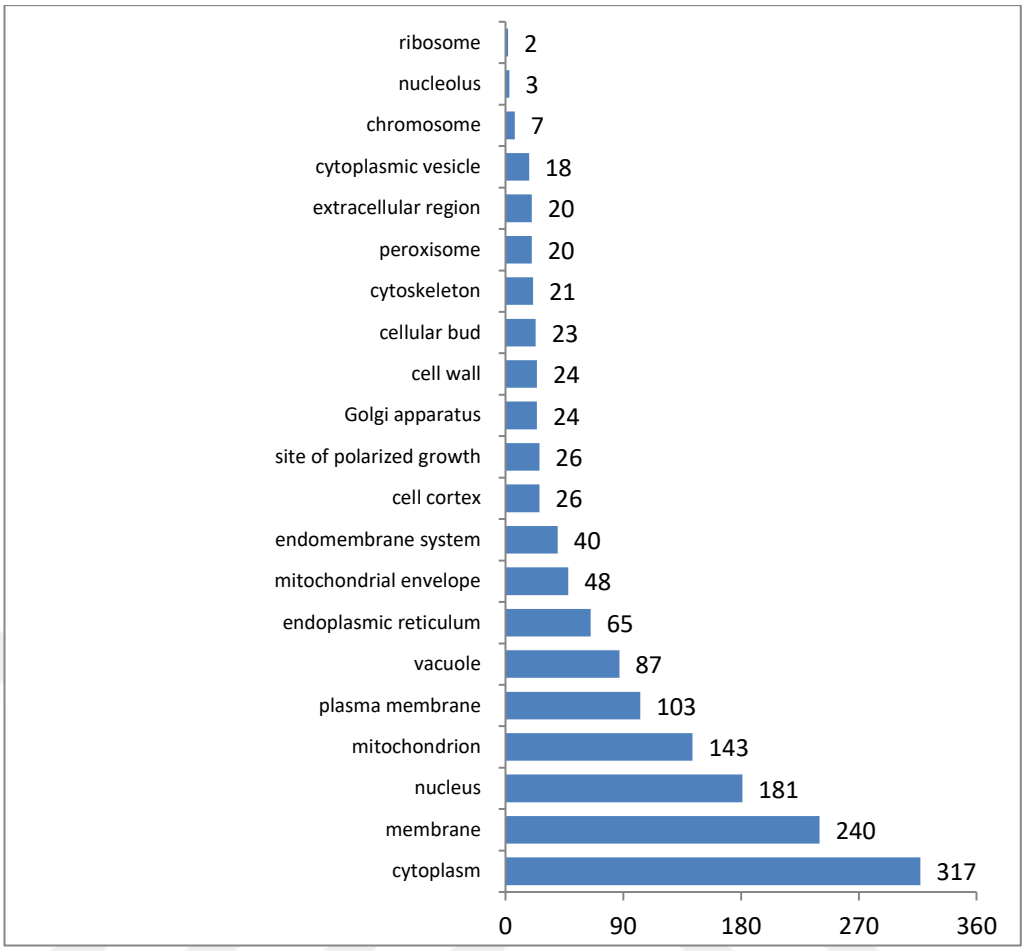

Figure 3.38 : Cellular components with the number of induced genes in 905 under stress condition, compared to non-stress condition.

3.3.4.2 Repressed genes of 905 under silver stress condition compared non-stress condition

767 genes were downregulated in 905 under silver stress condition, compared control conditions. 62 of these downregulated genes were unknown or dubious open reading frame unlikely to encode a functional protein or a protein, based on available experimental and comparative sequence data source SGD. Five-fold and higher downregulated genes are shown in Table 3.26. The genes that were downregulated by less than 5-fold and more than 2-fold are not shown. The genes named *BI2* and *ARO3* were the top downregulated ones with fold changes of 146 and 110, respectively.

The analysis of downregulated genes based on biological process revealed that 93 processes were repressed in the reference strain under silver stress conditions and the first 20 of them are shown in Figure 3.39. Additionally, the first 20 downregulated molecular functions based on the number of downregulated genes in the reference

strainare shown in Figure 3.40. It was observed that rRNA processing was significantly repressed in the reference strain under silver stress condition. Nearly all highly repressed biological processes were the same as in 2E.

Table 3.26 : Genes downregulated in 905 by at least 5-fold under silver stress condition, compared to control condition.

Fold (Down) Change	Systematic / Gene Name
>100	*BI2, ARO3*
50 - 100	*ERG20, AI1*
20 - 50	*ADH4, AI5_BETA, AI3, VAR1, PCS60, SDA1, KRE29, EHD3*
10 - 20	*ZRT1, DAD2, YBR255C-A, MTC7, DBP2, RNA14, PRP24, UTP23, SEO1, SAD1, MTC3*
5 - 10	*GRC3, FAR3, RLP24, HMT1, SET6, TIR2, SPS4, RPC53, KRE33, PHM6, FIN1, CBF5, AAH1, EFM2, YJR124C, IMD4, RPL41B, ECM1, YBL028C, MEP2, SFG1, YHL050C, ALB1, EKI1, YBR298C-A, MRT4, YLR413W, SUI1, YGR035C, RAS1, YNL024C, VPS62, RPB5, NOG2, NSR1, TRM1, GFD2, KNH1, RSC58, GAR1, TMA16, NIP7, RRP36, EFM1, DBP9, BFR2, EFG1, RFC4, YER156C, NOP7, DHR2, YIL096C, SEE1, CDC3, CIC1, TRM13, RSA4, SSP1, YLR363W-A, YLR297W, DAL7, RPC17, NOP58, EBP2, TDA6*

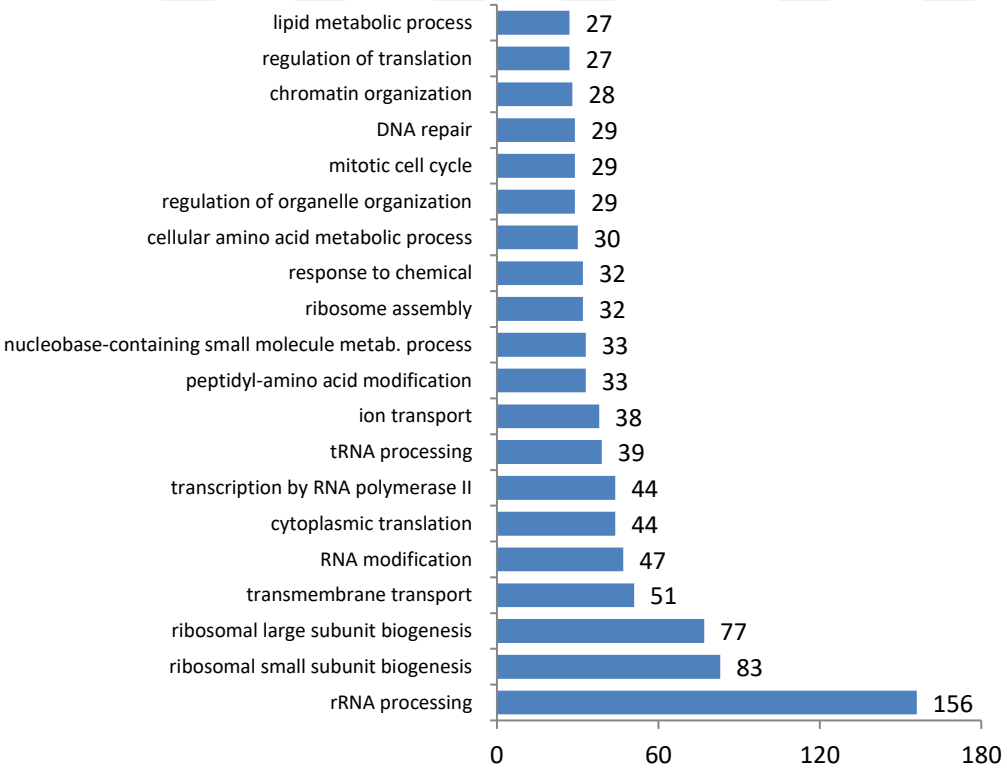

Figure 3.39 : The first 20 biological processes with the highest number of repressed genes in 905 under silver stress condition compared to non-stress condition.

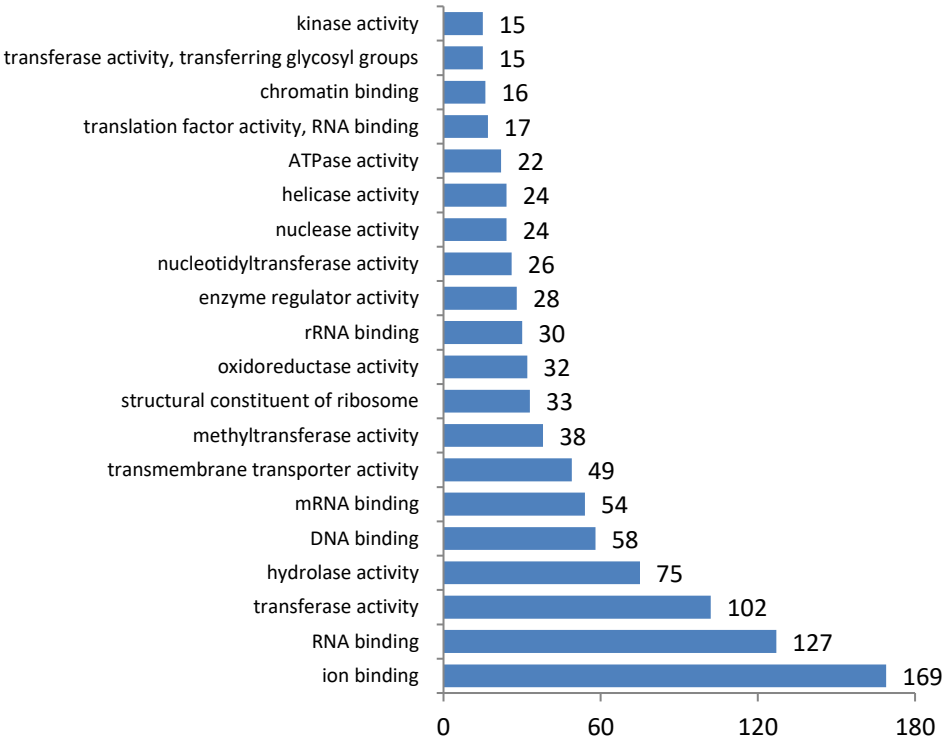

Figure 3.40 : The first 20 molecular functions with the highest number of repressed genes in 905 under silver stress condition compared to non-stress condition.

The analysis of downregulated genes based on cellular components revealed that many genes associated with 21 cellular components were repressed in the reference strain under stress conditions and they are shown in Figure 3.41.

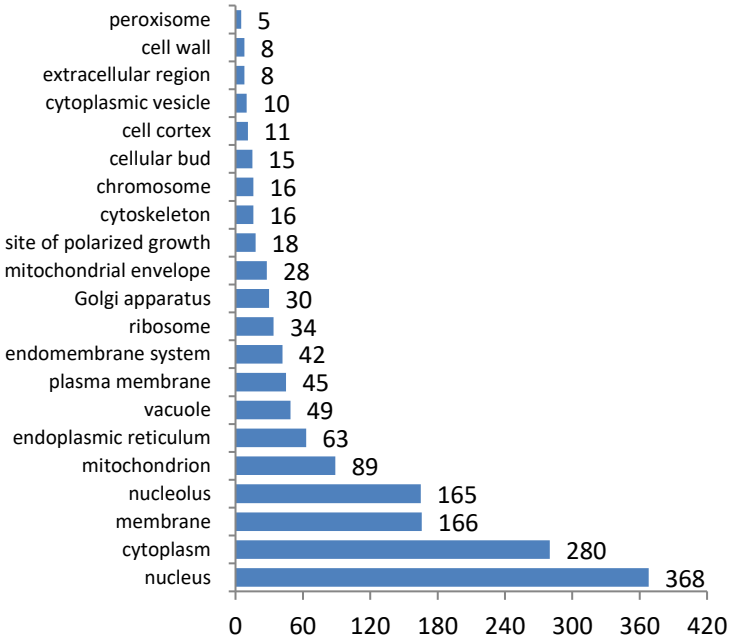

Figure 3.41 : Cellular components with the number of repressed genes in 905 under silver stress condition compared to non-stress condition.

3.4 Whole Genome Re-sequencing

In the silver resistant mutant 2E, 79 mutations were detected in comparison to the reference strain, by using whole genome-resequencing. The results are shown in Table 3.27. Three of these mutations were synonymous and 12 of them were intergenic. Three mutations were transversion type (transformation from A:T to G:C pair) that is typically observed in EMS mutagenesis. Finally, 61 mutations were transition mutations from G:C to A:T pairs.

Table 3.27 : Mutations found in 2E compared to 905 by whole genome-resequencing (Terzioğlu et al., 2020).

Chr	Position	Gene Name	Genetic Change	Amino Acid Substitution	GenInfo Identifier (GI)
XVI	293959	*GIP3*	c.2591 C>T	S864F	392295872
XVI	379191	*RLM1*	c.1928 C>T	T643I	392295920
XVI	795716	*RPS23A*	c.332 G>A	G111D	392296134
XV	256468	Hypothetical	c.23 C>T	P8L	392296295
XV	313108	*TOP1*	c.2017 G>A	E673K	392296327
XV	368141	Hypothetical	c.136 C>T	P46S	392296351
XV	375063	Hypothetical	c.678 G>A	M226I	392296355
XV	396795	*AKR2*	c.295 G>A	V99I	392296365
XV	456518	*GYP1*	c.1285 C>T	L429F	392296400
XV	500355	Hypothetical	c.2143 C>T	P715S	392296422
XV	742819	*STE4*	c.150 T>A	H50Q	392296540
XV	743642	*STE4*	c.973 G>A	A325T	392296540
XV	766792	Hypothetical	c.753 G>A	M251I	392296555
XV	857067	*SNF2*	c.2981 G>A	R994H	392296617
XV	966566	Hypothetical	c.843 A>T	K281N	392296669
XIII	251275	*GIS4*	c.1873 G>A	E625K	392297152
XIII	276393	*PLB1*	c.922 G>A	V308I	392297167
XIII	482542	*MYO5*	c.1430 C>T	P477L	392297270
XIII	523809	*POM152*	c.1492 C>T	P498S	392297291
XIII	534344	*GID8*	c.208 G>A	G70S	392297297
XIII	548220	Hypothetical	c.338 C>T	A113V	392297306
XIII	577584	*DNF3*	c.841 A>G	N281D	392297325
XIII	62944	*CAC2*	c.59 C>T	T20I	392297342
XIII	730295	*PEP5*	c.2008 C>T	P670S	392297401
XIII	143959	*PIF1*	c.2182 G>A	A728T	392297522
XIII	175639	Hypothetical	c.319 G>A	A107T	392297532
XII	531222	*NOP56*	c.481 G>A	A161T	392297708
XII	562269	*CCC1*	c.722 G>A	G241D	392297729
XII	674983	*PIG1*	c.679 C>T	L227F	392297779
XII	170817	*IZH3*	c.1564 G>A	V522M	392297999
XI	311636	*NUP100*	c.1777 G>A	A593T	392298069
XI	375825	*TTI1*	c.712 G>A	V238M	392298105
XI	489121	*GCN3*	c.277 C>T	H93Y	392298169

Table 3.27 (continued) : Mutations found in 2E compared to 905 by whole genome-sequencing (Terzioğlu et al., 2020).

Chr	Position	Gene Name	Genetic Change	Amino Acid Substitution	GenInfo Identifier (GI)
XI	582144	ECM4	c.209 A>C	*70S	392298218
XI	582145	*ECM4*	c.210 A>C	*70Y	392298218
X	97956	*JJJ2*	c.118 C>T	L40F	392298605
VIII	348925	*EPT1*	c.846 G>A	M282I	392298930
VIII	436555	*DBP8*	c.1204 G>A	E402K	392298981
VIII	448266	*FMO1*	c.857 G>A	G286D	392298986
VII	329759	*VPS45*	c.1036 G>A	A346T	392299168
VII	341160	*NUP145*	c.3068 C>T	P1023L	392299171
VII	453355	*STT3*	c.1115 C>T	A372V	392299237
VII	640952	Hypothetical	c.547 C>T	P183S	392299331
VII	806954	*NSR1*	c.436 G>A	A146T	392299413
VII	974878	*YAP1802*	c.1385 G>A	R462K	392299496
VI	261104	*IRC7*	c.815 C>T	A272V	392299619
V	341525	*TSC11*	c.3998 G>A	R1333H	392299796
V	342734	*TSC11*	c.2789 G>A	C930Y	392299796
V	207343	*GAL83*	c.829 G>A	A277T	392299975
IV	256039	*ATG20*	c.1289 C>T	A430V	392300003
IV	344835	*USO1*	c.349 G>A	V117M	392300059
IV	484035	*GCV1*	c.296 C>T	T99I	392300132
IV	537354	*ENA1*	c.218 C>T	A73V	392300150
IV	627378	*RLI1*	c.230 C>T	T77I	392300206
IV	1353090	*ECM11*	c.712 G>A	G238S	392300562
IV	167049	*ENT1*	c.661 G>A	G221S	392300663
II	451882	*ALG1*	c.1113 G>A	M371I	392300950
II	57837	*BOI1*	c.226 G>A	D76N	392300959
II	705697	*RRT2*	c.196 G>A	A66T	392301096
II	127990	*COR1*	c.1301 C>T	A434V	392301170
II	167474	*NCL1*	c.1175 G>A	R392K	392301195
II	193105	*RRN6*	c.2414 C>T	P805L	392301206
I	62204	*ERV46*	c.833 G>A	G278D	392301230
I	162709	*BUD14*	c.139 C>T	H47Y	392301280

Table 3.28 shows the list of the mutations found in 2E that seem to be closely related to silver resistance phenotype.

Table 3.28 : Selected mutations found in 2E compared to 905 by whole genome-resequencing, may be related to silver resistance (Terzioğlu et al., 2020).

Gene Name	Genetic Change	Amino Acid Substitution	Description
CCC1	c.722 G>A	G241D	Vacuolar Fe^{2+}/Mn^{2+} transporter
GIS4	c.1873 G>A	E625K	CAAX box containing protein of unknown function proposed to be involved in the RAS/cAMP signaling pathway

Table 3.28 (continued) : Selected mutations found in 2E compared to 905 by whole genome-resequencing, which may be related to silver resistance (Terzioğlu et al., 2020).

Gene Name	Genetic Change	Amino Acid Substitution	Description
IZH3	c.1564 G>A	V522M	Membrane protein involved in zinc ion homeostasis; member of the four-protein IZH family
MYO5	c.1430 C>T	P477L	One of two type I myosin motors that contains proline-rich tail homology 2 (TH2) and SH3 domains
NSR1	c.436 G>A	A146T	Nucleolar protein that binds nuclear localization sequences required for pre-rRNA processing and ribosome biogenesis
NUP100	c.1777 G>A	A593T	FG-nucleoporin component of central core of the nuclear pore complex
PIF1	c.2182 G>A	A728T	DNA helicase that promotes DNA synthesis during break-induced replication
RPS23A	c.332 G>A	G111D	Ribosomal protein 28 (rp28) of the small (40S) ribosomal subunit required for translational accuracy
TOP1	c.2017 G>A	E673K	Topoisomerase I; nuclear enzyme that relieves torsional strain in DNA by cleaving and re-sealing the phosphodiester backbone
TSC11	c.3998 G>A	R1333H	Subunit of TORC2 (Tor2p-Lst8p-Avo1-Avo2-Tsc11p-Bit61p); TORC2 is a membrane-associated complex that regulates actin cytoskeletal dynamics during polarized growth and cell wall integrity
	c.2789 G>A	C930Y	

4. DISCUSSION

A genetically stable and silver-resistant *Saccharomyces cerevisiae* strain was successfully obtained in this study by using evolutionary engineering. Previous studies showed that when *S. cerevisiae* was subjected to silver nanoparticles (AgNPs) causing silver ion release, its crucial cellular functions were disrupted or decreased including vesicular transport activities, endocytosis, RNA pocessing, oxidative metabolism, cellular respiration, transcription, and DNA replication activities (Marquez et al., 2018), cell wall and membrane integrity, cell wall formation (Horstmann et al., 2019), and copper homeostasis (Niazi et al., 2011). These studies used either wild-type *S. cerevisiae* S288C cells (Horstmann et al., 2019; Niazi et al., 2011) or its deletion collections (Marquez et al. , 2018), and observed their silver stress response. Unlike these previous studies, an evolved strain of *S. cerevisiae* that was highly resistant against silver stress was obtained through the mutation and systematic selection and the changes in global gene expression of this strain were also investigated in this study.

Holland et al. reported in 2011 that copper and silver had common resistance mechanisms in yeast cells as expected, because copper and silver are both transition metals participating in Group B in the Periodic Table and have similar electronic configurations of the monovalent cations. *S. cerevisiae* showed high copper resistance by upregulating *CUP1-1* and *CUP1-2* genes strongly (Niazi et al., 2011); these two genes encode a metallothionein protein and this metallothionein binds copper. Silver-resistant mutant 2E was also hyper-resistant to copper stress as it was detected in cross-resistance analysis and shown in Figure 3.8. When microarray analysis results of the silver-resistant mutant 2E were compared to those of the reference strain (shown in Table A.1), it was seen that the genes encoding the copper-binding proteins *CUP1-1, CUP1-2, CTR3,* and *CUP2* as the transcription factor were also induced. Copper-homeostasis is regulated by *CUP1-1, CUP1-2, CTR3,* and *CUP2* in eukaryotic cells (Rutherford and Bird, 2004).

The mutation lists (Table 3.27 and Table 3.28) prepared as a result of the comparison of the whole genome re-sequencing of both the silver resistant mutant and the

reference strain indicated that vacuolar Fe^{2+}/Mn^{2+} transporter encoding gene *CCC1* had a missense mutation in the mutant 2E and that might be one of the reasons of how 2E resisted against copper, as the transition metal sensitivity of the yeast cell is affected by Ccc1 through mitochondria–vacuole signaling pathway. In 2014, Xu et al. showed that copper resistance was improved as a result of the deletion of *CCC1* in *S. cerevisiae*. As copper and silver have common resistance mechanisms in yeast, improvement of the molecular components by the missense mutation in *CCC1* that provided copper resistance may have also improved silver resistance in the mutant 2E. In addition to its copper-homeostasis function in yeast, *CCC1* is also responsible for mediation of the storage of vacuolar iron by transferring iron from the cytosol to the vacuole. It has been proved that external iron sensitivity increased in Δccc1 yeast cells (Li, Miao, Jia, Ward, Kaplan, 2014). As shown in Figure 3.8 (B), the cross-resistance test results by spot assay in the media with 25 mM and 50 mM $(NH_4)_2Fe(SO_4)_2$ concentrations revealed that the silver-resistant mutant 2E was significantly sensitive to iron stress. As a result, iron sensitivity of 2E is expected with the potential contribution of missense mutation in *CCC1*.

Mitochondrial activities including cellular respiration decrease during silver stress, however, they are known to increase upon oxidative stress (Horstmann et al., 2019; Marquez et al., 2018). A recent study showed that when wild-type *S. cerevisiae* cells were subjected to silver stress, some oxidative stress responsive genes were differentially expressed: while *ZTA1* and *TSA2* were downregulated, *LTV1* was upregulated (Horstmann et al., 2019). Regarding the silver-resistant evolved strain 2E which has also a high oxidative stress resistance, *TSA2* and *ZTA1* were induced by 6.95-fold and 7.98-fold, respectively, and *LTV1* was repressed by 2.75-fold. It is not surprising that the observed changes in the gene expression of the silver-resistant evolved strain in the absence of any silver stress may be the opposite of the observed changes in the gene expression of wild-type *S. cerevisiae* strains in the presence of silver stress. With the downregulation of 100 and upregulation of 210 mitochondrial genes, the mitochondria-related gene expression profile of the evolved strain 2E was differential compared to the reference strain. A more active aerobic metabolism is indicated as a result of the upregulation of *NDI1*, *SDH1*, *SDH4*, *RIP1*, *SDH2*, *COX7*, *COX13*, *YTP1*, *SDH3*, and *CYC7*. These genes are among the 210 upregulated

mitochondrial genes in the evolved strain 2E and encode proteins functioning in the electron transfer system.

Many genes related to oxidoreductase activity (Table A.1) were upregulated in the evolved strain 2E, compared to the reference strain. As prominent examples, glutathione peroxidase 1 (*GPX1*) gene was upregulated along with the *SOD1* and *SOD2* genes encoding cytosolic and mitochondrial superoxide dismutases. Upregulation of *GRX1* and *GRX2* genes in 2E were also detected in comparison to the reference strain. Marquez et. al. observed in 2018 that *S. cerevisiae* mutants deleted in the genes *SOD1* and *ETR1* that encodes 2-enoyl thioester reductase showed sensitivity against silver stress. The silver-resistant mutant 2E had upregulated these two genes by 2.29 and 6.69-fold, respectively. Therefore, this upregulation supports the hypothesis that silver stress and oxidative stress resistance of the evolved strain 2E could be associated with these two genes.

CCC1 as the vacuolar iron transporter gene, and *PIF1* as the DNA helicase gene were both detected with missense mutations in the silver-resistant mutant 2E. These mutations might also have key roles in the oxidative stress resistance of 2E. Mmt1 and Mmt2 are both cation diffusion facilitator transporters. In 2014, Li et al. showed that overexpression of *MMT1* and *MMT2* genes led to an increase in hydrogen peroxide sensitivity, and their overexpression were suppressed by deletion of *CCC1*.

In addition to these studies, in 2010, Guirola et al. observed that *PIF1*-deleted cells grown in media with high zinc concentrations expressed oxidative stress response genes at higher levels. It was also shown that *S. cerevisiae* improved hydrogen peroxide resistance as a result of the deletion of the *TOP1*, *GIS4*, *RPS23A*, and *NUP100* genes (Brown et al., 2006) and the silver-resistant mutant 2E also has missense mutations in these genes. These studies might help explain how the evolved strain 2E resisted against oxidative stress along with the silver stress, as oxidative damage can be caused in cells by silver, as well as other metals. In 2012, Cherry et al. found that both the homozygous diploid null mutation in *BOI1* and null mutations in *GIP3, RRN6, NSR1, COR1, IZH3, USO1, VPS45, SNF2* led to a decrease in oxidative stress resistance and additionally *NCL1* generated oxidative stress hypersensitivity. On the other hand, upon 3 mM H_2O_2, resistance to oxidative stress increased with the null mutations in *GIS4, RPS23A, TOP1,* and *NUP100* genes (Brown et al., 2006). There are missense mutations in the silver-resistant mutant 2E in all of these genes (Table

3.27 and Table 3.28). Thus, further investigation of these significant changes regarding the mechanism of oxidative stress resistance observed in 2E is needed.

The studies investigating *S. cerevisiae* for its transcriptomic effects caused by silver nanoparticles and/or silver ions are limited and how the cell wall of yeast is affected by silver is yet to be clarified. In 2011, wild-type *S. cerevisiae* cells were exposed to ionic silver ($AgNO_3$) and AgNPs by Niazi et al. and it was found that the yeast cell wall was most likely damaged mechanically because of the significant changes in the expression of genes related to cell wall proteins by AgNPs during the initial growth phase of the yeast cells. Additionally, the expression of the genes related to membrane-bound transport proteins were also significantly changed during the exposure to AgNPs.

In 2018, Marquez et al. found that the deletion of genes participating in cell wall integrity and function in *S. cerevisiae* caused high sensitivity to zinc oxide nanoparticles (ZnOPs) and these *S. cerevisiae* deletion strains showed no sensitivity to AgNPs. A more recent investigation of wild-type *S. cerevisiae* cells affected by AgNPs revealed through transcriptomic analysis that many genes participating in cell wall biogenesis and organization were differentially expressed (Horstmann et al., 2019). Among these differentially expressed genes, the genes encoding cell wall mannoproteins *DAN1*, *TIP1*, *TIR1*, *TIR2*, *TIR3*, and *TIR4* were supressed and the genes *RNT1* and *YVH1* were induced. The silver-resistant mutant 2E repressed the genes *TIR1*, *TIR2*, *TIR3*, *TIR4* and *TIP1* (Table A.1). In addition to the downregulation of *TIP1* gene in 2E compared to the reference strain under control conditions, it was also strongly downregulated (8-fold and the most among downregulated genes) by the mutant 2E compared to the reference strain under silver stress conditions (Table 3.23). *TIP1* encodes the major cell wall mannoprotein of *Saccharomyces cerevisiae* functioning likely on lipase activity and *TIP1* gene expression is induced during cold- and heat-shock (Fujii et al., 1999). 2E also repressed the genes *YVH1* and *RNT1* by 3.69- and 2.91-fold, respectively, along with these downregulated cell wall mannoprotein genes. However, there was no differential expression of the gene *DAN1* in the mutant 2E, although the wild-type *S. cerevisiae* had downregulated *DAN1* strongly (174-fold) when exposed to AgNPs (Horstmann et al., 2019). In 2019, Horstmann et al. found that the reason for the thickness of yeast cell wall after AgNP treatment was the binding of Ag^+ ions on the cell wall and causing cell membrane

integrity disruption, by showing that there could not be an accumulation of these mannoproteins and glucans because of the downregulation of these cell wall-related genes. They thought that the thickness of the cell wall because of the Ag^+ ions caused the cell not to produce mannoproteins for a thick membrane which led to the cell wall degradation.

It was also indicated by Horstmann et al. that genes related to regeneration of NADH (*GUT2* and *ALD4*), synthesis of ergosterol (such as *ERG11, ERG28, ERG5, ERG3, ERG6* and *ERG25*), tricarboxylic acid (TCA) cycle (*CIT3, CIT2, ACO1*), and membrane sugar transporters (such as *HXT2, HXT17*, and *HXT13*) were repressed during the exposure of wild-type *S. cerevisiae* to AgNPs. Cell wall stability assay results of wild-type *S. cerevisiae* in the same study indicated that the yeast cells treated with AgNPs became more susceptible to cell wall damage in comparison to the yeast cells under control conditions. It can be concluded that when yeast cells are subjected to silver nanoparticles, integrity of the plasma membrane and the cell wall is disturbed significantly (Horstmann et al., 2019). However, there is no differential expression in the silver-resistant mutant 2E of these ergosterol synthesis genes, which had been reported by Horstmann et al. (2019) as downregulated. The evolved strain 2E also significantly induced NADH regeneration gene *GUT2* (10.70-fold), some TCA cycle genes (*MDH1* 2.83-fold, *CIT1* 4.06-fold), and many of the sugar transporter genes (such as *HXT2*, *HXT7* and *HXT6*) as shown in Table A.1.

Downregulation of *TIR1*, *TIR2*, *TIR3*, *TIR4*, and *TIP1* genes might also have resulted in a strong aerobic growth for the mutant 2E in addition to the upregulation of high-affinity glucose transporter genes *HXT2*, *HXT6*, *HXT7* and also most of the mitochondrial genes, as the yeast cell wall mannoprotein encoding genes, *TIR1*, *TIR2*, *TIR3*, and *TIR4*, are in fact called anaerobic genes and it was reported that they are expressed under anaerobic conditions and needed for anaerobic growth (Cohen et al., 2001 and Abramova, Sertil, Mehta, Lowry, 2001). It was also observed that lactate levels did not increase in *Daphnia magna* treated with silver nitrate, thus the silver ions apparently did not induce anaerobic metabolism in this organism (Li et al., 2015). This adaptation may help explain the better growth and lower death rate of the mutant under silver stress conditions.

In the silver-resistant mutant 2E, while the activator of *TIR* genes, *UPC2*, was downregulated by 3.75-fold, the repressor of *TIR* genes, *ROX1*, was upregulated by

2.91-fold. There were also other cell wall-associated genes in 2E that were strongly induced such as *SRL1* (2.21-fold), *YPS6* (6.48-fold), *USV1* (7.23-fold), and *YPK2* (7.46-fold) (Table A.1), although *TIR1*, *TIR2*, *TIR3*, *TIR4*, and *TIP1* genes were downregulated. One of the reasons for the change in the cell wall integrity of 2E may be the mutations identified in 2E genes participating in fungal type cell wall organization. As shown in Table 3.27 and Table 3.28, *RLM1*, *TSC11*, *ECM11*, and *MYO5* have missense mutations and *ECM4* has a stop-lost mutation in the silver-resistant mutant 2E. *TSC11* gene encodes the subunit of the membrane-associated complex that regulates cell wall integrity (Cherry et al., 2012). *ECM4* gene encodes proteins participating in cell wall structure. Along with these two genes related to cell wall integrity, the *RLM1* gene is also encoding a transcription factor located downstream of the *MPK1* gene known having two main functions as the maintenance of cell wall integrity and *MPK1* mitogen-activated protein kinase pathway activation (Cherry et al., 2012).

RLM1 has 707 potential gene targets according to the Yeastract+ database (Monteiro et al., 2019). 131 of those potential 707 targeted genes were expressed differentially (adj.p<0.05 and >2-fold) in the silver-resistant mutant 2E, thus, *RLM1* probably affects 2E significantly on silver resistance and cell wall integrity due to this differential expression profile. All these upregulated and downregulated genes in 2E related to cell wall integrity indicate that the mannoprotein genes induced anaerobically in yeast cell were repressed, but other cell wall-associated genes that are highly active during aerobic metabolism were upregulated. Additionally, mutations observed in the cell wall-associated genes and especially in *RLM1* as the transcription factor gene provided a more robust cell when compared to the cell wall integrity of the reference strain. The lyticase sensitivity test result shown in Figure 3.28 confirms this implication.

The silver-resistant mutant 2E contained in/on itself higher silver levels than the reference strain according to the results of F-AAS analysis (Figure 3.27). *PEP5* and *VPS45* genes are participating in vacuole biogenesis and vesicle protein sorting; *AKR2*, *YAP1802*, *ENT1*, and *MYO5* genes have important roles in endocytosis (Cherry et al., 2012). All these genes have missense mutations in the evolved strain 2E. Previous studies showed that aluminum, manganese, and zinc resistance decreased with the null mutation of *VPS45* in *S. cerevisiae* (Kakimoto et al., 2005; Yadav, Muend, Zhang, Rao, 2007; Pagani, Casamayor, Serrano, Atrian, Arino, 2007). In another study, it was

observed that resistance of *S. cerevisiae* against other metals such as nickel, cadmium, and zinc were decreased with the null mutation on *PEP5* gene (Ruotolo, Marchini, Ottonello, 2008; Pagani et al., 2007). Other null mutations in *S. cerevisiae* that led to a decrease in resistance against several chemicals were in *AKR2*, *MYO5*, *YAP1802*, and *ENT1* genes of yeast cell (Cherry et al., 2012). *AAC1*, *APL2*, *APL1*, *APM4*, and *ENT3* genes are participating in vesicular transport and clathrin-mediated endocytosis, and it was reported in 2018 by Marquez et al. that *S. cerevisiae* mutants obtained by deletion of these genes became highly sensitive to AgNPs. It was indicated in that study that AgNPs affected endocytosis through impairment of membrane functions which was a general effect of metal ions on yeast membrane. *AAC1* gene was 3.15-fold induced by the silver-resistant mutant 2E and it was among the genes reported by Marquez et al. in 2018. Expression profiles of these genes in the evolved strain 2E imply that one of the significant contributor for the improved silver resistance in 2E may be the modified transport and endocytosis processes.

In a study in 2016, Eid et al. investigated *RGI1* encoded protein for its pro-survival activities in *S. cerevisiae*. The sequence identity of the *RGI1* gene is at a level with the ferritin protein-encoding gene *Fth1*. *FTH1* decreases iron toxicity by binding and storing iron, and also damage of reactive oxygen species (ROS), and finally cell death due to stress. When treated with copper stress (as an apoptotic inducer) conditions, yeast viability was enhanced by the expression of *RGI1* by preventing ROS-induced stress. Apoptotic pathways stimulated by ROS or not by ROS were considered in *C. albicans* (Radhakrishnan et al., 2018), but the situation is not clear for *S. cerevisiae* as well as for *RGI1* with its unknown function in oxidative stress. It was also found that there was a condition at some level of AgNP which inhibited the growth but not led to cell death and ROS increase in *S. cerevisiae*, which means that the yeast was able to survive against oxidative stress at some level (Lee et al., 2019). *RGI1* was upregulated by 32-fold in the evolved mutant 2E (Table A.1) and this upregulation might also play a key role of survival of the silver-resistent mutant under silver-induced oxidative stress, because of the close relationship between copper and silver resistance pathways.

One of the four genes downregulated by the silver-resistant mutant 2E compared to the reference strain under silver stress condition is *HO*. It encodes homothallic switching endonuclease that is required for gene conversion at mating-type locus and involves in mating type switching, a two-directional conversion process of MATa and

MATalpha cells by changing activation of mating gene sets (Nasmyth, 1993). This kind of switching stimulated by *HO* expression occurs at the end of G1 period of the mitotic cell cycle *of Saccharomyces cerevisiae* when the cell cycle is arrested by mating factors. If *HO* gene is downregulated or turned off, the yeast cell remains stable in a/α diploid cell form (Herskowitz, 1988). *HO* gene was repressed by 7-fold (Table 3.23) in 2E under silver stress condition during mid-exponential growth phase and *HO* was also downregulated between 5- and 10-fold (Table 3.22) in 2E under control condition showing the mating tendency of mutant 2E with or without stress factors which may indicate that diploidization is a phenotype of the silver resistant mutant 2E. Haploid cells cope with DNA damage with the copy of chromosomes and also a/α diploids have the increased ability of DNA repair and recombination than α/α of a/a diploids (Mortimer, 1958). One of the toxic effects of silver and metals is the impairment of DNA repair and one of the responses of yeast cells against metal toxicity is changing cell cycle progression (Wysocki and Tamas, 2010). It was reported that response pathway of DNA damage targeted degradation of *HO* endonuclease (Kaplun et al., 2000). All these findings may indicate that the mutant 2E postpones its cell cycle progression, remains in diploid form and also improves DNA repair by downregulating *HO* gene which may also cause slower growth compared to the reference strain in control conditions. However, the whole genome re-sequencing analysis of 2E did not reveal any diploidization in its genome, despite a downregulation in the *HO* expression levels according to the transcriptomic results which remains to be investigated in more detail.

Copper ions inhibit the glucose-dependent H^+ efflux system in *Saccharomyces cerevisiae* and it was reported that calcium ions were used by the yeast cells to alleviate this inhibition (Karamushka et al., 1994). When yeast cells are exposed to high concentrations of copper ions, high level of calcium is stored in cytosol and causes cell death. On the other hand, it was reported that after the deletion of calcium channel gene *CCH1* and vacuolar calcium channel gene *YVC1*, lower elevations of copper-induced calcium ions were detected in cytoplasm and led to adaptation under copper stress (Ruta et al., 2016). It was also observed that oxidative stress caused a similar cell behavior as the response with Ca^{2+} (Popa et al., 2010). It was reported that the acetyltransferase gene *ATF2*-deleted *S. cerevisiae* mutant accumulated less calcium (URL-2). *ATF2* was downregulated in the silver-resistant mutant 2E compared to the

reference strain under control and silver stress conditions by 5-10 fold and 4 fold, respectively. As copper and silver are thought to stimulate similar response mechanisms and 2E has both copper and oxidative stress resistance, repression of the *ATF2* gene when compared to the reference strain may be one of the contributors of higher silver resistance than the reference strain, by providing cell viability upon preventing Ca^{2+} elevation in cytosol.

Copper, zinc, and chromium are essential metals and it was reported that due to the close relationship between silver and these metals, silver could be sensed as essential and used in some biological activities for substitution in deficiency of essential metals (Carri et al., 1991). *ARN1* gene encodes an iron transporter participating in the maintainance of iron homeostasis and being regulated by the iron transcription factors (Blaiseau et al., 2001). It was reported that yeast cells with increased expression of the genes functioning in iron transport were likely to remove the excessive metal and protect the cell (Jin et al., 2008). As expected with this report, both the silver-resistant mutant 2E and the reference strain increased their *ARN1* gene expression under silver stress condition compared to their expression levels under control condition, by 4-fold (Table 3.24) and 6-fold (Table 3.25), respectively. On the other hand, there was no expression difference under control condition and the expression level of *ARN1* gene in 2E was 3-fold lower than that of the reference strain under silver stress condition. In addition to *ARN1*, glutathione-dependent oxidoreductase and glutathione S-transferase *GRX4* gene were also downregulated by the silver resistant mutant 2E under stress condition, compared to control condition. *GRX4* participates in iron homeostasis regulation and iron signaling pathway, and it provides adaptation to high iron concentrations (Martinez-Pastor et al., 2017). Thus, the *ARN1* and *GRX4* gene repression profiles of 2E may be linked with the iron sensitivity.

The silver-resistant mutant 2E expressed a very low number of genes differentially under silver stress condition compared to control condition which means that it was evolved as it was always under stress conditions. There were genes that were upregulated by both 2E and the reference strain under silver stress, as shown in Table 3.24 and Table 3.25, respectively. Two of these induced genes were *YGP1* encoding cell wall-related secretory glycoprotein, and *SPI1* encoding glycosylphosphatidylinositol (GPI)-anchored cell wall protein (*YGP*1, 8-fold by 2E and more than 10-fold by reference strain; *SPI1*, 7-fold by 2E and more than 20-fold

by reference strain). It was reported that *S. cerevisiae* cell wall organization was strongly affected and cell wall-related genes such as *YGP1* and *SPI1*, and most of the high-osmolarity glycerol (HOG) pathway-dependent genes were induced by low environmental pH (Kapteyn et al., 2001). Silver nitrate was the silver compound used in this study. Silver nitrate is dissolved easily in water and its aqueous solution was acidic with the pH of between 5 and 6 (URL-3). Thus, even if the cell wall integrity of the silver-resistant mutant 2E was higher than that of the reference strain under both control and stress conditions, higher *YGP1* and *SPI1* expression in the reference strain (Figure 3.27) might be associated with the moderate improvement in the lyticase resistance of the reference strain under silver stress condition, compared to the control condition.

It was shown that heat shock, nitrogen starvation, and oxidative stress also induced most of the low pH-induced genes (Marchler et al., 1993). In 2011, Niazi et al. showed that heat shock genes, such as *HSP26* and *HSP12*, were one of the most strongly upregulated genes when *S. cerevisiae* was exposed to Ag ions and AgNPs. It was also reported that the expression of *SPI1* increased under osmotic stress and heat shock (Puig and PerezOrtin, 2000). *HSP26* and *HSP12* were upregulated in both 2E and the reference strain by 6-fold and by more than 50-fold, respectively (Table 3.24 and Table 3.25). *HSP82* gene was also upregulated, but less than the previously mentioned two heat shock protein-encoding genes. Additionally, it was observed that trehalose is a stabilizer of membrane and proteins in yeast, and there is an important role of trehalose during the heat shock survival (Crowe, 2007). Both 2E and the reference strain produced trehalose during stress conditions (Table 3.18). In 1996, Liu and Thiele suggested that in the oxidative stress resistance of eukaryotic cells, heat shock factors played a critical role. In order to activate gene transcription, signals of both oxidative and heat stress communicated to heat shock factor in a different way. Also in 2012, Morano et al. showed the wide and common scope of the resistance to heat and oxidative stress in yeast. Taken together, these were the transcriptional efforts of both 2E and reference strain against oxidative stress caused by the silver stress.

5. CONCLUSIONS

In this study, first a highly silver-resistant *S. cerevisiae* strain was obtained by evolutionary engineering and then genomic and transcriptomic analyses were performed to identify the mutations and the differentially expressed genes in the evolved strain. To our knowledge, there is no report showing the changes in the transcriptome and genome of a silver-resistant *S. cerevisiae* mutant obtained by evolutionary engineering. It was revealed by the results that the key genes that may contribute to the silver resistance of *S. cerevisiae* are participating in copper homeostasis, cellular respiration, oxidative metabolism, vesicular transport activities, endocytosis, and in cell wall/membrane integrity. To enlighten the mechanisms of silver resistance of yeast cells, further functional genomic analyses are needed, focusing on reverse engineering by introducing the mutations identified in the silver-resistant mutant 2E in this study, particularly in the cell wall integrity-related transcription factor gene *RLM1* into the prototrophic background strain. The overexpression or the disruption of the related genes and the analysis of the resulting strains are also needed for further investigation.

REFERENCES

Abdulrehman, D., Monteiro, P. T., Teixeira, M. C., Mira, N. P., Lourenco, A. B., dos Santos, S. C., ….. Freitas, A. T. (2011). YEASTRACT: providing a programmatic access to curated transcriptional regulatory associations in *Saccharomyces cerevisiae* through a web services interface. *Nucleic Acids Res, 39,* D136-140.

Abramova, N., Sertil, O., Mehta, S., and Lowry, C. V. (2001). Reciprocal regulation of anaerobic and aerobic cell wall mannoprotein gene expression in *Saccharomyces cerevisiae*. *Journal of Bacteriology, 183,* 2881-2887.

Alkım, C., Benbadis, L., Yılmaz, Ü., Çakar, Z. P., and Francois, J. M. (2013). Mechanisms other than activation of the iron regulon account for the hyper-resistance to cobalt of a *Saccharomyces cerevisiae* strain obtained by evolutionary engineering. *Metallomics, 5(8),* 1043-1060.

Argüello, J. M., Raimundo, D., and Gonzalez-Guerrero, M. (2012). Metal transport across biomembranes: Emerging models for a distinct chemistry. *The Journal of Biological Chemistry, 287(17),* 13510–13517.

Arslan, M., Holyavkin, C., Kisakesen, H. I., Topaloglu, A., Surmeli, Y., and Cakar, Z. P. (2018). Physiological and Transcriptomic Analysis of a Chronologically Long-Lived *Saccharomyces cerevisiae* Strain Obtained by Evolutionary Engineering. *Molecular Biotechnology, 60(7),* 468-484.

Bailey, J. E., Sburlati, A., Hatzimanikatis, V., Lee, K., Renner, V. A., and Tsai, P. S. (1996). Inverse metabolic engineering: A strategy for directed genetic engineering of useful phenotypes. *Biotechnol. Bioeng., 52,* 109-121.

Balaban, G., Yılmaz, Ü., Alkım, C., Topaloğlu, A., Kısakesen, H. I., ….. Çakar, Z. P. (2020). Evolutionary engineering of an iron-resistant *Saccharomyces cerevisiae* mutant and its physiological and molecular characterization. *Microorganism, 8,* 43 doi:10.3390/microorganisms8010043.

Blaiseau, P. L., Lesuisse, E., and Camadro, J. M. (2001). Aft2p, a novel iron-regulated transcription activator that modulates, with Aft1p, intracellular iron use and resistance to oxidative stress in yeast. *J Biol Chem, 276,* 34221–34226.

Bleackley, M. R., Young, B. P., Loewen, J. R., and MacGillivray, R. T. E. (2011). High density array screening to identify the genetic requirements for transition metal tolerance in *Saccharomyces cerevisiae*. *Metallomics, 3,* 195-205.

Botstein, D., Chervitz, S. A., and Cherry, J. M. (1997). Yeast as a model organism. *Science, 277(5330),* 1259-1260.

Brown, J. A., Sherlock, G., Myers, C. L., Burrows, N. M., Deng, C., Wu, H. I., ….. Brown, J. M. (2006). Global analysis of gene function in yeast by quantitative phenotypic profiling. *Molecular Systems Biology*, *2(1)*. https://doi.org/10.1038/msb4100043

Burke, D., Dawson, D., and Stearns, T. (2000). *Methods in Yeast Genetics: A Cold Spring Harbour Laboratory Course Manual*. New York: Cold Spring Harbor Laboratory Press.

Carri, M. T., Galiazzo, F., Ciriolo, M. R., and Rotilio, G. (1991). Evidence for co-regulation of Cu,Zn superoxide dismutase and metallothionein gene expression in yeast through transcriptional control by copper via the ACE 1 factor. *FEBS Lett*, *278*, 263–266.

Cherry, J. M., Hong, E. L., Amundsen, C., Balakrishnan, R., Binkley, G., Chan, E. T., ….. Wong, E. D. (2012). Saccharomyces Genome Database: The genomics resource of budding yeast. *Nucleic Acids Research*, *40 (D1)*, 700–705.

Chopra, I. (2007). The increasing use of silver-based products as antimicrobial agents: a useful development or a cause for concern? *Journal of Antimicrobial Chemotherapy*, *59(4)*, 587-90.

Cohen, B. D., Sertil, O., Abramova, N. E., Davies, K. J. A., and Lowry, C. V. (2001). Induction and repression of DAN1 and the family of anaerobic mannoprotein genes in *Saccharomyces cerevisiae* occurs through a complex array of regulatory sites. *Nucleic Acids Res*, *29(3)*, 799-808.

Cramp, D. G. (1967). New automated method for measuring glucose by glucose oxidase. *J Clin Pathol*, *20(6)*, 910-912.

Crowe, J. H., (2007). Trehalose as a "chemical chaperone": fact and fantasy. *Adv. Exp. Med. Biol.*, *594*, 143–158.

Çakar, Z. P., Alkım, C., Turanlı, B., Tokman, N., Akman, S., Sarıkaya, M., ….. Francois, J. M. (2009). Isolation of cobalt hyper-resistant mutants of *Saccharomyces cerevisiae* by in vivo evolutionary engineering approach. *Journal of Biotechnology*, *143(2)*, 130-138.

Çakar, Z. P., Turanli-Yildiz, B., Alkim, C., and Yilmaz, U. (2012). Evolutionary engineering of *Saccharomyces cerevisiae* for improved industrially important properties. *FEMS Yeast Research*, *12(2)*, 171-182.

Çakar, Z. P, Seker, U. O. S, Tamerler, C., Sonderegger, M., and Sauer, U. (2005). Evolutionary engineering of multiple-stress resistant *Saccharomyces cerevisiae*. *FEMS Yeast Research*, *5*, 569-578.

Dujon, B. (1996). The yeast genome project: what did we learn? *Trends Genet.*, *127*, 263-270.

Eid, R., Boucher, E., Gharib, N., Khoury, C., Arab, N. T. T., Murray, A., ….. Greenwood, M. T. (2016) Identification of human ferritin, heavy polypeptide1 (FTH1) and yeast RGI1 (YER067W) as pro-survival sequences that counteract the effects of Bax and copper in *Saccharomyces cerevisiae*. *Experimental Cell Research*, *342*, 52–61.

Fadeel, B., and Garcia-Bennett, A. E. (2010). Better safe than sorry: Understanding the toxicological properties of inorganic nanoparticles manufactured for biomedical applications. *Advanced Drug Delivery Reviews, 62,* 362-374.

Fuhrmann, G. F., and Rothstein, A. (1968). The transport of Zn^{+2}, Co^{+2} and Ni^{+2} into yeast cell. *Biochim Biophys Acta*., *163*, 325-330.

Fujii, T., Shimoi, H., and Iimura, Y. (1999). Structure of the glucan-binding sugar chain of Tip1p, a cell wall protein of *Saccharomyces cerevisiae*. *Biochim Biophys Acta, 1427(2),* 133-144.

Galagan, J. E., Henn, M. R., Ma, L. J., Cuomo, C. A., and Birren, B. (2005). Genomics of the fungal kingdom: insights into eukaryotic biology. *Genome Research, 15(12),* 1620-31.

Galaris, D., and Pantopoulos, K. (2008). Oxidative stress and iron homeostasis: mechanistic and health aspects. *Crit. Rev. Clin. Lab. Sci., 45,* 1-23.

Goffeau, A., Barrell, B. G., Bussey, H., Davis, R. W., Dujon, B., Feldmann, H., …… Oliver, S. G. (1996). Life with 6000 genes. *Science, 274(5287),* 546, 563-7.

Goldman, E. and Green, L. H. (2008). *Practical Handbook of Microbiology* (Second Edition). CRC Press.

Greenwood, N. N. and Earnshaw, A. (1997). Copper, Silver and Gold, *Chemistry of the Elements* (2nd ed., pp.1173-1200). Butterworth-Heinemann.

Greulich, C., Braun, D., Peetsch, A., Diendorf, J., Siebers, B., and Epple, M. (2012). The toxic effect of silver ions and silver nanoparticles towards bacteria and human cells occurs in the same concentration range. *RSC Advances, 2,* 6981-6987.

Guirola, M., Barreto, L., Pagani, A., Romagosa, M., Casamayor, A., Atrian, S., and Arino, J. (2010). Lack of DNA helicase Pif1 disrupts zinc and iron homoeostasis in yeast. *Biochemical Journal, 432(3),* 595-605.

Hacısalihoğlu, B., Holyavkin, C., Topaloğlu, A., Kısakesen, H. İ., and Çakar, Z. P. (2019). Genomic and transcriptomic analysis of a coniferyl aldehyde-resistant *Saccharomyces cerevisiae* strain obtained by evolutionary engineering. *FEMS Yeast Research, 19(3),* foz021.

Herskowitz, I. (1988). Life cycle of the budding yeast *Saccharomyces cerevisiae*. *Microbiol Rev, **52(4)**,* 536-53.

Holland, S. L., Dyer, P. S., Bond, C. J., James, S. A., Roberts, I. N., and Avery, S. V. (2011). Candida argentea sp. nov., a copper and silver resistant yeast species. *Fungal Biology, 115(9),* 909-18.

Horstmann, C., Campbell, C., Kim, D. S., and Kim, K. (2019). Transcriptome profile with 20 nm silver nanoparticles in yeast. *FEMS Yeast Research, 19,* foz003.

Hosiner, D., Gerber, S., Lichtenberg-Frate, H., Glaser, W., Schüller, C., and Klipp, E. (2014). Impact of Acute Metal Stress in *Saccharomyces cerevisiae*. *Plos One, 9(1),* e83330

Howe, P. D. and Dobson, S. (2002). Silver and silver compounds: environmental aspects (CICAD 44). Geneva : World Health Organization.

Jin, Y. H., Dunlap, P. E., McBride, S. J., Al-Refai, H., Bushel, P. R., and Freedman, J. H. (2008). Global transcriptome and deletome profiles of yeast exposed to transition metals. *PLoS Genetics*, *4(4)*, e1000053.

Kakimoto, M., Kobayashi, A., Fukuda, R., Ono, Y., Ohta, A., and Yoshimura, E. (2005). Genome-wide screening of aluminum tolerance in *Saccharomyces cerevisiae*. *BioMetals*, *18 (5)*, 467–474.

Kapteyn, J. C., ter Riet, B., Vink, E., Blad, S., De Nobel, H., Van Den Ende, H., and Klis, F. M. (2001). Low external pH induces HOG1-dependent c,hanges in the organization of the *Saccharomyces cerevisiae* cell wall. *Mol Microbiol*, *39(2)*, 469-79.

Karamushka, V. I., and Gadd, G. M. (1994). Influence of copper on proton efflux from *Saccharomyces cerevisiae* and the protective effect of calcium and magnesium. *FEMS Microbiology Letters*, *122(1-2)*, 33-38.

Kaplun, L., Ivantsiv, Y., Kornitzer, D., and Raveh, D. (2000). Functions of the DNA damage response pathway target Ho endonuclease of yeast for degradation via the ubiquitin-26S proteasome system. *Proc Natl Acad Sci U S A*, *97(18)*, 10077-10082.

Kuranda, K., Leberre. V., Sokol, S., Palamarczyk, G., and François, J. (2006). Investigating the caffeine effects in the yeast *Saccharomyces cerevisiae* brings new insights into the connection between TOR, PKC and Ras/cAMP signaling pathways. *Molecular Microbiology*, *61(5)*:1147–1166.

Küçükgöze, G., Alkım, C., Yılmaz, Ü., Kısakesen, H. İ., Gündüz, S., Akman, S., and Çakar, Z. P. (2013). Evolutionary engineering and transcriptomic analysis of nickel-resistant *Saccharomyces cerevisiae*. *FEMS Yeast Research*, *13(8)*, 731–746.

Lawrence, C. W. (2002). Classical mutagenesis techniques. *In Methods in Enzymology*, *194*, 189–199. https://doi.org/10.1016/S0076-6879(02)50963-0

Lederberg, J., and Lederberg, E. M. (1952). Replica plating and indirect selection of bacterial mutants. *J. Bacteriol.*, *63*, 399-406.

Lee, B., Lee, M. J., Yun, S. J., Kim K., Choi, I., and Park S. (2019) Silver nanoparticles induce reactive oxygen species-mediated cell cycle delay and synergistic cytotoxicity with 3-bromopyruvate in *Candida albicans*, but not in *Saccharomyces cerevisiae*. *International Journal of Nanomedicine*, *2019:14*, 4801-4816.

Li, L., Miao, R., Jia, X., Ward, D. M., and Kaplan, J. (2014). Expression of the yeast cation diffusion facilitators Mmt1 and Mmt2 affects mitochondrial and cellular iron homeostasis: evidence for mitochondrial iron export. *Journal of Biological Chemistry*, *289(24)*, 17132-41.

Li, L., Wu, H., Ji, C., van Gestel, C. A. M., Allen, H. E., and Peijnenburg, W. J. G. M. (2015). A metabolomic study on the responses of *Daphnia magna* exposed to silver nitrate and coated silver nanoparticles. *Ecotoxicology and Environmental Safety*, *119*, 66–73.

Limberger, K. M., Westphalen, G. H., Menezes, L. M., and Medina-Silva, R. (2011). Cytotoxicity of orthodontic materials assessed by survival tests in *Saccharomyces cerevisiae*. *Dental Materials*, *27(5)*, e81-6.

Liu, X., and Thiele, D. J. (1996). Oxidative stress induces heat shock factor phosphorylation and HSF-dependent activation of yeast metallothionein gene transcription. *Genes & Development*, *10*, 592-603.

Marchler, G., Schüller, C., Adam, G., and Ruis, H. (1993). A *Saccharomyces cerevisiae* UAS element controlled by protein kinase A activates transcription in response to a variety of stress conditions. *EMBO J*, *12*, 1997– 2003.

Márquez, I. G., Ghiyasvand, M., Massarsky, A., Babu, M., Samanfar, B., Omidi, K., ….. Golshani, A. (2018). Zinc oxide and silver nanoparticles toxicity in the baker's yeast, *Saccharomyces cerevisiae*. *PLoS One*. *13(3)*, e0193111. https://doi.org/10.1371/journal.pone.0193111

Martinez-Pastor, M. T., Perea-Garcia, A., and Puig, S. (2017). Mechanisms of iron sensing and regulation in the yeast *Saccharomyces cerevisiae*. *World J Microbiol Biotechnol.*, *33(4)*:75. doi: 10.1007/s11274-017-2215-8.

Matmati, N., and Hannun, Y. A. (2008). Thematic Review Series: Sphingolipids. ISC1 (inositol phosphosphingolipid-phospholipase C), the yeast homologue of neutral sphingomyelinases. *Journal of Lipid Research*, *49(5)*, 922-928.

Memarian, N., Jessulat, M., Alirezaie, M., Mir-Rashed, N., Xu, J., Zareie, M., ….. Golshani, A. (2007). Colony size measurement of the yeast gene deletion strains for functional genomics. *BMC Bioinformatics*, *8*, 117. doi: 10.1186/1471-2105-8-117.

Mijnendonckx, K., Leys, N., Mahillon, J., Silver, S., and Van Houdt, R. (2013). Antimicrobial silver: uses, toxicity and potential for resistance. *Biometals*, *26(4)*, 609-621.

Monteiro, P. T., Oliveira, J., Pais, P., Antunes, M., Palma, M., Cavalheiro, M., ….. Teixeira, M. C. (2019). YEASTRACT+: a portal for cross-species comparative genomics of transcription regulation in yeast. *Nucleic Acids Research*, *48(D1)*, D642-D649.

Morano, K. A., Grant C. M., and Moye-Rowley, W. S. (2012). The response to heat shock and oxidative stress in *Saccharomyces cerevisiae*. *Genetics*, *190(4)*, 1157-1195.

Mortimer, R. K. (1958). Radiobiological and genetic studies on a polyploidy series (haploid to hexaploid) of *Saccharomyces cerevisiae*. *Radiat. Res.*, *9*, 312-326.

Nasmyth, K. (1993). Regulating the HO endonuclease in yeast. *Curr Opin Genet Dev*, *3(2)*, 286-94.

Neovigt, E. (2008). Progress in metabolic engineering of *Saccharomyces cerevisiae*. *Microbiology and Molecular Biology Reviews*, *72*, 379-412.

Niazi, J. H., Sang, B. I., Kim, Y. S., and Gu, M. B. (2011). Global gene response in *Saccharomyces cerevisiae* exposed to silver nanoparticles. *Applied Biochemistry and Biotechnology*, *164(8)*, 1278-91.

Nies, D. H. (1999). Microbial heavy-metal resistance. *Appl Microbiol Biotechnol*, *51*, 730–750.

Ostergaard, S., Olsson, L., and Nielsen, J. (2000). Metabolic engineering of *Saccharomyces cerevisiae*. *Microbiology and Molecular Biology Reviews*, *64*, 34-50.

Pagani, M. A., Casamayor, A., Serrano, R., Atrian, S., and Arino, J. (2007). Disruption of iron homeostasis in *Saccharomyces cerevisiae* by high zinc levels: a genome-wide study. *Molecular Microbiology*, *65(2)*, 521-37.

Parrou, J. L., and François, J. (1997). A simplified procedure for a rapid and reliable assay of both glycogen and trehalose in whole yeast cells. *Anal. Biochem.*, *15*, 186-188.

Popa, C. V., Dumitru, I., Ruta, L. L., Danet, A. F., and Farcasanu, I. C. (2010). Exogenous oxidative stress induces Ca2+ release in the yeast *Saccharomyces cerevisiae*. *FEBS Journal*. *277(19)*, 4027- 4038. doi: 10.1111/j.1742-4658.2010.07794.x

Porro, D., Sauer, M., Braunduardi, P., and Mattanovich, D. (2005). Recombinant protein production in yeasts. *Mol. Biotechnol.*, *31*, 245-260.

Puig, S., and PerezOrtin, J. E. (2000). Stress response and expression patterns in wine fermentations of yeast genes induced at the diauxic shift. *Yeast*, *16*, 139– 148. doi: 10.1002/(sici)1097-0061(20000130)16:2<139::aid-yea512>3.0.co;2-j

R software (2017). R: A Language and Environment for Statistical Computing. Retrieved January 15, 2017, from https://www.rproject.org

Radhakrishnan, V. S., Dwivedi, S. P., Siddiqui, M. H., and Prasad, T. (2018) In vitro studies on oxidative stress-independent, Ag nanoparticles-induced cell toxicity of Candida albicans, an opportunistic pathogen. *Int J Nanomed*, *13*, 91–96.

Radhakrishnan, V. S., Reddy Mudiam, M. K., Kumar, M., Dwivedi, S. P., Singh, S. P., and Prasad, T. (2018) Silver nanoparticles induced alterations in multiple cellular targets, which are critical for drug susceptibilities and pathogenicity in fungal pathogen (Candida albicans). *Int J Nanomed*, *13*, 2647–2663.

Ramsay, L. M., and Gadd, G. M. (1997). Mutants of *Saccharomyces cerevisiae* defective in vacuolar function confirm a role for the vacuole in toxic metal ion detoxification. *FEMS Microbiology Letters*, *152*, 293-298.

Ruotolo, R., Marchini, G., and Ottonello, S. (2008). Membrane transporters and protein traffic networks differentially affecting metal tolerance: a genomic phenotyping study in yeast. *Genome Biology*, *9(4)*, R67.

Russek, E., and Colwell, R. R. (1983). Computation of most probable numbers. *Appl. Environ. Microbiol., 45*, 1646-1650.

Ruta, L. L., Popa, C. V., Nicolau, I., and Farcasanu, I. C. (2016) Calcium signaling and copper toxicity in *Saccharomyces cerevisiae* cells. *Environmental Science and Pollution Research International. 23(24)*, 24514-24526. doi: 10.1007/s11356-016-6666-5.

Rutherford, J. C., and Bird, A. J. (2004). Metal-responsive transcription factors that regulate iron, zinc, and copper homeostasis in eukaryotic cells. *Eukaryotic Cell, 3(1)*, 1-13.

Saulou, C., Jamme, F., Maranges, C., Fourquaux, I., Despax, B., Raynaud, P., ….. Mercier-Bonin, M. (2010). Synchrotron FTIR microspectroscopy of the yeast *Saccharomyces cerevisiae* after exposure to plasma-deposited nanosilver-containing coating. *Analytical and Bioanalytical Chemistry, 396(4)*, 1441-50.

Schacherer, J., Ruderfer, D. M., Gresham, D., Dolinski, K., Botstein, D., and Kruglyak, L. (2007). Genome-wide analysis of nucleotide-level variation in commonly used *Saccharomyces cerevisiae* strains. *PLoS ONE, 2(3)*, e322.

Sherman, F. (2002). Getting started with yeast. *Methods in Enzymology, 350*, 3-41.

Sherman, F., Fink, G. R., and Lawrence, C. W. (1979). *Methods in Yeast Genetics: Cold Spring Harbour Laboratory*. New York: Cold Spring Harbor Laboratory Press.

Shi, W., Zhan, C., Ignatov, A., Manjasetty, B. A., Marinkovic, N., Sullivan, M., ….. Chance, M. R. (2005). Metalloproteomics: high-throughput structural and functional annotation of proteins in structural genomics. *Structure, 13*, 1473-1486.

Solioz, M., and Odermatt, A. (1995). Copper and silver transport by CopB-ATPase in membrane vesicles of *Enterococcus hirae*. *Journal of Biological Chemistry, 270(16)*, 9217-9221.

Stephanopoulos, G. (1999). Metabolic fluxes and metabolic engineering. *Metab. Eng., 1*, 1-11.

Sürmeli, Y., Holyavkin, C., Topaloğlu, A., Arslan, M., Kısakesen, H. İ. and Çakar, Z. P. (2019). Evolutionary engineering and molecular characterization of a caffeine-resistant *Saccharomyces cerevisiae* strain. *World Journal of Microbiology and Biotechnology, 35*, 183.

Tamas, M. J., Labarre, J., Toledano, M. B., and Wysocki, R. (2005). Mechanisms of toxic metal tolerance in yeast. *Topics in Current Genetics, 14*, 395-454.

Terzioglu, E., Alkım, C., Arslan, M., Balaban, B. G., Holyavkin, C., Kısakesen, H. İ., ….. Çakar, Z. P. (2020). Genomic, transcriptomic and physiological analyses of silver-resistant *Saccharomyces cerevisiae* obtained by evolutionary engineering. *Yeast, 37*, 413-426. doi:10.1002/yea.3514.

Terzioğlu, E., Arslan, M., Kısakesen, H. İ., and Çakar, Z. P. (2020). Query DataSets for GSE143335. Retrieved January 9, 2020, from https://www.ncbi.nlm.nih.gov/geo/query/acc.cgi?acc=GSE14333

Turanli-Yildiz, B., Benbadis, L., Alkim, C., Sezgin, T., Aksit, A., Gokce, A., ….. Francois, J. M. (2017). In vivo evolutionary engineering for ethanol-tolerance of *Saccharomyces cerevisiae* haploid cells triggers diploidization. *Journal of Bioscience and Bioengineering*, *124(3)*, 309-318.

URL-1 <*https://chemed.chem.purdue.edu*>, date retrieved 17.07.2020.

URL-2 < *https://www.yeastgenome.org***>,** date retrieved 13.08.2020.

URL-3 <www.chemicalbook.com**>,** date retrieved 25.08.2020.

van Dijken, J.P., Bauer, J., Brambilla, L., Duboc, P., Francois, J. M., Gancedo, C., ….. Pronk, J. T. (2000). An interlaboratory comparison of physiological and genetic properties of four *Saccharomyces cerevisiae* strains. *Enzyme and Microbial Technology*, *26(9-10)*, 706-714.

Warheit, D. B., Sayes, C. M., Reed, K. L., and Swain, K. A. (2008). Health effects related to nanoparticle exposures: environmental, health and safety considerations for assessing hazards and risks. *Pharmacol. Ther.*, *120*, 35-42.

Winge, D. R. (1998). Copper-regulatory domain involve in gene expression, *Progress In Nucleic Acid Research and Molecular Biology* (Vol. 58, pp.165-195). Academic Press.

Wysocki, R., and Tamas, M. J. (2010). How *Saccharomyces cerevisiae* copes with toxic metals and metalloids. *FEMS Microbiology Reviews, 34(6)*, 925-951.

Xu, N., Dong, Y., Cheng, X., Yu, Q., Qian, K., Mao, J., ….. Li, M. (2014). Cellular iron homeostasis mediated by the Mrs4-Ccc1-Smf3 pathway is essential for mitochondrial function, morphogenesis and virulence in Candida albicans. Biochimica et Biophysica Acta - Molecular Cell Research, *1843(3)*, 629-39.

Yadav, J., Muend, S., Zhang, Y., and Rao, R. (2007). A phenomics approach in yeast links proton and calcium pump function in the Golgi. *Molecular Biology of the Cell*, *18 (4)*, 1480–1489.

Yu, G., Wang, L. G., Han, Y., and He, Q. Y. (2012). clusterProfiler: an R package for comparing biological themes among gene clusters. *OMICS: A Journal of Integrative Biology*, *16 (5)*, 284-287.

Yuan, D. S., Stearman, R., Dancis, A., Dunn, T., Beeler, T., and Klausner, R. D. (1995). The Menkes-Wilson-disease gene homolog in yeast provides copper to a ceruloplasmin like oxidase required for iron uptake. *Proceedings of the National Academy of Science of America*, *92(7)*, 2632-2636.

APPENDICES

APPENDIX A: Selected Functional Categories of Differentially Expressed Genes

APPENDIX A : Selected Functional Categories of Differentially Expressed Genes

Table A.1 : Selected functional categories of the upregulated and downregulated genes in 2E (Terzioğlu et al., 2020).

Systematic name	Gene name	Regulation	Fold change	Description
cellular respiration				
YEL024W	*RIP1*	up	2.46	Ubiquinol-cytochrome-c reductase
YEL039C	*CYC7*	up	46.70	Cytochrome c isoform 2, expressed under hypoxic conditions
DNA repair				
YDL059C	*RAD59*	up	2.64	Protein involved in DNA double-strand break repair
YDR314C	*RAD34*	up	2.97	Protein involved in nucleotide excision repair (NER)
YNL133C	*FYV6*	up	2.19	Protein of unknown function; proposed to regulate double-strand break repair via non-homologous end-joining
hydrolase activity				
YBR098W	*MMS4*	up	2.63	Subunit of structure-specific Mms4p-Mus81p endonuclease
YPL123C	*RNY1*	up	6.57	Vacuolar RNase of the T(2) family
YER142C	*MAG1*	up	2.29	3-methyl-adenine DNA glycosylase
YAL015C	*NTG1*	up	2.20	DNA N-glycosylase and apurinic/apyrimidinic (AP) lyase
YMR173W	*DDR48*	up	3.35	DNA damage-responsive protein
YML095C	*RAD10*	up	2.75	Single-stranded DNA endonuclease (with Rad1p)
kinase activity and transferase activity				
YFR053C	*HXK1*	up	113.19	Hexokinase isoenzyme 1
YGL208W	*SIP2*	up	7.34	One of three beta subunits of the Snf1 kinase complex

Table A.1 (continued) : Selected functional categories of the upregulated and downregulated genes in 2E (Terzioğlu et al., 2020).

Systematic name	Gene name	Regulation	Fold change	Description
lipid binding				
YFL014W	*HSP12*	up	11.83	Plasma membrane protein involved in maintaining membrane organization
lyase activity				
YNL036W	*NCE103*	up	16.31	Carbonic anhydrase
YOR386W	*PHR1*	up	4.52	DNA photolyase involved in photoreactivation
mitochondrial electron transport				
YNL237W	*YTP1*	up	2.81	Probable type-III integral membrane protein of unknown function; has regions of similarity to mitochondrial electron transport proteins
nucleic acid binding transcription factor activity and DNA binding				
YIL101C	*XBP1*	up	7.68	Transcriptional repressor
YGL166W	*CUP2*	up	2.30	Copper-binding transcription factor
oxidoreductase activity				
YDR178W	*SDH4*	up	3.16	Membrane anchor subunit of succinate dehydrogenase (SDH)
YDR453C	*TSA2*	up	6.95	Stress inducible cytoplasmic thioredoxin peroxidase
YHR008C	*SOD2*	up	2.37	Mitochondrial manganese superoxide dismutase
YJR104C	*SOD1*	up	2.29	Cytosolic copper-zinc superoxide dismutase
YKL026C	*GPX1*	up	3.31	Phospholipid hydroperoxide glutathione peroxidase
YKL086W	*SRX1*	up	13.58	Sulfiredoxin
YKL141W	*SDH3*	up	2.39	Subunit of succinate dehydrogenase and of TIM22 translocase
YLL041C	*SDH2*	up	2.20	Iron-sulfur protein subunit of succinate dehydrogenase

Table A.1 (continued) : Selected functional categories of the upregulated and downregulated genes in 2E (Terzioğlu et al., 2020).

Systematic name	Gene name	Regulation	Fold change	Description
YML120C	*NDI1*	up	4.20	NADH:ubiquinone oxidoreductase
YOR374W	*ALD4*	up	32.21	Mitochondrial aldehyde dehydrogenase
YHR053C	*CUP1-1*	up	4.79	Metallothionein
YHR055C	*CUP1-2*	up	4.71	Metallothionein
YKL148C	*SDH1*	up	4.01	Flavoprotein subunit of succinate dehydrogenase
YCL035C	*GRX1*	up	6.11	Glutathione-dependent disulfide oxidoreductase
YDR513W	*GRX2*	up	4.75	Cytoplasmic glutaredoxin
YMR256C	*COX7*	up	4.71	Subunit VII of cytochrome c oxidase (Complex IV)
YGL191W	*COX13*	up	3.61	Subunit VIa of cytochrome c oxidase
YOR120W	*GCY1*	up	6.12	Glycerol dehydrogenase
peroxisome organization				
YIL065C	*FIS1*	up	2.29	Protein involved in mitochondrial fission and peroxisome abundance
phosphatase activity, hydrolase activity and DNA binding				
YMR156C	*TPP1*	up	2.51	DNA 3'-phosphatase
response to chemical and signaling				
YNL305C	*BXI1*	up	5.08	Protein involved in apoptosis
sporulation and meiotic cell cycle				
YNL194C	YNL194C	up	100.75	Integral membrane protein
stress response				
YOL052C-A	*DDR2*	up	18.18	Multi-stress response protein
transferase activity				
YGL087C	*MMS2*	up	4.36	Ubiquitin-conjugating enzyme variant
transmembrane ion transport				
YER145C	*FTR1*	down	2.97	High affinity iron permease
YMR319C	*FET4*	down	2.81	Low-affinity Fe(II) transporter of the plasma membrane

Table A.1 (continued): Selected functional categories of the upregulated and downregulated genes in 2E (Terzioğlu et al., 2020).

Systematic name	Gene name	Regulation	Fold change	Description
YML123C	*PHO84*	down	68.56	High-affinity inorganic phosphate (Pi) transporter
transmembrane transporter activity				
YDR342C	*HXT7*	up	48.42	High-affinity glucose transporter
YDR343C	*HXT6*	up	52.53	High-affinity glucose transporter
YJR095W	*SFC1*	up	6.64	Mitochondrial succinate-fumarate transporter
YLR411W	*CTR3*	up	3.01	High-affinity copper transporter of the plasma membrane
YMR011W	*HXT2*	up	39.54	High-affinity glucose transporter of the major facilitator superfamily
vacuolar membrane transporter				
YMR243C	*ZRC1*	down	2.01	Vacuolar membrane zinc transporter
v-SNARE binding				
YGR142W	*BTN2*	up	3.86	v-SNARE binding protein
cell wall component				
YER011W	*TIR1*	down	9.19	Cell wall mannoprotein of the Srp1p/Tip1p family
YOR010C	*TIR2*	down	11.41	Putative cell wall mannoprotein of the Srp1p/Tip1p family
YIL011W	*TIR3*	down	3.65	Cell wall mannoprotein of the Srp1p/Tip1p family
YOR009W	*TIR4*	down	2.27	Cell wall mannoprotein of the Srp1p/Tip1p family
energy reserve				
YER067W	*RGI1*	up	32.84	Protein of unknown function involved in energy metabolism under respiratory conditions

CURRICULUM VITAE

Name Surname **:** Ergi TERZİOĞLU

EDUCATION **:**

- **B.Sc.** **:** 2003, İstanbul Technical University, Faculty of Management, Industrial Engineering Department
- **M.Sc.** **:** 2009, İstanbul Technical University, Graduate School of Science Engineering and Technology, Department of Molecular Biology-Genetics and Biotechnology

PUBLICATIONS, PRESENTATIONS AND PATENTS ON THE THESIS:

- **Terzioğlu, E.**, Alkım, C., Arslan, M., Kısakesen, H. İ., Yılmaz, Ü., Balaban, B. G., Selçuki, C., and Çakar, Z. P. 2015: Physiological and transcriptomic analysis of a silver-resistant *Saccharomyces cerevisiae* strain obtained by evolutionary engineering. International Conference - Microbial Stress Meeting: from Molecules to Systems, November 12-14, 2015, Sitges, Spain. (Oral Presentation, Abstract Book p.23)
- **Terzioğlu, E.**, Alkım, C., Arslan, M., Balaban, B. G., Holyavkin, C., Kısakesen, H. İ., Topaloğlu, A., Yılmaz Şahin, Ü., Gündüz Işık, S., Akman, S., and Çakar, Z. P. 2020. Genomic, transcriptomic and physiological analyses of silver-resistant *Saccharomyces cerevisiae* obtained by evolutionary engineering. *Yeast*, ***2020 (37)***, 413-426. doi:10.1002/yea.3514.

OTHER PUBLICATIONS, PRESENTATIONS AND PATENTS:

- **Terzioğlu, E.**, Çakar, Z.P., Köprülüoğlu, C., Eyrilmez, S.M., Acar, N., and Selçuki, C. 2011: Investigation of interactions of Cu ions with the MXCXXC motif of the Atx1 protein by density functional theory. The International Conference on Enzyme Science and Technology 'ICEST 2011', October 31-November 4, 2011, Kuşadası, Turkey. (Poster Presentation, Abstract Book p. 120)
- **Terzioğlu, E.**, Kahveci, M.Ü., Çakar, Z.P., and Selçuki, C. 2008: A computational study of MXCXXC motif in yeast copper chaperons with Cu^{+} and Cu^{2+}. HIBIT 2008, 3rd International Symposium on Health Informatics and Bioinformatics, May 18-20, 2008, Istanbul, Turkey. (Oral Presentation)
- **Terzioğlu, E.**, Kahveci, M.Ü., Çakar, Z.P., and Selçuki, C. 2008: A computational analysis of interactions between copper and MXCXXC peptide motif with varying X's in yeast. Chemical Physics Conference VIII, 24-25 April, 2008, Istanbul Technical University, Istanbul, Turkey. (Poster Presentation, Abstract Book p. 19)
- **Terzioğlu, E.**, Kahveci, M.Ü., Çakar, Z.P., and Selçuki, C. 2007: Computational conformational analysis of MXCXXC motif of ATX1 in *Saccharomyces cerevisiae*. *Drugs Fut*. 2007 (*32*, *Suppl. A*): 6th AFMC International Medicinal Chemistry Symposium, July 8-11, 2007, Istanbul, Turkey. (Poster Presentation, Abstract Book p. PB-44)
- Kahveci, M.Ü., **Terzioğlu, E.**, Çakar, Z.P., and Selçuki, C. 2007: Computational conformational analysis of REXLE motif of iron permease FTR1 in *Saccharomyces cerevisiae*. *Drugs Fut.* ***2007*** *(32, Suppl. A)*: 6th AFMC International Medicinal Chemistry Symposium, July 8-11, 2007, Istanbul, Turkey. (Poster Presentation, Abstract Book p. PB-45)